

Linton, Oliver Bruce; Wu, Jianbin

**Working Paper**

## A coupled component GARCH model for intraday and overnight volatility

cemmap working paper, No. CWP05/17

**Provided in Cooperation with:**

Institute for Fiscal Studies (IFS), London

*Suggested Citation:* Linton, Oliver Bruce; Wu, Jianbin (2017) : A coupled component GARCH model for intraday and overnight volatility, cemmap working paper, No. CWP05/17, Centre for Microdata Methods and Practice (cemmap), London, <https://doi.org/10.1920/wp.cem.2017.0517>

This Version is available at:

<https://hdl.handle.net/10419/189690>

**Standard-Nutzungsbedingungen:**

Die Dokumente auf EconStor dürfen zu eigenen wissenschaftlichen Zwecken und zum Privatgebrauch gespeichert und kopiert werden.

Sie dürfen die Dokumente nicht für öffentliche oder kommerzielle Zwecke vervielfältigen, öffentlich ausstellen, öffentlich zugänglich machen, vertreiben oder anderweitig nutzen.

Sofern die Verfasser die Dokumente unter Open-Content-Lizenzen (insbesondere CC-Lizenzen) zur Verfügung gestellt haben sollten, gelten abweichend von diesen Nutzungsbedingungen die in der dort genannten Lizenz gewährten Nutzungsrechte.

**Terms of use:**

*Documents in EconStor may be saved and copied for your personal and scholarly purposes.*

*You are not to copy documents for public or commercial purposes, to exhibit the documents publicly, to make them publicly available on the internet, or to distribute or otherwise use the documents in public.*

*If the documents have been made available under an Open Content Licence (especially Creative Commons Licences), you may exercise further usage rights as specified in the indicated licence.*

# A coupled component GARCH model for intraday and overnight volatility

---

Oliver Linton  
Jianbin Wu

The Institute for Fiscal Studies  
Department of Economics, UCL

**cemmap** working paper CWP05/17

# A coupled component GARCH model for intraday and overnight volatility\*

Oliver Linton<sup>†</sup>                      Jianbin Wu<sup>‡</sup>  
University of Cambridge              Xiamen University

January 20, 2017

## Abstract

We propose a semi-parametric coupled component GARCH model for intraday and overnight volatility that allows the two periods to have different properties. To capture the very heavy tails of overnight returns, we adopt a dynamic conditional score model with  $t$  innovations. We propose a several step estimation procedure that captures the nonparametric slowly moving components by kernel estimation and the dynamic parameters by  $t$  maximum likelihood. We establish the consistency and asymptotic normality of our estimation procedures. We extend the modelling to the multivariate case. We apply our model to the study of the Dow Jones industrial average component stocks over the period 1991-2016 and the CRSP cap based portfolios over the period of 1992-2015. We show that actually the ratio of overnight to intraday volatility has increased in importance for big stocks in the last 20 years. In addition, our model provides better intraday volatility forecast since it takes account of the full dynamic consequences of the overnight shock and previous ones.

## 1 Introduction

The balance between intraday and overnight returns is of considerable interest as it sheds light on many issues in finance: the efficient markets hypothesis, the calendar time versus trading time models, the process by which information is impacted into stock prices, the relative merits of auction versus continuous trading, the effect of high frequency trading on market quality, and the globalization and connectedness of international markets. We propose a time series model for intraday and overnight returns that respects their temporal ordering and permits them to have different properties. In particular, we propose a volatility model for each return series that has a long run component that slowly evolves over time, and is treated nonparametrically, and a parametric dynamic volatility

---

\*We would like to thank Piet Sercu, Haihan Tang and Chen Wang for helpful comments.

<sup>†</sup>Faculty of Economics, Austin Robinson Building, Sidgwick Avenue, Cambridge, CB3 9DD. Email: ob120@cam.ac.uk. Thanks to the Cambridge INET for financial support.

<sup>‡</sup>School of Management, Xiamen, China. Email: jianbin.wu@xmu.edu.cn

component that allows for short run deviations from the long run process, which depend on previous intraday and overnight shocks. We adopt a dynamic conditional score (DCS) model, Harvey (2013) and Harvey and Luati (2014), that links the news impact curves of the innovations to the shock distributions, which we assume to be t-distributions with unknown degrees of freedom (which may differ between day and night). In practice, the overnight return distribution is more heavy tailed than the intraday return, and in fact very heavily tailed. Our model allows for a difference in tail thickness in the conditional distributions. The short run dynamic process allows for leverage effects and separates the overnight shock from the intraday shock. Our model extends Blanc, Chicheportiche, and Bouchaud (2014) who consider an asymmetric ARCH( $\infty$ ) process with t shocks. We also introduce a multivariate model that allows for time varying correlations.

We apply our model to the study of 28 Dow Jones industrial average component stocks over the period 1991-2016, a period which saw several substantial institutional changes. There are several purposes for our application. First, many authors have argued that the introduction of computerized trading and the increased prevalence of high frequency trading strategies in the period post 2005 has led to an increase in volatility, see Linton, O'Hara, and Zigrand (2013). A direct comparison of volatility before and after would be problematic here because of the Global Financial Crisis (GFC), which raised volatility during the same period that High Frequency Trading (HFT) was becoming more prevalent. However, this hypothesis would suggest that the ratio of intraday to overnight volatility should have increased during this period because trading is not taking place during the market close period. We would like to evaluate whether this has occurred. One could just compare the daily return volatility from the intraday segment with the daily return volatility from the overnight segment, as many studies such as French and Roll (1986) have done. However, this would ignore both fast and slow variation in volatility through business cycle and other causal factors. Also, overnight raw returns are very heavy tailed and so sample variances are not very accurate. We use our dynamic two component model that allows for both fast and slow dynamic components to volatility, as is now common practice ( Engle and Lee, 1999; Engle and Rangel, 2008; Hafner and Linton, 2010; Rangel and Engle, 2012; and Han and Kristensen, 2015). Our model also allows dynamic feedback between overnight and intraday volatility, which is of interest in itself. Our model generates heavy tails in observed returns and parameter estimates that are robust to this phenomenon. Our model therefore allows us to compare the long run components of volatility over this period without over reliance on Gaussian-type theory. We show that for the Dow Jones stocks actually the long run component of overnight volatility has increased in importance during this period relative to the long run component of intraday volatility. We provide a formal test statistic that quantifies the strength of this effect. This seems to be hard to reconcile with the view that trading has increased volatility. We also document the short run dynamic processes. Notably, we find, unlike Blanc, Chicheportiche, and Bouchaud (2014), that overnight returns significantly affect future intraday volatility. We also find overnight return shocks to have t-distributions with degrees of freedom roughly equal to three, which emphasizes the potential fragility of Gaussian-based estimation routines that earlier work has been based on. We also estimate the multivariate model and document that there has been an upward trend in the long run component of contemporary overnight correlation between stocks as well as in

the long run component of contemporary intraday correlation between stocks. However, the trend development for the overnight correlations started later than for intraday, and started happening only after 2005, whereas the intraday correlations appear to have slowly increased more or less from the beginning of the period.

We also apply our model to 10 cap based portfolios over the period 1992-2015. The ratio of overnight to intraday volatility has indeed increased for large stocks, but has decreased for small stocks. Notably, the slope increases monotonically from the smallest to the largest cap decile. From the multivariate model, we find small stocks had rather weak co-movement with the market in the early 90s. But the co-movement has been increased considerably during this period, although still smaller than that of big stocks.

A second practical purpose for our model is to improve forecasts of intraday volatility or close to close volatility. Our model allows us to condition on the opening price to forecast intraday volatility or to update the close to close volatility forecast and also to take account of the full dynamic consequences of the overnight shock and previous ones. We compare forecast performance of our model with a procedure based only on close to close returns and find in most cases superior performance.

Overnight returns have attracted much attention during recent years. Specifically, Cooper, Cliff, and Gulen (2008) suggest that the US equity premium over the last decade is solely due to overnight returns. Berkman, Koch, Tuttle, and Zhang (2012) find positive overnight returns tend to be followed by reversals in the subsequent trading day, because retail investors who dominating open prices tend to buy high-attention stocks, driving up the open price. Following this, Aboody, Even-Tov, Lehavy, and Trueman (forthcoming) suggest to use overnight returns as a firm-specific sentiment. On the other hand, Aretz and Bartram (2015) find evidence that intraday returns outperform overnight returns from a sample with stocks in 35 countries, and suggest this also holds in the US market. In contrast with the mixed evidence for mean values, it is generally agreed that overnight returns are less volatile at least in the US market (Lockwood and Linn, 1990; French and Roll, 1986; Aretz and Bartram, 2015), but more leptokurtic (Ng and Masulis, 1995; Blanc, Chicheportiche, and Bouchaud, 2014). We are going to provide some new evidences for these questions with our coupled component GARCH model.

## 2 Model and Properties

We let  $r_t^D$  denote intraday returns and  $r_t^N$  denote overnight returns on day  $t$ . We take the ordering that night precedes day so that  $r_t^D = \ln(P_t^C/P_t^O)$  and  $r_t^N = \ln(P_t^O/P_{t-1}^C)$ , where  $P_t^O$  denotes the opening price on day  $t$  and  $P_t^C$  denotes the closing price on day  $t$ . Our model allows intraday returns to depend on overnight returns with the same  $t$ , but overnight returns just depend on lagged variables. Suppose that

$$\begin{pmatrix} 1 & \delta \\ 0 & 1 \end{pmatrix} \begin{pmatrix} r_t^D \\ r_t^N \end{pmatrix} = \begin{pmatrix} \mu_D \\ \mu_N \end{pmatrix} + \Pi \begin{pmatrix} r_{t-1}^D \\ r_{t-1}^N \end{pmatrix} + \begin{pmatrix} u_t^D \\ u_t^N \end{pmatrix}, \quad (1)$$

where  $u_t^D$  and  $u_t^N$  are conditional mean zero shocks. Under the EMH,  $\delta = 0$  and  $\Pi = 0$ , but we allow these coefficients to be nonzero to pick up small short run effects such as due to microstructure, Scholes and Williams (1977).

We further suppose that the error process has conditional heteroskedasticity, with both long run and short run effects. Specifically, we suppose that

$$u_t = \begin{pmatrix} \exp(\lambda_t^D) \exp(\sigma^D(t/T)) & 0 \\ 0 & \exp(\lambda_t^N) \exp(\sigma^N(t/T)) \end{pmatrix} \begin{pmatrix} \varepsilon_t^D \\ \varepsilon_t^N \end{pmatrix}, \quad (2)$$

where:  $\varepsilon_t^D$  and  $\varepsilon_t^N$  are i.i.d. mean zero shocks from  $t$  distributions with  $v_D$  and  $v_N$  degrees of freedom, respectively, while  $\sigma^D(\cdot)$  and  $\sigma^N(\cdot)$  are unknown but smooth functions that will represent the slowly varying (long-run) scale of the process, and  $T$  is the number of observations. Suppose that for  $j = D, N$ :

$$\sigma^j(s) = \sum_{i=1}^{\infty} \theta_i^j \psi_i^j(s), \quad s \in [0, 1] \quad (3)$$

for some orthonormal basis  $\{\psi_i^j(s)\}_{i=1}^{\infty}$  with  $\int_0^1 \psi_i^j(s) ds = 0$  and

$$\int \psi_i^j(s) \psi_k^j(s) ds = \begin{cases} 1 & \text{if } i = k \\ 0 & \text{if } i \neq k. \end{cases}$$

Different from Hafner and Linton (2010), we suppose  $\sigma^D(\cdot)$  and  $\sigma^N(\cdot)$  integrate to zero to achieve identification. So we do not have to restrict the parameters of the short run dynamic processes. In the following,  $j$  is always used to denote  $D, N$  without further mentioning.

Regarding the short run dynamic part of (2), we adopt a dynamic conditional score approach, Creal, Koopman, and Lucas (2012) and Harvey and Luati (2014). Let  $e_t^j = \exp(-\sigma^j(t/T))u_t^j$ , and the conditional score function is defined as

$$m_t^j = \frac{(1 + v_j)(e_t^j)^2}{v_j \exp(2\lambda_t^j) + (e_t^j)^2} - 1, \quad v_j > 0.$$

We suppose that  $\lambda_t^D$  and  $\lambda_t^N$  are linear combinations of past values of the shocks determined by the conditional score function

$$\lambda_t^D = \omega_D(1 - \beta_D) + \beta_D \lambda_{t-1}^D + \gamma_D m_{t-1}^D + \rho_D m_t^N + \gamma_D^*(m_{t-1}^D + 1)\text{sign}(e_{t-1}^D) + \rho_D^*(m_t^N + 1)\text{sign}(e_t^N) \quad (4)$$

$$\lambda_t^N = \omega_N(1 - \beta_N) + \beta_N \lambda_{t-1}^N + \gamma_N m_{t-1}^N + \rho_N m_{t-1}^D + \gamma_N^*(m_{t-1}^N + 1)\text{sign}(e_{t-1}^N) + \rho_N^*(m_{t-1}^D + 1)\text{sign}(e_{t-1}^D). \quad (5)$$

This gives two dynamic processes for the short run scale of the overnight and intraday return. We allow the overnight shock to affect the intraday scale through the parameter  $\rho_D$ , and we allow for leverage effects through the parameters  $\gamma_D^*$ ,  $\rho_D^*$ ,  $\rho_N^*$ , and  $\gamma_N^*$ .<sup>1</sup> Let

$$\phi = (\omega_D, \beta_D, \gamma_D, \gamma_D^*, \rho_D, \rho_D^*, v_D, \omega_N, \beta_N, \gamma_N, \gamma_N^*, \rho_N, \rho_N^*, v_N)^\top \in \mathbb{R}^{14}$$

<sup>1</sup>The shock variable  $m_t^j$  can be expressed as  $m_t^j = (v_j + 1)b_t^j - 1$ , where  $b_t^j$  has a beta distribution,  $beta(1/2, v_j/2)$ .

be the finite dimensional parameters of interest.

Harvey (2013) argues that the quadratic innovations that feature in GARCH models naturally fit with the Gaussian distribution for the shock, but once one allows heavier tail distributions like the t-distribution, it is anomalous to focus on quadratic innovations, and indeed this focus leads to a lack of robustness because large shocks are fed substantially into the volatility update. He argues it is more natural to link the shock to volatility to the distribution of the rescaled return shock, which in the case of the t distribution has the advantage that large shocks are automatically down weighted, and in such a way driven by the shape of the error distribution.<sup>2</sup> The DCS model has the incidental advantage that there are analytic expressions for moments, autocorrelation functions, multi-step forecasts, and their mean squared errors. In the appendix we prove that if  $|\beta_j| < 1$ ,  $j = D, N$ , then  $e_t^j$  and  $\lambda_t^j$  are strongly stationary and  $\beta$ -mixing with exponential decay.

## 2.1 Further properties of the model

Before introducing our estimation procedure we gather together some properties of our model that are useful in applications. For example, we may obtain the dynamic intraday value at risk conditional on overnight returns and past information as follows

$$\begin{aligned} VaR_t^D(\alpha) &= \mu_t^D + s_t^D t_\alpha(v_D), \\ \mu_t^D &= E(r_t^D | \mathcal{F}_{t-1}, r_t^N) = \mu_D - \delta r_t^N - \Pi_{11} r_{t-1}^D - \Pi_{12} r_{t-1}^N \\ s_t^D &= \text{sd}(r_t^D | \mathcal{F}_{t-1}, r_t^N) = \exp(\lambda_t^D) \exp(\sigma^D(t/T)), \end{aligned}$$

where  $t_\alpha(v)$  is the  $\alpha$  quantile of the t-distribution with degrees of freedom  $v$ . Here,  $\mathcal{F}_{t-1}$  is the sigma field generated by  $\{r_{t-1}^D, r_{t-1}^N, r_{t-2}^D, r_{t-2}^N, \dots\}$  and  $\mathcal{F}_{t-1} \cup \{r_t^N\}$  is the sigma field generated by  $\{r_t^N, r_{t-1}^D, r_{t-1}^N, r_{t-2}^D, r_{t-2}^N, \dots\}$ . To obtain the value at risk given only past intraday returns say, requires some further arguments.

The conditional second order moments conditioning on different information sets are:

$$\begin{aligned} \text{var}(r_t^D | \mathcal{F}_{t-1}, r_t^N) &= \frac{v_D}{v_D - 2} \exp(2\lambda_t^D + 2\sigma^D(t/T)) \\ \text{var}(r_t^N | \mathcal{F}_{t-1}) &= \frac{v_N}{v_N - 2} \exp(2\lambda_t^N + 2\sigma^N(t/T)) \\ \text{var}(r_t^D | \mathcal{F}_{t-1}) &= \delta^2 \frac{v_N}{v_N - 2} \exp(2\lambda_t^N + 2\sigma^N(t/T)) + \frac{v_D}{v_D - 2} \exp(2\sigma^D(t/T)) E [\exp(2\lambda_t^D) | \mathcal{F}_{t-1}] \\ \text{cov}(r_t^D, r_t^N | \mathcal{F}_{t-1}) &= -\delta \frac{v_N}{v_N - 2} \exp(2\lambda_t^N + 2\sigma^N(t/T)) \\ \text{corr}(r_t^D, r_t^N | \mathcal{F}_{t-1}) &= \frac{-\delta \sqrt{\frac{v_N}{v_N - 2}} \exp(\lambda_t^N + \sigma^N(t/T))}{\sqrt{\delta^2 \frac{v_N}{v_N - 2} \exp(2\lambda_t^N + 2\sigma^N(t/T)) + \frac{v_D}{v_D - 2} \exp(2\sigma^D(t/T)) E [\exp(2\lambda_t^D) | \mathcal{F}_{t-1}]}} \\ \text{var}(r_t^D + r_t^N | \mathcal{F}_{t-1}) &= \frac{v_N(1 - \delta)^2}{v_N - 2} \exp(2\lambda_t^N + 2\sigma^N(t/T)) + \frac{v_D}{v_D - 2} \exp(2\sigma^D(t/T)) E [\exp(2\lambda_t^D) | \mathcal{F}_{t-1}]. \end{aligned}$$

---

<sup>2</sup>This type of argument is similar to the argument in limited dependent variable models such as binary choice where a linear function of covariates is connected to the observed outcome by a link function determined by the distributional assumption.

In the online appendix we show that

$$E [\exp(2\lambda_t^D)|\mathcal{F}_{t-1}] = \frac{1}{2} \exp(-2\rho_D)\Lambda_t \times {}_1F_1(1/2, 1/2 + v_N/2, (2\rho_D + 2\rho_D^*)(v_N + 1)) \\ + \frac{1}{2} \exp(-2\rho_D)\Lambda_t \times {}_1F_1(1/2, 1/2 + v_N/2, (2\rho_D - 2\rho_D^*)(v_N + 1)), \quad (6)$$

where  $\Lambda_t = \exp(2\omega_D(1 - \beta_D) + 2\beta_D\lambda_{t-1}^D + 2\gamma_D m_{t-1}^D + 2\gamma_D^*(m_{t-1}^D + 1)\text{sign}(e_{t-1}^D))$  and  ${}_1F_1$  is the Kummer's function

$${}_1F_1(\alpha, \beta, c) = 1 + \sum_{k=0}^{\infty} \left( \prod_{r=1}^{k-1} \frac{\alpha + r}{\beta + r} \right) \frac{c^k}{k!}, \quad \alpha, \beta > 0.$$

From this we obtain an explicit formula for  $\text{var}(r_t^D|\mathcal{F}_{t-1})$ ,  $\text{corr}(r_t^D, r_t^N|\mathcal{F}_{t-1})$ , and  $\text{var}(r_t^D + r_t^N|\mathcal{F}_{t-1})$ , which can be used for forecasting. In the online appendix we also give explicit expressions for the unconditional moments.

### 3 Estimation

We first outline our estimation strategy. Taking unconditional expectations of the absolute errors we have for  $j = N, D$ ,

$$E(|u_t^j|) = E(|\varepsilon_t^j|)E(\exp(\lambda_t^j)) \exp(\sigma^j(t/T)) = c^j(\phi) \times \exp(\sigma^j(t/T)),$$

where  $c^j$  is a constant that depends in a complicated way on the parameter vector  $\phi$ . Therefore, we can estimate  $\sigma^N(s), \sigma^D(s)$  as follows. Suppose that we know  $\delta, \mu, \Pi$  (in practice these can be replaced by root-T consistent estimators). Although we defined the sieve expansion of  $\sigma$ , we use kernel technology to estimate the nonparametric part. Let  $K(u)$  be a kernel with support  $[-1, 1]$  and  $h$  a bandwidth, and let  $K_h(\cdot) = K(\cdot/h)/h$ . Then let

$$\tilde{\sigma}^j(s) = \log \left( \frac{1}{T} \sum_{t=1}^T K_h(s - t/T) |u_t^j| \right) \quad (7)$$

for any  $s \in (0, 1)$ . In fact, we employ a boundary modification for  $s \in [0, h] \cup [1 - h, 1]$ , whereby  $K$  is replaced by a boundary kernel, which is a function of two arguments  $K(u, c)$ , where the parameter  $c$  controls the support of the kernel; thus left boundary kernel  $K(u, c)$  with  $c = s/h$  has support  $[-1, c]$  and satisfies  $\int_{-1}^c K(u, c)du = 1$ ,  $\int_{-1}^c uK(u, c)du = 0$ , and  $\int_{-1}^c u^2K(u, c)du < \infty$ . Similarly for the right boundary. The purpose of the boundary modification is to ensure that the bias property holds throughout  $[0, 1]$ . For identification, we rescale  $\tilde{\sigma}^j(t/T)$  as

$$\tilde{\sigma}^j(t/T) = \tilde{\sigma}^j(t/T) - \frac{1}{T} \sum_{t=1}^T \tilde{\sigma}^j(t/T). \quad (8)$$

Note that  $\tilde{\sigma}^j(u)$  can be written as  $\tilde{\sigma}^j(u) = \sum_{i=1}^{\infty} \tilde{\theta}_i^j \psi_i^j(s)$  for some coefficients  $\tilde{\theta}_i^j$  determined uniquely by the sample value. For notational convenience we will represent  $\tilde{\sigma}^j$  in terms of  $\{\tilde{\theta}_i^j\}_{i=1}^{\infty}$  or just  $\tilde{\theta}$  for shorthand.



Let  $\tilde{e}_t^N = \exp(-\tilde{\sigma}^N(t/T))u_t^N$  and  $\tilde{e}_t^D = \exp(-\tilde{\sigma}^D(t/T))u_t^D$ , and let  $\tilde{\theta}$  denote  $\{\tilde{\sigma}^j(s), s \in [0, 1], j = N, D\}$ . Define the global log-likelihood function for  $\phi$  (apart from an unnecessary constant and conditional on the estimated values of  $\theta$ )

$$l_T(\phi; \tilde{\theta}) = \frac{1}{T} \sum_{t=1}^T \left( l_t^N(\phi; \tilde{\theta}) + l_t^D(\phi; \tilde{\theta}) \right),$$

$$l_t^j(\phi; \tilde{\theta}) = -\lambda_t^j(\phi; \tilde{\theta}) - \frac{v_j + 1}{2} \ln \left( 1 + \frac{(\tilde{e}_t^j)^2}{v_j \exp(2\lambda_t^j(\phi; \tilde{\theta}))} \right) + \ln \Gamma \left( \frac{v_j + 1}{2} \right) - \frac{1}{2} \ln v_j - \ln \Gamma \left( \frac{v_j}{2} \right),$$
(9)

where  $\lambda_t^j(\phi; \tilde{\theta})$  are defined in (4) and (5). For practical purposes,  $\lambda_{1|0}^j$  may be set equal to the unconditional mean,  $\lambda_{1|0}^j = \omega_j$ . We estimate  $\phi$  by maximizing  $l_T(\phi; \tilde{\theta})$  with respect to  $\phi$ . Let  $\tilde{\phi}$  denote these estimates.

Given estimates of  $\phi$  and the preliminary estimates of  $\sigma^D(\cdot), \sigma^N(\cdot)$ , we calculate

$$\tilde{\eta}_t^N = \exp(-\tilde{\lambda}_t^N)u_t^N; \quad \tilde{\eta}_t^D = \exp(-\tilde{\lambda}_t^D)u_t^D,$$

where  $\tilde{\lambda}_t^j = \lambda_t^j(\tilde{\phi}; \tilde{\theta})$ . We then update the estimates of  $\sigma^D(\cdot), \sigma^N(\cdot)$  using the local likelihood function in Severini and Wong (1992) given  $\tilde{\eta}_t^j$  and  $\tilde{v}_j$ , i.e., we minimize the objective function

$$\tilde{L}_T^j(\gamma; \tilde{\lambda}^j, s) = \frac{1}{T} \sum_{t=1}^T K_h(s - t/T) \left[ \gamma + \frac{\tilde{v}_j + 1}{2} \ln \left( 1 + \frac{(\tilde{\eta}_t^j \exp(-\gamma))^2}{\tilde{v}_j} \right) \right]$$
(10)

with respect to  $\gamma \in \mathbb{R}$ , for  $j = D, N$  separately, where  $\tilde{\lambda}^j = (\tilde{\lambda}_1^j, \dots, \tilde{\lambda}_T^j)^\top$ . Likewise here we use a boundary kernel for  $s \in [0, h] \cup [1 - h, 1]$ . In practice we use Newton-Raphson iterations making use of the derivatives of the objective functions, which are given in (23).

To summarize, the estimation algorithm is as follows.

### Algorithm

STEP 1. Estimate  $\delta, \mu^j, \Pi$  by least squares and  $\tilde{\sigma}^j(u), u \in [0, 1], j = N, D$  from (7) and (8)

STEP 2. Estimate  $\phi$  by optimizing  $l_T(\phi; \tilde{\theta})$  with respect to  $\phi$  (by Newton-Raphson) to give  $\tilde{\phi}$ .

STEP 3. Given the initial estimates  $\tilde{\theta}$  and  $\tilde{\phi}$ , we replace  $\lambda_t^j$  with  $\tilde{\lambda}_t^j = \lambda_t^j(\tilde{\phi}; \tilde{\theta})$ . Then let  $\hat{\sigma}^j(s)$  optimize  $\tilde{L}_T^j(\sigma^j(s); \tilde{\lambda}, s)$  with respect to  $\sigma^j(s)$ . For identification, we rescale  $\hat{\sigma}^j(t/T) = \hat{\sigma}^j(t/T) - \frac{1}{T} \sum_{t=1}^T \hat{\sigma}^j(t/T)$ .

STEP 4. Repeat Steps 2-3 to update  $\hat{\theta}$  and  $\hat{\phi}$  until convergence. We define convergence in terms of the distance measure

$$\Delta_r = \sum_{j=D, N} \int [\hat{\sigma}^{j, [r]}(u) - \hat{\sigma}^{j, [r-1]}(u)]^2 du + \left( \hat{\phi}^{[r]} - \hat{\phi}^{[r-1]} \right)^\top \left( \hat{\phi}^{[r]} - \hat{\phi}^{[r-1]} \right),$$

that is, we stop when  $\Delta_r \leq \epsilon$  for some prespecified small  $\epsilon$ .

## 4 Large Sample Properties of Estimators

In this section we give the asymptotic distribution theory of the estimators considered above. The proofs of all results are given in the Appendix. Let  $h_t^j = \lambda_t^j + \sigma^j(t/T)$ , and let:

$$A_t = \begin{bmatrix} 1 & a_t^{DN} \\ 0 & 1 \end{bmatrix}, \quad B_{t-1} = \begin{bmatrix} (\beta_D + a_{t-1}^{DD}) & 0 \\ a_{t-1}^{ND} & (\beta_N + a_{t-1}^{NN}) \end{bmatrix},$$

$$a_{t-1}^{DD} = -2(\gamma_D + \gamma_D^* \text{sign}(u_{t-1}^D)) (v_D + 1) b_{t-1}^D (1 - b_{t-1}^D)$$

$$a_t^{DN} = -2(\rho_D + \rho_D^* \text{sign}(u_t^N)) (v_N + 1) b_t^N (1 - b_t^N)$$

$$a_{t-1}^{NN} = -2(\gamma_N + \gamma_N^* \text{sign}(u_{t-1}^N)) (v_N + 1) b_{t-1}^N (1 - b_{t-1}^N)$$

$$a_{t-1}^{ND} = -2(\rho_N + \rho_N^* \text{sign}(u_{t-1}^D)) (v_D + 1) b_{t-1}^D (1 - b_{t-1}^D)$$

$$b_t^D = \frac{(e_t^D)^2}{v_D \exp(2\lambda_t^D) + (e_t^D)^2} \quad ; \quad b_t^N = \frac{(e_t^N)^2}{v_D \exp(2\lambda_t^N) + (e_t^N)^2}.$$

We use the maximum row sum matrix norm,  $\|\cdot\|_\infty$ , defined by

$$\|A\|_\infty = \max_{1 \leq i \leq n} \sum_{j=1}^n |a_{ij}|.$$

### Assumptions A

1.  $\|E(A_t \otimes A_t)\|_\infty < \infty$ ,  $\|EB_t EA_t\|_\infty < 1$ ,  $\|E(B_{t-1} A_{t-1} \otimes B_{t-1} A_{t-1})\|_\infty < \|EB_t EA_t\|_\infty$ , and the top-Lyapunov exponent of the sequence of  $A_t B_{t-1}$  is strictly negative. The top Lyapunov exponent is defined as Theorem 4.26 of Douc, Moulines, and Stoffer (2014).
2.  $0 \leq |\beta_j| < 1$ .
3.  $h_t^j$  starts from infinite past. The parameter  $\phi_0$  is an interior point of  $\Phi \subset \mathbb{R}^{14}$ , where  $\Phi$  is the parameter space of  $\phi_0$ .
4. The functions  $\sigma^j$  are twice continuously differentiable on  $[0, 1]$ ,  $j = D, N$ .
5.  $E|u_t^j|^{2+\delta} < \infty$  for some  $\delta > 0$ ,  $j = D, N$ .
6. The kernel function  $K$  is bounded, symmetric about zero with compact support, that is  $K(v) = 0$  for all  $|v| > C_1$  with some  $C_1 < \infty$ . Moreover, it is Lipschitz, that is  $|K(v) - K(v')| \leq L|v - v'|$  for some  $L < \infty$  and all  $v, v' \in \mathbb{R}$ . Denote  $\|K\|_2^2 = \int K(s)^2 ds$ .
7.  $h(T) \rightarrow 0$ , as  $T \rightarrow \infty$  such that  $T^{1/2-\delta} h \rightarrow \infty$  for some small  $\delta > 0$ .

Assumptions A3-A7 are used to derive the properties of  $\tilde{\sigma}^j(s)$ , in line with Vogt and Linton (2014) and Vogt (2012). But we only require that  $E|u_t^j|^{2+\delta} < \infty$ , since we use  $\tilde{\sigma}^j(s) = \log\left(\frac{1}{T} \sum_{t=1}^T K_h(s - t/T) |u_t^j|\right)$ . This is in line with the fact that the fourth-order moment of overnight

returns often does not exist. The mixing condition in Vogt and Linton (2014) is replaced by Assumption A2, because of our tight model structure. Assumption A1 is required to derive the stationarity of score functions, where  $\|E(A_t \otimes A_t)\|_\infty < \infty$  can be verified easily, since  $b_t^N$  in  $A_t$  follows a beta distribution.

The first result gives the uniform convergence rate of the initial estimator  $\tilde{\sigma}^j(s)$ . The proof mainly follows Theorem 3 in Vogt and Linton (2014).

**Lemma 1** *Suppose that Assumptions A2-A7 hold. Then,*

$$\sup_{s \in [0,1]} |\tilde{\sigma}^j(s) - \sigma_0^j(s)| = O_p \left( h^2 + \sqrt{\frac{\log T}{Th}} \right).$$

We next present an important orthogonality condition that allows us to establish a simple theory for the parametric component.

**Theorem 1** *Suppose that Assumptions A1-A4 hold. Then, for each  $k$  and  $i$ , for  $k \in \{1, \dots, \infty\}$  and  $i \in \{1, \dots, 14\}$ , we have*

$$\frac{1}{T} \sum_{t=1}^T E \left[ \frac{\partial l_t(\phi_0; \theta_0)}{\partial \theta_k} \frac{\partial l_t(\phi_0; \theta_0)}{\partial \phi_i} \right] = O\left(\frac{1}{T}\right).$$

The proof of Theorem 1 is provided in Appendix A. Theorem 1 implies that the score functions with respect to  $\theta$  and  $\phi$  are asymptotic orthogonal. The intuition behind is that  $\sigma^j$  is a function of a deterministic variable,  $t/T$ , while  $\lambda_t^j$  is a stationary process independent of time  $t$ . The cross product of their score functions can be somehow separated. The asymptotic orthogonality implies the particular asymptotic property of  $\tilde{\phi}$  and  $\hat{\phi}$  in Theorem 2 follows.

Let

$$I(\phi_0) = E \left[ \frac{\partial l_t(\phi_0; \theta_0)}{\partial \phi} \frac{\partial l_t(\phi_0; \theta_0)}{\partial \phi^\top} \right].$$

**Theorem 2** *Suppose that Assumptions A1-A7 hold. Then*

$$\sqrt{T} (\tilde{\phi} - \phi_0) = \sqrt{T} (\hat{\phi} - \phi_0) + o_P(1) \implies N(0, I(\phi_0)^{-1})$$

**Theorem 3** *Suppose that Assumptions A1-A7 hold. Then for  $u \in (0, 1)$*

$$\sqrt{Th} \begin{pmatrix} \hat{\sigma}^D(u) & -\sigma_0^D(u) \\ \hat{\sigma}^N(u) & -\sigma_0^N(u) \end{pmatrix} \implies N \left( 0, \|K\|_2^2 \begin{pmatrix} \frac{(v_D+3)}{2v_D} & 0 \\ 0 & \frac{(v_N+3)}{2v_N} \end{pmatrix} \right). \quad (11)$$

Theorem 2 shows that  $\tilde{\phi}$  and  $\hat{\phi}$  have the same asymptotic property. Together with Theorem 3, we obtain the consistency and asymptotic normality of  $\tilde{\phi}$ ,  $\hat{\phi}$  and  $\hat{\sigma}^j(s)$ . The form of the limiting variance in (11) is consistent with the known Fisher information for the estimation of scale parameter of a t-distribution with known location and degrees of freedom (these quantities are estimated at a faster rate), which makes this part of the procedure also efficient in the sense considered in Tibshirani (1984).

The proofs of Theorem 2 and 3 are provided in Appendix A. The information matrix,  $I(\phi_0)$ , can be computed explicitly. We can conduct inference with Theorem 2 and Theorem 3 using plug-in estimates of the unknown quantities.

The kernel estimator  $\tilde{\sigma}(s)$  in the initial step can be replaced by the sieve estimator of  $\theta$ . It is easy to show that  $\tilde{\theta}$  converges to  $\theta$  paralleling Lemma 1, and Theorem 1, 2 and 3 remain the same.

## 5 A Multivariate model

We next consider an extension to a multivariate model. We keep a similar structure to the univariate model except that we allow the slowly moving component to be matrix valued. Suppose that

$$r_t = \begin{pmatrix} r_t^D \\ r_t^N \end{pmatrix}; \quad \mu = \begin{pmatrix} \mu_D \\ \mu_N \end{pmatrix},$$

where  $r_t^D, r_t^N$  are  $n \times 1$  vectors containing all the intraday and overnight returns respectively, and let

$$\mathbf{D}r_t = \mu + \Pi r_{t-1} + u_t,$$

where  $u_t^D$  and  $u_t^N$  are mean zero shocks, while

$$\mathbf{D} = \begin{pmatrix} I_n & \text{diag}(\Delta) \\ 0 & I_n \end{pmatrix}; \quad \Pi = \begin{pmatrix} \text{diag}(\Pi_{11}) & \text{diag}(\Pi_{12}) \\ \text{diag}(\Pi_{21}) & \text{diag}(\Pi_{22}) \end{pmatrix},$$

and  $\Delta, \Pi_{11}, \Pi_{12}, \Pi_{21},$  and  $\Pi_{22}$  are  $n \times 1$  vectors.

Alternatively, to investigate the unsystematic risk, we can specify  $r_t$  using a capital asset pricing model (CAPM)

$$r_{it}^D = a_i^D + \beta_i^{DD} r_{mt}^D + \beta_i^{DN} r_{mt}^N + u_{it}^D \quad (12)$$

$$r_{it}^N = a_i^N + \beta_i^{NN} r_{mt}^N + \beta_i^{ND} r_{mt-1}^D + u_{it}^N, \quad (13)$$

where  $r_{mt}^D$  and  $r_{mt}^N$  are the market returns and  $r_{it}^D$  and  $r_{it}^N$  are the returns of stock  $i$ .

For the variance equation, we suppose that

$$u_t = \begin{pmatrix} \Sigma^D(\frac{t}{T})^{\frac{1}{2}} \text{diag}(\exp(\lambda_t^D)) & 0 \\ 0 & \Sigma^N(\frac{t}{T})^{\frac{1}{2}} \text{diag}(\exp(\lambda_t^N)) \end{pmatrix} \begin{pmatrix} \varepsilon_t^D \\ \varepsilon_t^N \end{pmatrix},$$

where:  $\varepsilon_{it}^j$  is i.i.d. shocks from univariate  $t$  distributions with  $v_{ij}$  degrees of freedom, while  $\lambda_t^j$  are  $n \times 1$  vectors.

We assume that  $\Sigma^D(\cdot)$  and  $\Sigma^N(\cdot)$  are smooth matrix functions but are otherwise unknown. We can write these covariance matrices in terms of the correlation matrices and the variances as follows

$$\Sigma^j(s) = \text{diag}(\exp(\sigma^j(s))) R^j(s) \text{diag}(\exp(\sigma^j(s))), \quad j = D, N, \quad (14)$$

with  $\text{diag}(\exp(\sigma^j(s)))$  being the volatility matrix and  $R^j(s)$  being the correlation matrix with unit diagonal elements. For identification, we still assume  $\int_0^1 \sigma_i^j(s) ds = 0$ , for  $i \in \{1, \dots, n\}$ .

As with the univariate model, define  $e_t^j = \text{diag}(\exp(\lambda_t^j)) \varepsilon_t^j$ , and suppose that

$$m_{it}^j = \frac{(1 + v_{ij})(e_{it}^j)^2}{v_{ij} \exp(2\lambda_{it}^j) + (e_{it}^j)^2} - 1,$$

$$\begin{aligned} \lambda_{it}^D &= \omega_{iD}(1 - \beta_{iD}) + \beta_{iD}\lambda_{it-1}^D + \gamma_{iD}m_{it-1}^D + \rho_{iD}m_{it}^N \\ &\quad + \gamma_{iD}^*(m_{it-1}^D + 1)\text{sign}(u_{it-1}^D) + \rho_{iD}^*(m_{it}^N + 1)\text{sign}(u_{it}^N), \\ \lambda_{it}^N &= \omega_{iN}(1 - \beta_{iN}) + \beta_{iN}\lambda_{it-1}^N + \gamma_{iN}m_{it-1}^N + \rho_{iN}m_{it-1}^D \\ &\quad + \rho_{iN}^*(m_{it-1}^D + 1)\text{sign}(u_{it-1}^D) + \gamma_{iN}^*(m_{it-1}^N + 1)\text{sign}(u_{it-1}^N). \end{aligned}$$

For each  $i$  define the parameter vector  $\phi_i = (\omega_{iD}, \beta_{iD}, \gamma_{iD}, \gamma_{iD}^*, \rho_{iD}, \rho_{iD}^*, v_{iD}, \omega_{iN}, \beta_{iN}, \gamma_{iN}, \gamma_{iN}^*, \rho_{iN}, \rho_{iN}^*, v_{iN})^\top \in \mathbb{R}^{14}$  and let  $\phi = (\phi_1^\top, \dots, \phi_n^\top)^\top$  denote all the dynamic parameters.

Define  $l_i$  the vector with the  $i^{\text{th}}$  element 1 and all others 0, so that  $\varepsilon_{it}^j = l_i^\top \text{diag}(\exp(-\lambda_t^j)) (\Sigma^j(\frac{t}{T}))^{-1/2} u_t^j$ . The normalized global log-likelihood function is

$$l_T(\phi, \Sigma(\cdot)) = \frac{1}{T} \sum_{t=1}^T (l_t^N + l_t^D)$$

$$\begin{aligned} l_t^j(\phi, \Sigma(\cdot)) &= \sum_{i=1}^n \left( - \prod_{i=1}^n \lambda_{it}^j - \frac{v_{ij} + 1}{2} \ln \left( 1 + \frac{(l_i^\top \text{diag}(\exp(-\lambda_t^j - \sigma^j(t/T))) (\Sigma^j(\frac{t}{T}))^{-1/2} u_t^j)^2}{v_{ij}} \right) \right) \\ &\quad - \frac{1}{2} \log \left| \Sigma^j \left( \frac{t}{T} \right) \right| + \sum_{i=1}^n \left( \ln \Gamma \left( \frac{v_{ij} + 1}{2} \right) - \frac{1}{2} \ln v_{ij} - \ln \Gamma \left( \frac{v_{ij}}{2} \right) \right). \end{aligned}$$

We first define an initial estimator for  $\Sigma^j(\frac{t}{T})$  and then obtain an estimator of  $\phi$ , and then we update them. Suppose that we know  $\Delta, \Pi$  and  $\mu$ . To give an estimator of  $\Sigma^j(\frac{t}{T})$  robust to heavy tails, we estimate the volatility parameter

$$\tilde{\sigma}_i^j(s) = \log \left( \frac{1}{T} \sum_{t=1}^T K_h(s - t/T) |u_{it}^j| \right). \quad (15)$$

For identification, we rescale  $\tilde{\sigma}^j(t/T)$  as

$$\tilde{\sigma}_i^j(t/T) = \tilde{\sigma}_i^j(t/T) - \frac{1}{T} \sum_{t=1}^T \tilde{\sigma}_i^j(t/T). \quad (16)$$

Supposing that the heavy tails issue is less severe in the estimation of correlation, which seems reasonable; we estimate the correlation parameter by standard procedures

$$\tilde{R}_{ik}^j(s) = \frac{\sum_{t=1}^T K_h(s - t/T) u_{ik}^j u_{ik}^j}{\sqrt{\sum_{t=1}^T K_h(s - \frac{t}{T}) u_{it}^j u_{it}^j \sum_{t=1}^T K_h(s - \frac{t}{T}) u_{kt}^j u_{kt}^j}} \quad (17)$$

for  $s \in (0, 1)$ , and boundary modification as previously detailed.

Alternatively, we can use a robust correlation estimator. Omitting the superscript  $j = D, N$  here, we first compute the pairwise Kendall tau

$$\hat{\tau}_{k,l}(s) = \frac{\sum_{i=1}^T \sum_{j=i}^{T-1} K_h(s - \frac{i}{T}) K_h(s - \frac{j}{T}) (I \{(u_{i,k} - u_{j,k})(u_{i,l} - u_{j,l}) > 0\} - I \{(u_{i,k} - u_{j,k})(u_{i,l} - u_{j,l}) < 0\})}{\sum_{i=1}^T \sum_{j=i}^{T-1} K_h(s - \frac{i}{T}) K_h(s - \frac{j}{T}) (I \{(u_{i,k} - u_{j,k})(u_{i,l} - u_{j,l}) > 0\} + I \{(u_{i,k} - u_{j,k})(u_{i,l} - u_{j,l}) < 0\})}. \quad (18)$$

Then applying the relation between Kendall tau and the linear correlation coefficient for the elliptical distribution suggested by Linskog, Mcneil, and Schmock (2003) and Battay and Linton (2014), we obtain the robust linear correlation estimator,

$$\hat{\rho}_{k,l}(s) = \sin\left(\frac{\pi}{2} \hat{\tau}_{k,l}(s)\right).$$

In some cases, the matrix of pairwise correlations must be adjusted to ensure that the resulting matrix is positive definite.

We have

$$\tilde{\Sigma}^j(s) = \text{diag}(\exp(\tilde{\sigma}^j(s))) \tilde{R}^j(s) \text{diag}(\exp(\tilde{\sigma}^j(s))), \quad j = D, N. \quad (19)$$

Letting  $\tilde{e}_t^j = \tilde{\Sigma}^j(\frac{t}{T})^{-1/2} u_t^j$ , we obtain  $\tilde{\phi}_i$  by maximizing the univariate log-likelihood function of  $\tilde{e}_{it}^j$  in (9) for each  $i = 1, \dots, n$ . To update the estimator for each  $\Sigma^j(\frac{t}{T})$ , denote  $\Theta = (\Sigma^j)^{-1/2}$ . We first obtain  $\hat{\Theta}$  with the local likelihood function given  $\tilde{\lambda}_t^j$  and  $\tilde{v}_j$ , i.e., maximize the local objective function

$$L_T^j(\Theta; \tilde{\lambda}, s) = \frac{1}{T} \sum_{t=1}^T K_h(s - t/T) \left[ \log |\Theta| - \sum_{i=1}^n \left( \frac{\tilde{v}_{ij} + 1}{2} \ln \left( 1 + \frac{(t_i^\top \text{diag}(\exp(-\tilde{\lambda}_t^j)) \Theta u_t^j)^2}{\tilde{v}_{ij}} \right) \right) \right]$$

with respect to  $\text{vech}(\Theta)$ , and let  $\hat{\Sigma}^j(t/T) = \hat{\Theta}^{-2}$ . The derivatives of the objective function are given in (33) and (34) in Appendix B.

To summarize, the estimation algorithm is as follows.

### Algorithm

STEP 1. Estimate  $\mathbb{D}, \mu, \Pi$  (or the CAPM structure) by least squares,  $\tilde{\sigma}^j(u)$ ,  $u \in [0, 1]$ ,  $j = N, D$  from (15) and (16), and  $\tilde{R}_{ik}^j$  from (17).

STEP 2. Let  $\tilde{e}_t^j = \tilde{\Sigma}^j(\frac{t}{T})^{-1/2} u_t^j$ . We obtain  $\tilde{\phi}_i$  by maximizing the univariate log-likelihood function of  $\tilde{e}_{it}^j$  in (9) for each  $i = 1, \dots, n$ .

STEP 3. We replace  $\lambda_t^j$  with  $\tilde{\lambda}_t^j = \lambda_t^j(\tilde{\phi}; \tilde{\theta})$ . For each  $\Sigma_j(\frac{t}{T})$ , denote  $\Theta^j = (\Sigma^j)^{-1/2}$ . Then obtain  $\hat{\Theta}$  with the local likelihood function given  $\tilde{\lambda}_t^j$  and  $\tilde{v}_j$ , with the Newton-Raphson iterations making use of the derivatives of the objective functions.

STEP 4. Repeat Steps 2-3 to update  $\hat{\phi}$  and  $\hat{\Sigma}^j(\frac{t}{T})$  until convergence.

Our multivariate model can be considered as a GARCH model with a slowly moving correlation matrix. Assuming diagonality on the short run component  $\lambda_t^j$  enables us to estimate the model easily and rapidly. In particular, the computation time of the initial estimator is only of order  $n$ , with  $n$  being the number of assets considered; it is thus feasible even with quite large  $n$ . The extension to models with non-diagonal short run components is possible, but only feasible with small  $n$ .

Blanc, Chicheportiche, and Bouchaud (2014) impose a pooling assumption in their modelling, which translates here to the restriction that  $\phi_i = \phi_1$  for all  $i = 1, \dots, n$ . This improves efficiency when the restriction is true. We can test the restriction by a standard Wald procedure or Likelihood ratio statistic. In the application we find these pooling restrictions are strongly rejected by the data.

## 6 Application to Dow Jones stocks

### 6.1 Descriptive statistics

We investigate 28 components of the Dow Jones industrial average index over the period 1991-11-12 to 2016-04-13. The 28 stocks are: MMM, AXP, AAPL.O, BA, CAT, CVX, CSCO.O, KO, DD, XOM, GE, HD, IBM, INTC.O, JNJ, JPM, MCD, MRK, MSFT.O, NKE, PFE, PG, TRV, UNH, UTX, VZ, WMT, DIS. The stocks GS and V are excluded since they did not officially go public until 1999 and 2008, respectively. The data is obtained from Thompson Reuters Eikon, and has been adjusted for corporate actions. We define overnight returns as the log price change between the close of one trading day to the opening of the next trading day. We do not incorporate weekend and holiday effects into our model, since they are not the focus of this paper, and our model is already rather complicated in terms of both model specification and estimation. In addition, although the weekend effect is documented by studies such as French (1980) and Rogalski (1984), and further supported by Cho, Linton, and Whang (2007) with a stochastic dominance approach, many studies suggest the disappearance of the weekend effect, including Mehdian and Perry (2001) and Steeley (2001). In particular, Sullivan, Timmermann, and White (2001) claim that calendar effects are the result of data-snooping.

Many studies find significantly higher overnight returns, for example, Cooper, Cliff, and Gulen (2008) and Berkman, Koch, Tuttle, and Zhang (2012). Cooper, Cliff, and Gulen (2008) even suggest the US equity premium is solely due to overnight returns during the research period from 1993 to 2006. To investigate this overnight anomaly, Figure B.1 in the online appendix plots the cumulative returns for these 28 stocks. For AAPL, CAT, CSCO, HD, INTC, JPM, PFE, UTX and WMT, positive cumulative returns mainly stem from overnight periods, while for MMM, KO, DD, XOM, JNJ, MCD, MRK, NKE, PG, TRV, VZ and DIS, positive cumulative returns mainly come from intraday periods. There is no clear dominance of positive overnight returns from these Dow Jones stocks.

Berkman, Koch, Tuttle, and Zhang (2012) find significant positive mean overnight returns of +10 basis points (bp) per day, along with -7 bp for intraday returns from 3000 largest U.S. stocks. Following their procedure, we first compute the cross-sectional mean (or median) returns for each

day, then compute the time series mean and the standard deviation of these cross-sectional mean (or median) values. The mean intraday return is 2.18 bp with standard error 1.22 bp, while the mean overnight return is 1.60 bp with standard error 0.70 bp. The difference between overnight and intraday mean is not statistically significant.

Table B.1 in the online appendix provides summary statistics for intraday and overnight returns. Compared with intraday returns, overnight returns exhibit more negative skewness and leptokurtosis. More specifically, 10 of these 28 stocks exhibit negative intraday skewness, while 26 of 28 stocks have negative overnight skewness. The largest sample kurtosis for overnight returns is extremely high, suggesting non-existence of the population kurtosis.

## 6.2 Results of the univariate model

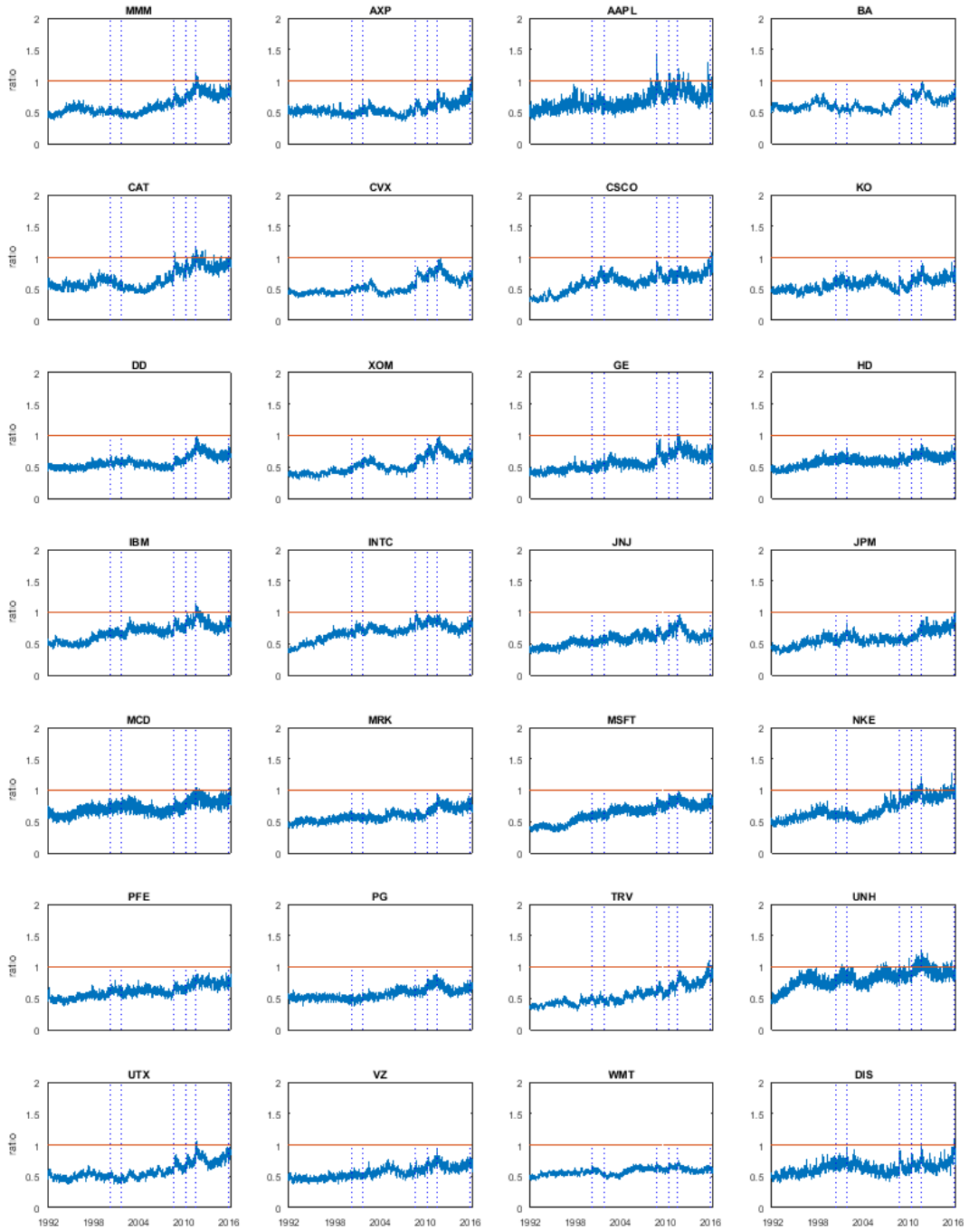
Table B.2 in the online appendix reports the estimates and their robust standard errors in the mean equations. We multiply returns by 100 to give more readable coefficients.  $\Pi_{ij}$  refers to the element of the  $i$ th row  $j$ th column in the coefficient matrix  $\Pi$ . For the prediction of intraday returns, 12 of the 28 stocks have significant  $\Pi_{11}$  that are all negative, and 7 of 28 stocks have significant  $\delta$  which are all positive. This suggests that both overnight and intraday returns tend to have a negative effect in their subsequent intraday return. However, we do not find clear patterns for predicting overnight returns. The constant terms,  $\mu_D$  and  $\mu_N$ , are positive for most Dow Jones stocks.

Table B.3 in the online appendix gives the estimates of dynamic parameters. Parameters  $\beta_D$  and  $\beta_N$  are significantly different from 1, and  $\rho_D$ ,  $\gamma_D$ ,  $\rho_N$  and  $\gamma_N$  are positive and significant. In addition, we find significant leverage effects, with negative and significant  $\rho_D^*$ ,  $\gamma_D^*$ ,  $\rho_N^*$  and  $\gamma_N^*$ , suggesting higher volatility after negative returns.

We are also concerned about the difference between overnight and intraday parameters. Table B.4 in the online appendix reports Wald tests with the null hypothesis that the intraday and overnight parameters are equal within each stock. The parameter  $\omega_D$ , determining the unconditional short-run scale, is significantly larger than  $\omega_N$ . The overnight degree-of-freedom parameter is around 3, significantly smaller than the intraday counterpart at approximately 8. Both are in line with the descriptive statistics in Table B.1 in the online appendix and previous studies that suggest overnight returns are more leptokurtic but less volatile. With other pairs of intraday and overnight parameters,  $\beta_j$ ,  $\gamma$ ,  $\rho_j$ ,  $\gamma_j^*$ ,  $\rho_j^*$ , the null hypothesis is seldom rejected. However, the joint null hypothesis,  $(\beta_D, \gamma, \rho_D, \gamma_D^*, \rho_D^*) = (\beta_N, \gamma, \rho_N, \gamma_N^*, \rho_N^*)$ , is rejected by many stocks. It is noteworthy that the null hypothesis  $H_0 : \gamma_N = \rho_D$  is not rejected by our data, which is inconsistent with Blanc, Chicheportiche, and Bouchaud (2014). They suggest that past overnight returns weakly affect future intraday volatilities, except for the very next one, but substantially impact future overnight volatilities. This inconsistency is probably because the dynamic conditional score model shrinks the impact of extreme overnight observations. After this shrinkage, overnight innovations become closer to the intraday innovations.

Many paper have argued that the introduction of high frequency trading in the period post 2005 has led to an increase in volatility. Figure A.1 in Appendix C plots the intraday and overnight





This figure shows the dynamic ratio of overnight to intraday volatility, based on the univariate coupled component model with one subplot for each stock. The five dashed vertical lines from left to right represent the dates: 10 March 2000(dot-com bubble), 11 September 2001(the September 11 attacks), 16 September 2008(financial crisis), 6 May 2010 (flash crash) and 1 August 2011 (August 2011 stock markets fall), respectively. Intraday and overnight volatiles are defined as  $\sqrt{\frac{\nu_j}{\nu_j - 2} \exp(2\lambda_t^j + 2\sigma^j(\frac{t}{T}))}$ , for  $j = D, N$ .

Figure 1: Ratios of overnight to intraday volatility: univariate model

volatilities,  $\sqrt{\frac{\nu_j}{\nu_j-2} \exp(2\lambda_t^j + 2\sigma^j(\frac{t}{T}))}$ , for  $j = D, N$ . The intraday volatility (red lines) significantly dominated than the overnight volatility (black lines) in the first half period, but this domination has disappeared gradually, especially after the 2008 financial crisis. We can also notice that the intraday volatilities after 2005 are in general smaller than that before 2005, except the financial crisis period. This is contrary to what often argued about high frequency trading increasing volatilities. To further investigate this, we plot the ratios of overnight to intraday volatility in Figure 1. The stocks all exhibit upward trends over the 24-year period considered here, and many of them experienced peaks around August 2011, corresponding to the August 2011 stock markets fall. As a robustness check, we investigate the ratio of VIX to the Rogers and Satchell (1991) volatility (RS volatility). The idea is that the VIX measures one-month ahead volatility, total volatility including presumably intraday and overnight, whereas the aggregated RS volatility only includes intraday volatility. Therefore, the ratio reflects the variability of intraday to overnight to some extent, although it is quite noisy. Figure B.4 in the online appendix presents: (1) the RS volatility on daily Dow Jones stocks,  $V_{rs,t}$ ; (2) one-month ahead RS volatility,  $\sqrt{\sum_{i=1}^{22} V_{rs,t+i}^2}$ ; (3) VIX; and (4) the ratio of VIX to the one month ahead RS volatility. The reported RS volatility is the average RS volatility across the 28 stocks. The ratio of VIX to the one month ahead RS volatility still shows an upward trend during the sample period.

Figure B.2 in the online appendix depicts the long-run intraday and overnight components,  $\sigma^D(t/T)$  and  $\sigma^N(t/T)$ , and their 95% point-wise confidence intervals. Most stocks arrived at their first peaks around 10 March 2000, corresponding to the Dot-com bubble event, while some arrived at around September 2011, right after the 9-11 attacks. The intraday components reached their second peaks during the financial crisis in September 2008, while overnight components continued to rise and reaching their highest points during the 2010 Flash crash. Roughly speaking, the intraday components were larger than the overnight ones before the first peaks, but smaller after the financial crisis of September 2008. However, it is imperative to remember that the long-run components are constructed with rescaling  $\int_0^1 \sigma(s) ds = 0$ . In general, the intraday volatility are still larger.

We test the constancy of the ratio of long run overnight to intraday volatility through the null hypothesis

$$H_0 : \exp(\sigma_0^N(\cdot)) = \rho \exp(\sigma_0^D(\cdot)) \quad (20)$$

for some  $\rho \in \mathbb{R}_+$  versus the general alternative. By Theorem 3 and the delta method,  $\exp(\hat{\sigma}^D(s))$  and  $\exp(\hat{\sigma}^N(s))$  converge jointly to a normal distribution, and are asymptotically mutually independent. It follows that for  $s \in (0, 1)$ ,

$$\begin{aligned} \hat{\tau}(s) &= \sqrt{Th} (\exp(\hat{\sigma}^N(s)) - \hat{\rho} \exp(\hat{\sigma}^D(s))) \implies N(0, \rho^2 V_s^D + V_s^N) \\ \hat{\rho} &= \frac{1}{T} \sum_{t=1}^T \frac{\exp(\hat{\sigma}^N(t/T))}{\exp(\hat{\sigma}^D(t/T))}, \end{aligned}$$

where  $V_s^j = \exp(2\sigma_0^j(s)) \frac{(v_j+3)}{2v_j} \|K\|_2^2$ , for  $j = D, N$ .

Figure B.3 in the online appendix displays the test statistics  $\hat{\tau}(s)$  and the 95 % point-wise confidence intervals for  $s \in [0, 1]$ . Consistent with the results above, the equal ratio null hypothesis is mostly rejected before the first peaks occurred (in 2000) and after the second peaks (in 2010).

All these evidences indicate that the intraday volatility has decreased in importance during the last 24 years relative to the overnight volatility for the Dow Jones stocks.

We also want to compare our coupled component GARCH model with its one component version for the open to close return to assess the improvement in volatility forecast from using overnight returns. We construct 10 rolling windows, each containing 5652 in-sample and 50 out-of-sample observations. In each rolling window, the parameters in the short-run variances are estimated with the in-sample data once and stay the same during the one-step out-of-sample forecast. In the one-step ahead forecast of the long-run covariance matrices, the single-side weight function is used. For instance, to forecast the long-run covariance matrix of period  $\tau$  ( $s = \tau/T$ ), we set the two-side weight function  $K_h(s - t/T) = 0$ , for  $t \geq \tau$ , and then rescale  $K_h(s - t/T)$  to obtain a sum of 1. Table B.5 in the online appendix reports Giacomini and White (2006) model pair-wise comparison tests with the out-of-sample quasi Gaussian and student t log-likelihood loss functions. For most stocks, the coupled component GARCH model dominates the one component model. Some dominances are statistically significant. We omit the comparison for overnight variance forecast between the one component and the coupled component model, since it is not plausible to estimate a GARCH model with overnight returns alone.

Ljung-Box tests on the absolute and squared standardized residuals are used to verify whether the coupled component GARCH model is adequate to capture the heteroskedasticity, shown in Table B.6 in the online appendix. With the absolute form, strong heteroskedasticity exists in both intraday and overnight returns, but disappears in the standardized residuals, implying that our model captures the heteroskedasticity well. On the other hand, we are sometimes unable to detect the heteroskedasticity in overnight returns with squared values. In general, the use of the absolute form is more robust when the distribution is heavy tailed.

Figure B.5 in the online appendix displays the quantile-quantile(Q-Q) plots of the intraday innovations, comparing with the student t distribution with  $\hat{\nu}_D$  degrees of freedom. The points in the Q-Q plots approximately lie on a line, showing that the intraday innovations closely approximate the t distribution. Figure B.6 in the online appendix displays the Q-Q plots of the overnight innovations. Many stocks have several outliers in the lower left corners. Our model only partly captures the negative skewness and leptokurtosis of overnight innovations.

### 6.3 Results of the multivariate model

Figure A.2 and Figure A.3 in Appendix C present the long run correlations between intraday and overnight returns, respectively. Each subplot presents the 27 time series of long run correlations between that individual stock and the remaining stocks. The correlations exhibit an obvious upward trend during our sample period of 1998-2016, and are typically high during the 2008 financial crisis.

Figure B.7 in the online appendix plots the eigenvalues of the dynamic covariance matrices, as well as their proportions (the eigenvalues divided by the sum of eigenvalues). The dynamic of eigenvalues reinforces the previous remark that the stock markets experienced high risk in the 2001 9-11 attacks and in the 2008 financial crisis. The largest eigenvalue represents a strong common component, illustrating that a large proportion of the market financial risk can be explained by one single factor.

More specifically, the largest eigenvalue proportion increased substantially between 1998 and 2016. The second and third largest eigenvalues still accounted for a considerable proportion of risk in the volatile period from 2000 to 2002, but became rather insignificant in the volatile period from 2008 to 2011. The largest intraday eigenvalue proportion reached its peak in 2008, while the largest overnight eigenvalue proportion remained consistently high until 2011. Remarkably, the largest eigenvalue explained nearly 50% of intraday risk in the 2008 financial crisis, and 70% of overnight risk in the August 2011 stock markets fall.

Table B.7 in the online appendix provides estimates of the multivariate model. Compared to the univariate models, the average  $\beta_D$  decreases to 0.8796 from 0.9515, and the average  $\beta_N$  decreases to 0.8926 from 0.9553. Together with the increase of  $\gamma_j$  and  $\rho_j$ , this shows that more weights are given to information in the most recent trading days by taking correlations into consideration.

One concern is that our initial correlation estimator is based on the Pearson product moment correlation. This Pearson estimator may perform poorly due to the heavy tails of overnight innovations. Therefore, we also try the robust correlation estimator in the initial step. But the results remain similar as shown in Figure B.2 in the online appendix. It plots the largest eigenvalue proportions of the estimated covariance matrices to see the difference between using robust (in black) and non-robust (in red) correlation estimators in the initial step. We use solid lines for the initial estimators, and dash lines for the updated estimators. The updated estimators are obtained in the final estimation step, as previously detailed. Despite the large difference of initial estimators, in particular for overnight returns, the updated estimators are roughly similar. Like the eigenvalues, the updated covariances themselves also remain unchanged for different initial estimators.

To investigate the idiosyncratic risk, we estimate the mean equation with a CAPM structure. As reported in Table B.8 in the online appendix, the intraday alpha ( $\alpha_D$ ) is significant in 6 stocks, and the overnight alpha ( $\alpha_N$ ) is significant in 15 stocks. The intraday and overnight beta coefficients,  $\beta^{DD}$  and  $\beta^{NN}$ , are very close, varying from 0.5 to 1.5 and all significantly positive. For several stocks, the beta coefficients associated with previous market returns,  $\beta^{DN}$  and  $\beta^{NN}$ , are also significant with absolute values larger than 0.1. We then investigate the dynamic covariance of the residuals in the CAPM model. The idiosyncratic risk is indeed quite small for most Dow Jones stocks, implied by Figure (B.9–B.10) in the online appendix.

## 7 Application to CRSP stocks

In this section, we investigate 10 cap based portfolios with CRSP stocks from July 1992 to December 2015. July 1992 is the first month that CRSP provides opening stock prices. The prices are adjusted for stock splits and dividends with the cumulative factor in CRSP. Stocks with non-active trade status are excluded for that day, as well as stocks with overnight or intraday returns larger than 50% in absolute value.<sup>3</sup> CRSP sorts all stocks into 10 deciles based on their market capitalization values, and provide the portfolio assignment for each stock each year. We compute three versions of value

---

<sup>3</sup>In CRSP, if the closing price is not available on any given trading day, the number in the price field has a negative sign to indicate that it is a bid/ask average and not an actual closing price. We exclude these negative closing price.

weighted intraday and overnight returns for 10 cap based deciles, according to the assignment with three market types: NYSE/AMEX/NASDAQ, NASDAQ, and NYSE.

## 7.1 Overnight returns

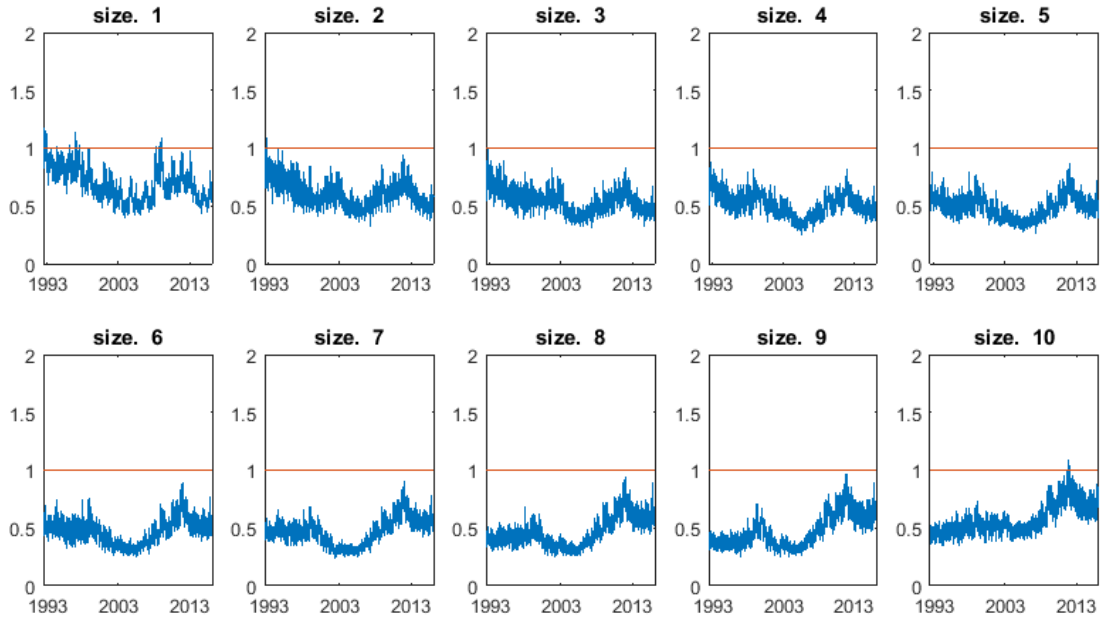
Table A.1 in Appendix C reports descriptive statistics for overnight and intraday returns of the deciles constructed with NYSE/AMEX/NASDAQ stocks (Panel A). The standard errors are estimated based on the standard deviations of the value weighted returns cross time. The mean intraday and overnight returns are positive and significant, except the mean intraday return in the largest cap decile. Small stocks show higher returns than large stocks, especially during intraday, probably suggesting the existence of size effects. Specifically, the mean intraday (overnight) return is 9.4 bp (6.0 bp) per day in the smallest decile, 9.6 pb (3.2 bp) in the second smallest decile, and only 1.6 bp (2.7 bp) in the largest decile. However, the median values of intraday returns are often larger than 10 bp while their overnight counterparts are overall much smaller around 6 bp. This indicates the right skewness of intraday returns. Panel B and C give the descriptive statistics for NASDAQ deciles and NYSE deciles, respectively. In general, NASDAQ deciles have higher returns than NYSE deciles.

Figure A.4 in Appendix C plots the sample autocorrelation function of intraday and overnight returns for deciles with stocks on NYSE /AMEX/NASDAQ. Both intraday and overnight returns exhibit large and significant positive autocorrelations in small cap deciles. It is worth noting that the autocorrelations of overnight returns decay at a very slow rate, which suggests the existence of long memory. This is somehow consistent with Aboody, Even-Tov, Lehavy, and Trueman (forthcoming). They documented overnight returns can serve as a measure of firm-specific investor sentiment, partly by showing overnight returns are persistent for periods extending several weeks, and argued that short-term persistence is stronger for harder-to-value firms.

We also notice that the overnight returns in large cap deciles (deciles 5-10) show significant negative first-order autocorrelations, with magnitude around  $-0.1$ . For intraday deciles, only the largest cap decile exhibits significantly negative first order autocorrelation, around  $-0.07$ . In addition to the autocorrelations, Figure A.5 in Appendix C shows the cross correlations between overnight returns and intraday returns. The correlation between  $r_t^D$  and  $r_t^N$  on the same day is around 0.1 and significant in most cap deciles, but insignificant in the largest decile. The cross correlation between  $r_{t-1}^D$  and  $r_t^N$  is significant for all cap deciles, with magnitude even larger than the correlation between  $r_t^D$  and  $r_t^N$  for decile 1, 2, 3 and 10, which indicates strong positive effects from intraday (overnight) returns to the subsequent overnight (intraday) returns.

## 7.2 Results of the univariate model

We estimate the univariate coupled component GARCH model for each cap decile. Table A.2 of Appendix C reports the estimates and their robust standard errors in the mean equations. Most deciles exhibit negative and significant  $\delta$ , indicating overnight returns have positive effects on the subsequent intraday returns. One exception is the largest decile, with insignificantly  $\delta$ . These positive effects seem to be conflicted with the strong reversal effects reported in Berkman, Koch, Tuttle, and



This figure plots the ratio of overnight to intraday volatility for cap based deciles. Decile 1 has the smallest capitalization and decile 10 has the largest. The intraday and overnight volatility are  $\sqrt{\frac{\nu_j}{\nu_j-2} \exp(2\lambda_t^j + 2\sigma^j(\frac{t}{T}))}$  for  $j = D, N$ , respectively.

Figure 2: Ratio of overnight to intraday volatility of cap based deciles: NYSE/AMEX/NASDAQ

Zhang (2012). But note that the reversal effects describe the cross-sectional difference in returns, while our positive effects describe the time-series properties of each return series.

Table A.4 in Appendix C reports the estimates of the dynamic parameters for NYSE/AMEX/NASDAQ deciles. Parameters  $\beta_D$  and  $\beta_N$  are significantly different from 1, and  $\rho_D$ ,  $\gamma_D$ ,  $\rho_N$  and  $\gamma_N$  are significantly positive. The leverage effects are significant, suggesting higher volatility after negative returns. Now the overnight degrees of freedom are larger than 4, less heavy tailed than that of individual stocks in the previous section.

One main advantage of the coupled component model, relative to the traditional one component version, is that it allows us to investigate the overnight and intraday volatility separately, and to obtain their ratios. As depicted in Figure 2 for NYSE/AMEX/NASDAQ stocks, the ratio of overnight to intraday volatility exhibits a downward trend in small cap deciles and an upward trend in large cap deciles. We also notice that the slopes increases monotonically from the smallest cap decile to the largest cap decile. Moreover, the ratio was considerably higher during the crisis period. Results remain similar when we consider NASDAQ stocks or NYSE stocks alone (Figure A.6), although the slope is somehow flatter for NYSE stocks. Actually, according to the market capitalization values in 2015, the average capitalization value of the smallest NYSE decile is 0.0993 million, which is between decile 2 and decile 3 in NYSE/AMEX/NASDAQ, and between decile 3 and decile 4 in NASDAQ, as shown in Table A.3 of Appendix C. If we look at the decile 1 of NYSE and decile 3 or decile 4 of NASDAQ, they indeed exhibit similar ratios of overnight to intraday volatility.

With the same approach, we also conduct 10 beta sorted portfolios and 10 standard deviation sorted portfolios. The beta and standard deviation values decrease from decile 1 to decile 10. Most deciles exhibit increasing overnight to intraday volatility ratio during the period, but there is no monotonic pattern across deciles.

Overall, the ratio of overnight to intraday volatility has been increased during the sample period at least for large stocks, and the ratio was typically higher during the financial crisis period, which is quite consistent with what we observed from the Dow Jones stocks in the previous section.

### 7.3 Results of the multivariate model

We next investigate the correlations between overnight and intraday returns with the multivariate model. Figure A.8 in Appendix C presents the long run correlations between intraday and overnight returns in Panel A and Panel B, respectively. Each subplot presents the 9 time series of long run correlations between that decile and the remaining deciles. Both intraday and overnight correlations have increased gradually during the sample period. Especially, the smallest cap decile had rather low correlations with other deciles, around 0.2 (0.3) for overnight (intraday) in 1992, and this number increased considerably to around 0.8 (0.6) for overnight (intraday) in 2015. Despite this substantial increase, comparing with large stocks, small stocks still co-move less with remaining stocks. We may expect different correlations during trading and non-trading hours. Indeed, the short run intraday and overnight correlations might be different. But the correlations reported here are the slowly moving long run correlations. We can not observe big difference between these long run intraday and overnight correlations.

## 8 Conclusion

We have introduced a new coupled component GARCH model for intraday and overnight volatility. This model is able to capture the heavy tails of overnight returns. For each component, we further specify a non-parametric long run smoothly evolving component with a parametric short term fluctuates. The large sample properties of the estimators are provided for the univariate model.

The empirical results show that the ratio of overnight to intraday volatility for specially large stocks has increased during the last 20 years when accounting for both slowly changing and rapidly changing components. This is contrary to what is often argued with regard to the change in market structure and the predatory practices of certain traders.

The information in overnight returns is valuable for updating the forecast of the close to close volatility. In the multivariate model we find that (slowly moving) correlations between assets have increased during our sample period. In particular, the co-movement of small stocks with the market has increased considerably.

## References

- Aboody, David, Omri Even-Tov, Reuven Lehavy, and Brett Trueman (forthcoming), “Overnight returns and firm-specific investor sentiment.” *Journal of Financial and Quantitative Analysis*.
- Aretz, Kevin and Söhnke M Bartram (2015), “Making money while you sleep? anomalies in international day and night returns.” Working paper, available at: <https://ssrn.com/abstract=2670841>.
- Battey, Heather and Oliver Linton (2014), “Nonparametric estimation of multivariate elliptic densities via finite mixture sieves.” *Journal of Multivariate Analysis*, 123, 43–67.
- Berkman, Henk, Paul D Koch, Laura Tuttle, and Ying Jenny Zhang (2012), “Paying attention: overnight returns and the hidden cost of buying at the open.” *Journal of Financial and Quantitative Analysis*, 47, 715–741.
- Blanc, Pierre, Rémy Chicheportiche, and Jean-Philippe Bouchaud (2014), “The fine structure of volatility feedback ii: Overnight and intra-day effects.” *Physica A: Statistical Mechanics and its Applications*, 402, 58–75.
- Branch, Ben S and Aixin Ma (2006), “The overnight return, one more anomaly.” Working paper, available at: <https://ssrn.com/abstract=937997>.
- Carrasco, Marine and Xiaohong Chen (2002), “Mixing and moment properties of various garch and stochastic volatility models.” *Econometric Theory*, 18, 17–39.
- Cho, Young-Hyun, Oliver Linton, and Yoon-Jae Whang (2007), “Are there monday effects in stock returns: A stochastic dominance approach.” *Journal of Empirical Finance*, 14, 736–755.



- Cooper, Michael J, Michael T Cliff, and Huseyin Gulen (2008), “Return differences between trading and non-trading hours: Like night and day.” Working paper, available at: <https://ssrn.com/abstract=1004081>.
- Creal, Drew, Siem Jan Koopman, and André Lucas (2012), “A dynamic multivariate heavy-tailed model for time-varying volatilities and correlations.” *Journal of Business & Economic Statistics*, 29, 552–563.
- Douc, Randal, Eric Moulines, and David Stoffer (2014), *Nonlinear time series: Theory, methods and applications with R examples*. CRC Press.
- Engle, Robert F and Gary Lee (1999), “A long-run and short-run component model of stock return volatility.” *Cointegration, Causality, and Forecasting: A Festschrift in Honour of Clive WJ Granger*, 475–497.
- Engle, Robert F and Jose Gonzalo Rangel (2008), “The spline-garch model for low-frequency volatility and its global macroeconomic causes.” *Review of Financial Studies*, 21, 1187–1222.
- French, Kenneth R (1980), “Stock returns and the weekend effect.” *Journal of Financial Economics*, 8, 55–69.
- French, Kenneth R and Richard Roll (1986), “Stock return variances: The arrival of information and the reaction of traders.” *Journal of Financial Economics*, 17, 5–26.
- Giacomini, Raffaella and Halbert White (2006), “Tests of conditional predictive ability.” *Econometrica*, 74, 1545–1578.
- Hafner, Christian M and Oliver Linton (2010), “Efficient estimation of a multivariate multiplicative volatility model.” *Journal of Econometrics*, 159, 55–73.
- Han, Heejoon and Dennis Kristensen (2015), “Semiparametric multiplicative garch-x model: Adopting economic variables to explain volatility.” Working paper.
- Harvey, Andrew and Alessandra Luati (2014), “Filtering with heavy tails.” *Journal of the American Statistical Association*, 109, 1112–1122.
- Harvey, Andrew C (2013), *Dynamic models for volatility and heavy tails: with applications to financial and economic time series*, volume 52. Cambridge University Press.
- Kristensen, Dennis (2009), “Uniform convergence rates of kernel estimators with heterogeneous dependent data.” *Econometric Theory*, 25, 1433–1445.
- Lindskog, Filip, Alexander Mcneil, and Uwe Schmock (2003), “Kendalls tau for elliptical distributions.” In *Credit Risk* (Bol Georg, Nakhaeizadeh Gholamreza, T. Rachev Svetlozarm, Ridder Thomas, and Vollmer Karl-Heinz, eds.), 149–156, Springer.

- Linton, Oliver, Maureen O'Hara, and Jean-Pierre Zigrand (2013), "The regulatory challenge of high-frequency markets." 207–230, Risk Books, London.
- Lockwood, Larry J and Scott C Linn (1990), "An examination of stock market return volatility during overnight and intraday periods, 1964–1989." *The Journal of Finance*, 45, 591–601.
- Mehdian, Seyed and Mark J Perry (2001), "The reversal of the monday effect: new evidence from us equity markets." *Journal of Business Finance & Accounting*, 28, 1043–1065.
- Ng, Victor and Ronald W Masulis (1995), "Overnight and daytime stock return dynamics on the London stock exchange." *Journal of Business and Economic Statistics*, 13, 365–378.
- Rangel, José Gonzalo and Robert F Engle (2012), "The factor–spline–garch model for high and low frequency correlations." *Journal of Business & Economic Statistics*, 30, 109–124.
- Rogalski, Richard J (1984), "New findings regarding day-of-the-week returns over trading and non-trading periods: a note." *The Journal of Finance*, 39, 1603–1614.
- Rogers, L Christopher G and Stephen E Satchell (1991), "Estimating variance from high, low and closing prices." *The Annals of Applied Probability*, 1, 504–512.
- Scholes, Myron and Joseph Williams (1977), "Estimating betas from nonsynchronous data." *Journal of Financial Economics*, 5, 309–327.
- Severini, Thomas A and Wing Hung Wong (1992), "Profile likelihood and conditionally parametric models." *The Annals of Statistics*, 20, 1768–1802.
- Steeley, James M (2001), "A note on information seasonality and the disappearance of the weekend effect in the UK stock market." *Journal of Banking & Finance*, 25, 1941–1956.
- Sullivan, Ryan, Allan Timmermann, and Halbert White (2001), "Dangers of data mining: The case of calendar effects in stock returns." *Journal of Econometrics*, 105, 249–286.
- Tasaki, Hiroyuki (2009), "Convergence rates of approximate sums of riemann integrals." *Journal of Approximation Theory*, 161, 477–490.
- Tibshirani, RJ (1984), *Local likelihood estimation*. Ph.D. thesis, Stanford University.
- Vogt, Michael (2012), "Nonparametric regression for locally stationary time series." *The Annals of Statistics*, 40, 2601–2633.
- Vogt, Michael and Oliver Linton (2014), "Nonparametric estimation of a periodic sequence in the presence of a smooth trend." *Biometrika*, 101, 121–140.

## 9 Appendix

### 9.1 Appendix A: Proof of theorems and lemmas in the univariate model

#### 9.1.1 Proof of Lemma 1

Denote  $H^j(s) = \exp(\sigma^j(s))$ . We drop the superscript  $j$  in what follows and have

$$\begin{aligned} |u_t| &= H(t/T) |e_t| = E |e_t| H(t/T) + H(t/T) (|e_t| - E |e_t|) \\ \frac{|u_t|}{E |e_t|} &= H(t/T) + \frac{H(t/T)}{E |e_t|} (|e_t| - E |e_t|) \\ &=: H(t/T) + \xi_t \end{aligned}$$

where  $E\xi_t = 0$ . Suppose we know  $E |e_t|$ . This gives a non-parametric regression function, so we can invoke the Nadaraya-Waston estimator

$$\tilde{H}(s)^* = \frac{\sum_{t=1}^T K_h(s - t/T) \frac{|u_t|}{E |e_t|}}{\sum_{t=1}^T K_h(s - t/T)}.$$

From Lemma 2,  $\{e_t\}$  is a  $\beta$  mixing process with exponential decay, and  $\xi_t$  thereby is also a  $\beta$  mixing process with exponential decay. Invoking Theorem 3 in Vogt and Linton (2014), Theorem 4.1 in Vogt (2012) or Kristensen (2009) yields:

$$\sup_{s \in [C_1 h, 1 - C_1 h]} \left| \tilde{H}(s)^* - H_0(s) \right| = O_p \left( \sqrt{\frac{\log T}{Th}} + h^2 \right).$$

Denote  $\tilde{\sigma}(s)^* = \log \tilde{H}(s)^*$ . Taylor expansion at  $H_0(s)$  gives

$$\tilde{\sigma}(s)^* = \sigma(s) + \left( \tilde{H}(s)^* - H(s) \right) \frac{1}{H(s)} - \frac{1}{2} \left( \tilde{H}(s)^* - H(s) \right)^2 \frac{1}{H(s)^2},$$

where  $\bar{H}(s)$  is function between  $\tilde{H}(s)^*$  and  $H_0(s)$ . Therefore,

$$\sup_{s \in [C_1 h, 1 - C_1 h]} \left| \tilde{\sigma}(s)^* - \sigma_0(s) \right| = O_p \left( h^2 + \sqrt{\frac{\log T}{Th}} \right).$$

For  $s \in [0, h] \cup [1 - h, 1]$ , we use a boundary kernel to ensure the bias property holds through  $[0, 1]$ .

Until now we have obtained the property for the un-rescaled estimator  $\tilde{\sigma}(s)^*$ . Next, we are going to show the convergence rate of the rescaled estimator  $\tilde{\sigma}(s)$ . Recall that

$$\tilde{\sigma}(s) = \tilde{\sigma}(s)^* - \frac{1}{T} \sum_{t=1}^T \tilde{\sigma}\left(\frac{t}{T}\right),$$

and we can rewrite  $\tilde{\sigma}(s)$  as:

$$\tilde{\sigma}(s) = \tilde{\sigma}(s)^* - \frac{1}{T} \sum_{t=1}^T \tilde{\sigma}\left(\frac{t}{T}\right)^*,$$

as  $E|e_t|$  in  $\tilde{\sigma}(s)^*$  has vanished due to the rescaling. Plugging this into  $\sup_{s \in [C_1 h, 1 - C_1 h]} |\tilde{\sigma}(s) - \sigma_0(s)|$  gives

$$\begin{aligned}
& \sup_{s \in [0, 1]} |\tilde{\sigma}(s) - \sigma_0(s)| \\
&= \sup_{s \in [0, 1]} \left| \tilde{\sigma}(s)^* - \frac{1}{T} \sum_{t=1}^T \tilde{\sigma}\left(\frac{t}{T}\right)^* - \sigma_0(s) \right| \\
&= \sup_{s \in [0, 1]} \left| \tilde{\sigma}(s)^* - \frac{1}{T} \sum_{t=1}^T \tilde{\sigma}\left(\frac{t}{T}\right)^* - \sigma_0(s) - \frac{1}{T} \sum_{t=1}^T \sigma_0\left(\frac{t}{T}\right) + \frac{1}{T} \sum_{t=1}^T \sigma_0\left(\frac{t}{T}\right) \right| \\
&\leq \sup_{s \in [0, 1]} |\tilde{\sigma}(s)^* - \sigma_0(s)| + \left| \frac{1}{T} \sum_{t=1}^T \left( \tilde{\sigma}\left(\frac{t}{T}\right)^* - \sigma_0\left(\frac{t}{T}\right) \right) \right| + \left| \frac{1}{T} \sum_{t=1}^T \sigma_0\left(\frac{t}{T}\right) \right| \\
&= O_p \left( h^2 + \sqrt{\frac{\log T}{Th}} \right) + O_p \left( h^2 + \sqrt{\frac{\log T}{Th}} \right) + \left| \frac{1}{T} \sum_{t=1}^T \sigma_0\left(\frac{t}{T}\right) \right| \\
&= O_p \left( h^2 + \sqrt{\frac{\log T}{Th}} \right) + \left| \frac{1}{T} \sum_{t=1}^T \sigma_0\left(\frac{t}{T}\right) \right|.
\end{aligned}$$

We only have to work out the second term  $\left| \frac{1}{T} \sum_{t=1}^T \sigma_0\left(\frac{t}{T}\right) \right|$ . According to Theorem 1.3 in Tasaki (2009),

$$\lim_{T \rightarrow \infty} T^2 \left( \int_0^1 \sigma_0(s) ds - \frac{1}{2T} \sum_{t=1}^T \sigma_0\left(\frac{t}{T}\right) - \frac{1}{2T} \sum_{t=0}^{T-1} \sigma_0\left(\frac{t}{T}\right) \right) = -\frac{1}{12} (\sigma_0'(1) - \sigma_0'(0)).$$

Since  $\int_0^1 \sigma_0(s) ds = 0$  and  $\sigma_0'(1) - \sigma_0'(0)$  is bounded by Assumption A4, it follows

$$\begin{aligned}
\left| \frac{1}{T} \sum_{t=1}^T \sigma_0\left(\frac{t}{T}\right) \right| &\leq \left| \frac{1}{2T} \sum_{t=1}^T \sigma_0\left(\frac{t}{T}\right) + \frac{1}{2T} \sum_{t=0}^{T-1} \sigma_0\left(\frac{t}{T}\right) \right| + \left| \frac{1}{2T} \sum_{t=1}^T \sigma_0\left(\frac{t}{T}\right) - \frac{1}{2T} \sum_{t=0}^{T-1} \sigma_0\left(\frac{t}{T}\right) \right| \\
&= O(T^{-2}) + \frac{1}{2T} |\sigma_0(1) - \sigma_0(0)| \\
&= O(T^{-1}).
\end{aligned}$$

Therefore, the uniform convergence rate is

$$\begin{aligned}
\sup_{s \in [0, 1]} |\tilde{\sigma}(s) - \sigma_0(s)| &= O_p \left( h^2 + \sqrt{\frac{\log T}{Th}} \right) + O(T^{-1}) \\
&= O_p \left( h^2 + \sqrt{\frac{\log T}{Th}} \right).
\end{aligned}$$

■

### 9.1.2 Proof of Theorem 1

Let  $\phi_i = \beta_D$  and  $\theta_k$  be an element in function  $\sigma^D(\cdot)$  (for simplicity, the subscript  $k$  is omitted in the following explanation). Recall that  $h_t^j = \lambda_t^j + \sigma^j(t/T)$ , and the log-likelihood function, without

unnecessary constant, can be rewritten as a function of  $h_t^j$

$$l_t^j = -h_t^j - \frac{v_j + 1}{2} \ln \left( 1 + \frac{(u_t^j)^2}{v_j \exp(2h_t^j)} \right) + \ln \Gamma \left( \frac{v_j + 1}{2} \right) - \frac{1}{2} \ln v_j - \ln \Gamma \left( \frac{v_j}{2} \right)$$

with the score functions

$$\begin{aligned} \frac{\partial l_t}{\partial \theta} &= \frac{\partial l_t^D}{\partial h_t^D} \frac{\partial h_t^D}{\partial \theta} + \frac{\partial l_t^N}{\partial h_t^N} \frac{\partial h_t^D}{\partial \theta} = m_t^D \frac{\partial h_t^D}{\partial \theta} + m_t^N \frac{\partial h_t^D}{\partial \theta} \\ \frac{\partial l_t}{\partial \beta_D} &= \frac{\partial l_t^D}{\partial h_t^D} \frac{\partial h_t^D}{\partial \beta_D} = m_t^D \frac{\partial h_t^D}{\partial \beta_D} + m_t^N \frac{\partial h_t^D}{\partial \beta_D}. \end{aligned}$$

Recall that  $m_t^j = (v_j + 1)b_t^j - 1$ , with  $b_t^j$  independent and identically beta distributed, we have  $E(m_t^N m_t^D) = 0$ ,  $E(m_t^j)^2$  is time invariant, and  $E(m_t^j) < \infty$ . Therefore, we can write

$$\sum_{t=1}^T E \frac{\partial l_t}{\partial \theta} \frac{\partial l_t}{\partial \beta_D} = E(m_t^D)^2 \sum_{t=1}^T \frac{\partial h_t^D}{\partial \theta} \frac{\partial h_t^D}{\partial \beta_D} + E(m_t^N)^2 \sum_{t=1}^T E \frac{\partial h_t^N}{\partial \theta} \frac{\partial h_t^N}{\partial \beta_D}.$$

To prove the theorem, it then suffices to show that

$$\left\| \sum_{t=1}^T E \begin{pmatrix} \frac{\partial h_t^D}{\partial \theta} \\ \frac{\partial h_t^N}{\partial \theta} \end{pmatrix} \begin{pmatrix} \frac{\partial h_t^D}{\partial \beta_D} & \frac{\partial h_t^N}{\partial \beta_D} \end{pmatrix} \right\|_{\infty} = O(1).$$

By expressing  $\lambda_t^j$  as a function of  $\varphi$  and  $\{(\sigma^j(\frac{t-i}{T}), u_{t-i}^j), i \geq 0\}$ , we can write  $\frac{\partial h_t^j}{\partial \theta}$  as

$$\begin{aligned} \begin{pmatrix} \frac{\partial h_t^D}{\partial \theta} \\ \frac{\partial h_t^N}{\partial \theta} \end{pmatrix} &= \sum_{k=0}^T \begin{pmatrix} \frac{\partial h_t^D}{\partial \sigma^D(\frac{t-k}{T})} \frac{\partial \sigma^D(\frac{t-k}{T})}{\partial \theta} \\ \frac{\partial h_t^N}{\partial \sigma^D(\frac{t-k}{T})} \frac{\partial \sigma^D(\frac{t-k}{T})}{\partial \theta} \end{pmatrix} \\ &= \sum_{k=0}^T \begin{pmatrix} \frac{\partial h_t^D}{\partial \sigma^D(\frac{t-k}{T})} \\ \frac{\partial h_t^N}{\partial \sigma^D(\frac{t-k}{T})} \end{pmatrix} \psi_i^D \left( \frac{t-k}{T} \right), \end{aligned}$$

when the limit exists. Thus we obtain,

$$\begin{aligned} &\frac{1}{T} \sum_{t=1}^T E \begin{pmatrix} \frac{\partial h_t^D}{\partial \theta} \\ \frac{\partial h_t^N}{\partial \theta} \end{pmatrix} \begin{pmatrix} \frac{\partial h_t^D}{\partial \beta_D} & \frac{\partial h_t^N}{\partial \beta_D} \end{pmatrix} \\ &= \frac{1}{T} \sum_{k=0}^T \sum_{t=1}^T E \begin{pmatrix} \frac{\partial h_t^D}{\partial \sigma^D(\frac{t-k}{T})} \\ \frac{\partial h_t^N}{\partial \sigma^D(\frac{t-k}{T})} \end{pmatrix} \begin{pmatrix} \frac{\partial h_t^D}{\partial \beta_D} & \frac{\partial h_t^N}{\partial \beta_D} \end{pmatrix} \psi_i^D \left( \frac{t-k}{T} \right) \\ &= \frac{1}{T} \sum_{k=0}^T E \begin{pmatrix} \frac{\partial h_t^D}{\partial \sigma^D(\frac{t-k}{T})} \\ \frac{\partial h_t^N}{\partial \sigma^D(\frac{t-k}{T})} \end{pmatrix} \begin{pmatrix} \frac{\partial h_t^D}{\partial \beta_D} & \frac{\partial h_t^N}{\partial \beta_D} \end{pmatrix} \sum_{t=1}^T \psi_i^D \left( \frac{t-k}{T} \right). \end{aligned}$$

The second equality follows since  $E \begin{pmatrix} \frac{\partial h_t^D}{\partial \sigma^j(\frac{t-k}{T})} \\ \frac{\partial h_t^N}{\partial \sigma^j(\frac{t-k}{T})} \end{pmatrix} \begin{pmatrix} \frac{\partial h_t^D}{\partial \beta_D} & \frac{\partial h_t^N}{\partial \beta_D} \end{pmatrix}$  is invariant across time  $t$  by Lemma 4.

Taylor expansion of  $\sum_{t=1}^T \psi_i^D \left( \frac{t-k}{T} \right)$  around  $\sum_{t=1}^T \psi_i^D \left( \frac{t}{T} \right)$  gives

$$\begin{aligned} \frac{1}{T} \sum_t \psi_i^D \left( \frac{t-k}{T} \right) &= \frac{1}{T} \sum_t \psi_i^D \left( \frac{t}{T} \right) - \frac{1}{T} \frac{k}{T} \sum_t \psi_i^{D'} \left( \frac{t}{T} \right) + O \left( \frac{k}{T} \right)^2 \\ &= O \left( \frac{1}{T} \right) + O \left( \frac{k}{T} \right) + O \left( \frac{k}{T} \right)^2 \\ &= O \left( \frac{k}{T} \right). \end{aligned}$$

Hence, it suffices to show

$$\sum_{k=0}^T \left\| k \left( E \left( \begin{array}{c} \frac{\partial h_t^D}{\partial \sigma^{D(\frac{t-k}{T})}} \\ \frac{\partial h_t^N}{\partial \sigma^{D(\frac{t-k}{T})}} \end{array} \right) \left( \begin{array}{cc} \frac{\partial h_t^D}{\partial \beta_D} & \frac{\partial h_t^N}{\partial \beta_D} \end{array} \right) \right) \right\|_{\infty} < \infty,$$

which is obtained by Lemma 3.

The proof with respect to  $v_D$  is similar, but the score function is slightly different. The score functions of  $l_t^D$  and  $l_t^N$  with respect to  $v_D$  are

$$\begin{aligned} \frac{\partial l_t^D}{\partial v_D} &= -\frac{1}{2} \ln \left( 1 + \frac{(u_t^D)^2}{v_D \exp(2h_t^D)} \right) + \frac{\partial}{\partial v_D} \left( \ln \Gamma \left( \frac{v_D+1}{2} \right) - \ln \Gamma \left( \frac{v_D}{2} \right) \right) - \frac{1}{2v_D} \\ &\quad + \frac{v_D+1}{2 \left( 1 + \frac{(u_t^D)^2}{v_D \exp(2h_t^D)} \right)} \frac{(u_t^D)^2}{v_D^2 \exp(2h_t^D)} \left( 1 + 2v_D \frac{\partial h_t^D}{\partial v_D} \right) + \frac{\partial h_t^D}{\partial v_D} \\ \frac{\partial l_t^N}{\partial v_D} &= \frac{v_N+1}{2 \left( 1 + \frac{(u_t^N)^2}{v_N \exp(2h_t^N)} \right)} \frac{(u_t^N)^2}{v_N^2 \exp(2h_t^N)} \left( 1 + 2v_N \frac{\partial h_t^N}{\partial v_D} \right) + \frac{\partial h_t^N}{\partial v_D}. \end{aligned} \tag{21}$$

Then we can have

$$\begin{aligned} &\sum_{t=1}^T E \frac{\partial l_t^D}{\partial \theta} \frac{\partial l_t^D}{\partial v_D} \\ &= \sum_{t=1}^T E m_t^D \frac{\partial h_t^D}{\partial \theta} \left[ \frac{\partial h_t^D}{\partial v_D} - \frac{1}{2} \ln \left( 1 + \frac{(u_t^D)^2}{v_D \exp(2h_t^D)} \right) \right] \\ &\quad + \sum_{t=1}^T E m_t^D \frac{\partial h_t^D}{\partial \theta} \frac{\partial \ln \Gamma \left( \frac{v_D+1}{2} \right) - \frac{1}{2} \ln v_D - \ln \Gamma \left( \frac{v_D}{2} \right)}{\partial v_D} \\ &\quad + \sum_{t=1}^T E m_t^D \frac{\partial h_t^D}{\partial \theta} \left[ \frac{v_D+1}{2 \left( 1 + \frac{(u_t^D)^2}{v_D \exp(2h_t^D)} \right)} \frac{(u_t^D)^2}{v_D^2 \exp(2h_t^D)} \left( 1 + 2v_D \frac{\partial h_t^D}{\partial v_D} \right) \right] \\ &= \frac{1}{2} E \left( m_t^D \left( -\ln \left( 1 + \frac{(\varepsilon_t^D)^2}{v_D} \right) + \frac{v_D+1}{2v_D + (\varepsilon_t^D)^2} \frac{(\varepsilon_t^D)^2}{v_D} \right) \right) \frac{1}{T} \sum_{t=1}^T E \frac{\partial h_t^D}{\partial \theta} \\ &\quad + E \left( m_t^D \left( 1 + \frac{(v_D+1)(\varepsilon_t^D)^2}{2v_D + (\varepsilon_t^D)^2} \right) \right) \frac{1}{T} \sum_{t=1}^T E \frac{\partial h_t^D}{\partial v_D} \frac{\partial h_t^D}{\partial \theta}. \end{aligned}$$

The first term vanishes by Lemma 5. Then we can use the same procedure above to obtain  $\sum_{t=1}^T E \frac{\partial h_t^D}{\partial v_D} \frac{\partial h_t^D}{\partial \theta} = O(1)$ , and to finish the proof for  $v_D$ . ■

### 9.1.3 Proof of Theorem 2

The general strategy is we first show the estimator obtained by maximizing  $\sum l(\phi; \tilde{\theta})$  and  $\sum l(\phi; \theta)$  has the same asymptotic distribution, provided  $\|\tilde{\theta} - \theta_0\|$  converges to 0. Then we show  $\|\tilde{\theta} - \theta_0\|$  converges to 0, given the uniform convergence rate for  $\sigma(s)$  in Lemma 1. As a result, the asymptotic property of  $\tilde{\phi}$  follows as in a parameter model.

Following Severini and Wong (1992), the expansion of  $\frac{1}{\sqrt{T}} \sum_{t=1}^T \frac{\partial l_t(\phi_{i0}; \tilde{\theta})}{\partial \phi}$  at  $\theta_0$  gives

$$\frac{1}{\sqrt{T}} \sum_{t=1}^T \frac{\partial l_t(\phi_0; \tilde{\theta})}{\partial \phi} = \frac{1}{\sqrt{T}} \sum_{t=1}^T \frac{\partial l_t(\phi_0; \theta_0)}{\partial \phi} + \frac{1}{\sqrt{T}} \sum_k \sum_{t=1}^T \frac{\partial^2 l_t(\phi_0; \theta_0)}{\partial \phi \partial \theta_k} (\tilde{\theta}_k - \theta_{k,0}) + o_p(1). \quad (22)$$

According to Theorem 1, we have  $E \sum_{t=1}^T \frac{\partial^2 l_t(\phi; \theta)}{\partial \phi_i \partial \theta_k} = O(1)$ , for each  $k$  and  $i$ ,  $k \in \{1, \dots, \infty\}$  and  $i \in \{1, \dots, 14\}$ . It follows that

$$\sum_{t=1}^T \frac{\partial^2 l_t(\phi_0; \theta_0)}{\partial \phi_i \partial \theta_k} = O_p(\sqrt{T}).$$

Given that the dimension of the sieve space grows slowly and  $\tilde{\theta}$  converges to  $\theta$ , the second term in (22) will be of order  $o_p(1)$ .

Next we investigate the relationship between the kernel estimator and  $\tilde{\theta}$  in a very general setting. Recall that  $\sigma(s) = \sum_{j=1}^{\infty} \theta_j \psi_j(s)$  for some orthogonal basis  $\psi_j$ . We assume that  $\tilde{\sigma}(s)$  is a member of the same normed space as  $\sigma(s)$  in which case we can write

$$\tilde{\sigma}(s) = \sum_{j=1}^{\infty} \tilde{\theta}_j \psi_j(s)$$

for some coefficients  $\tilde{\theta}_j$ ,  $j = 1, 2, \dots$ . We have

$$\begin{aligned} \int (\tilde{\sigma}(s) - \sigma(s))^2 ds &= \int \left( \sum_{j=1}^{\infty} (\tilde{\theta}_j - \theta_j) \psi_j(s) \right)^2 ds \\ &= \sum_{j=1}^{\infty} (\tilde{\theta}_j - \theta_j)^2 \int \psi_j^2(s) ds \\ &= \sum_{j=1}^{\infty} (\tilde{\theta}_j - \theta_j)^2 \end{aligned}$$

under the assumption that  $\psi_j$  are orthonormal. So given the  $L_2$  rate of convergence of  $\tilde{\sigma}$  we have the same convergence rate for the implied coefficients. Hence, given the uniform convergence rate for  $\tilde{\sigma}(s)$  in Lemma 1, we have  $\|\tilde{\theta} - \theta_0\|$  converges to 0, and the estimator obtained by maximizing  $\sum l(\phi; \tilde{\theta})$  and  $\sum l(\phi; \theta)$  has the same property.

Therefore, the asymptotic property of  $\tilde{\phi}$  can be obtained with the similar procedure of Harvey (2013). He gives the consistency and asymptotic normality of the estimator for the parametric beta-egarch model. The basic idea is that the first three derivatives of  $l_t$  with respect to  $\phi$  (except  $v_j$ ) are linear combinations of  $b_t^h (1 - b_t)^k$ ,  $h, k = 0, 1, 2, \dots$ , with  $b_t = \frac{(1+v)(e_t)^2}{v \exp(2\lambda_t) + (e_t)^2}$ . Since  $b_t$  is beta distributed, these first three derivatives are all bounded. It is then straightforward to show that the

score function satisfies a CLT, and its derivative converges to the information matrix by the ergodic theorem.

Obviously,  $\hat{\phi}$  has the same asymptotic property of  $\tilde{\phi}$ , since  $\sum_{t=1}^T \frac{\partial l_t(\phi_{i0}, \tilde{\theta})}{\partial \phi}$  and  $\sum_{t=1}^T \frac{\partial l_t(\phi_{i0}, \theta)}{\partial \phi}$  have the same asymptotic property.  $\blacksquare$

#### 9.1.4 Proof of Theorem 3

Consider the local likelihood function given  $\eta_t^j$  and  $v_j$ , i.e., minimize the objective function

$$L_T^j(\sigma^j; s) = \frac{1}{T} \sum_{t=1}^T K_h(s - t/T) \left[ \sigma^j + \frac{v_j + 1}{2} \ln \left( 1 + \frac{(\eta_t^j \exp(-\sigma^j))^2}{v_j} \right) \right]$$

with respect to  $\omega$ , for  $j = D, N$  separately. The first order and second order derivatives are:

$$\begin{aligned} \frac{\partial L_T^j(\sigma^j; s)}{\partial \sigma^j} &= \frac{1}{T} \sum_{t=1}^T K_h(s - t/T) [-(v_j + 1)b_t^j(\sigma^j) + 1] \\ \frac{\partial^2 L_T^j(\sigma^j; s)}{\partial \sigma^{j2}} &= 2(v_j + 1) \frac{1}{T} \sum_{t=1}^T K_h(s - t/T) [b_t^j(\sigma^j) (1 - b_t^j(\sigma^j))], \end{aligned} \quad (23)$$

where

$$b_t^j(\sigma^j) = \frac{\frac{(\eta_t^j)^2}{v_j}}{\exp(2\sigma^j) + \frac{(\eta_t^j)^2}{v_j}}.$$

We have

$$\sqrt{Th} \left( \hat{\sigma}^j(s) - \sigma_0^j(s) \right) = \left[ \frac{1}{Th} \frac{\partial^2 L_T^j(\sigma_0^j; s)}{\partial \sigma^{j2}} \right]^{-1} \frac{1}{\sqrt{Th}} \frac{\partial L_T^j(\sigma_0^j; s)}{\partial \sigma^j} + o_p(1),$$

This is asymptotically normal with mean zero and variance (when the t distribution is correct)

$$\text{var} \left[ \frac{1}{\sqrt{Th}} \frac{\partial L_T^j(\sigma_0^j; s)}{\partial \sigma^j} \right] = \|K\|_2^2 E \left[ (1 - (v_j + 1)b_t^j(\sigma_0^j(s)))^2 \right]_{t/T=s}.$$

This follows because

$$E \left[ (1 - (v_j + 1)b_t^j(\sigma_0^j(s)))^2 \right] = f(t/T)$$

for some smooth function  $f$ , and recall  $\eta_t^j = \exp(\sigma^j(t/T))\varepsilon_t^j$ . It follows that

$$\frac{h^2}{Th} \sum_{t=1}^T K_h^2(s - t/T) f(t/T) \rightarrow \|K\|_2^2 f(s),$$

Therefore,

$$\sqrt{Th} \left( \hat{\sigma}^j(s) - \sigma_0^j(s) \right) \Rightarrow N \left( 0, \frac{\|K\|_2^2}{E \left[ (1 - (v_j + 1)b_t^j)^2 \right]_{t/T=s}} \right)$$



Further, since  $b_t^j$  is distributed as  $beta(\frac{1}{2}, \frac{v_j}{2})$ , with

$$E \left[ (1 - (v_j + 1)b_t^j)^2 \right]_{t/T=s} = \frac{2v_j}{(v_j + 3)}.$$

It thus follows that

$$\sqrt{T}h \left( \widehat{\sigma}^j(s) - \sigma_0^j(s) \right) \implies N \left( 0, \sqrt{\frac{(v_j + 3)}{2v_j}} \|K\|_2^2 \right).$$

when the t distribution is correct. ■

### 9.1.5 Other Lemmas

**Lemma 2** *If  $|\beta_j| < 1$ ,  $j = D, N$ , then  $e_t^j$  and  $\lambda_t^j$  are strictly stationary and  $\beta$ -mixing with exponential decay.*

**Proof.** For simplicity, we consider the model without leverage effects

$$\begin{aligned} \lambda_t^D &= \omega_D(1 - \beta_D) + \beta_D \lambda_{t-1}^D + \gamma_D m_{t-1}^D + \rho_D m_t^N \\ \lambda_t^N &= \omega_N(1 - \beta_N) + \beta_N \lambda_{t-1}^N + \gamma_N m_{t-1}^N + \rho_N m_{t-1}^D. \end{aligned}$$

Let us write it as

$$\begin{pmatrix} \lambda_t^D \\ \lambda_t^N \\ m_t^D \\ m_t^N \end{pmatrix} = \begin{pmatrix} \beta_D & 0 & \gamma_D & 0 \\ 0 & \beta_N & \rho_N & \beta_N \\ 0 & 0 & 0 & 0 \\ 0 & 0 & 0 & 0 \end{pmatrix} \begin{pmatrix} \lambda_{t-1}^D \\ \lambda_{t-1}^N \\ m_{t-1}^D \\ m_{t-1}^N \end{pmatrix} + \begin{pmatrix} \rho_D m_t^N + \omega_D(1 - \beta_D) \\ \omega_N(1 - \beta_N) \\ m_t^D \\ m_t^N \end{pmatrix}.$$

Since  $m_t^N$  and  $m_t^D$  are i.i.d random variables and follow a beta distribution, we can easily find an integer  $s \geq 1$  to satisfy

$$E \left| \begin{array}{c} \rho_D m_t^N + \omega_D(1 - \beta_D) \\ \omega_N(1 - \beta_N) \\ m_t^D \\ m_t^N \end{array} \right|^s < \infty$$

(Condition A<sub>2</sub> in Carrasco and Chen (2002)). The largest eigenvalue of the matrix

$$\begin{vmatrix} \beta_D & 0 & \gamma_D & 0 \\ 0 & \beta_N & \rho_N & \beta_N \\ 0 & 0 & 0 & 0 \\ 0 & 0 & 0 & 0 \end{vmatrix}$$

is smaller than 1 by assumption. Define  $X_t = \left( \lambda_t^D \quad \lambda_t^N \quad m_t^D \quad m_t^N \right)^\top$ . According to Proposition 2 in Carrasco and Chen (2002), the process  $X_t$  is Markov geometrically ergodic and  $E|X_t|^s < \infty$ . Moreover, if  $X_t$  is initialized from the invariant distribution, it is then strictly stationary and  $\beta$ -mixing with exponential decay. The process  $\{e_t^j\}$  is a generalized hidden Markov model and stationary  $\beta$ -mixing with a decay rate at least as fast as that of  $\{\lambda_t^j\}$  by Proposition 4 in Carrasco and Chen (2002). The extension to the model with leverage effects is straightforward, by defining  $X_t = \left( \lambda_t^D \quad \lambda_t^N \quad m_t^D \quad m_t^N \quad \text{sign}(e_t^D) \quad \text{sign}(e_t^N) \right)^\top$ . ■

**Lemma 3** *Under Assumption A1-A4, it holds that*

$$\sum_k k \left\| E \left( \left[ \begin{array}{c} \frac{\partial h_t^D}{\partial \sigma^{D(t-k/T)}} \\ \frac{\partial h_t^N}{\partial \sigma^{D(t-k/T)}} \end{array} \right] \left( \frac{\partial}{\partial \beta_D} h_t^D \quad \frac{\partial}{\partial \beta_D} h_t^N \right) \right) \right\|_{\infty} < \infty.$$

**Proof.** By (26) and (27), we have

$$\begin{aligned} E \left( \frac{\frac{\partial h_{t+1}^D}{\partial \sigma^{D(t+k/T)}}}{\frac{\partial h_{t+1}^N}{\partial \sigma^{D(t+k/T)}}} \right) \left( \frac{\partial}{\partial \beta_D} h_{t+1}^D \quad \frac{\partial}{\partial \beta_D} h_{t+1}^N \right) &= E A_{t+1} \begin{pmatrix} a_t^{DD} \\ a_t^{ND} \end{pmatrix} \begin{pmatrix} \lambda_t^D - \omega_D & 0 \end{pmatrix} A_{t+1}^T; k = 1 \\ E \left( \frac{\frac{\partial h_{t+1}^D}{\partial \sigma^{D(t+k/T)}}}{\frac{\partial h_{t+1}^N}{\partial \sigma^{D(t+k/T)}}} \right) \left( \frac{\partial}{\partial \beta_D} h_{t+1}^D \quad \frac{\partial}{\partial \beta_D} h_{t+1}^N \right) &= E \begin{pmatrix} 1 \\ 0 \end{pmatrix} \begin{pmatrix} \lambda_t^D - \omega_D & 0 \end{pmatrix} A_{t+1}^T = 0; k = 0. \end{aligned}$$

When  $k > 1$ , it holds

$$\begin{aligned} &\text{vec} \left( \frac{\frac{\partial h_t^D}{\partial \sigma^{D(t-k/T)}}}{\frac{\partial h_t^N}{\partial \sigma^{D(t-k/T)}}} \right) \left( \frac{\partial}{\partial \beta_D} h_t^D \quad \frac{\partial}{\partial \beta_D} h_t^N \right) \\ &= \text{vec} A_t \left( \prod_{i=1}^{k-1} B_{t-i} A_{t-i} \right) \Lambda_{t-k} \begin{pmatrix} \lambda_{t-1}^D - \omega_D & 0 \end{pmatrix} A_t^T \\ &+ \text{vec} A_t \left( \prod_{i=1}^{k-1} B_{t-i} A_{t-i} \right) \Lambda_{t-k} \begin{pmatrix} \lambda_{t-2}^D - \omega_D & 0 \end{pmatrix} A_{t-1}^T B_{t-1}^T A_t^T \\ &+ \dots \\ &+ \text{vec} A_t \left( \prod_{i=1}^{k-1} B_{t-i} A_{t-i} \right) \Lambda_{t-k} \begin{pmatrix} \lambda_{t-k+1}^D - \omega_D & 0 \end{pmatrix} A_{t-k+2}^T B_{t-k+2}^T \dots A_{t-1}^T B_{t-1}^T A_t^T \\ &= \sum_{j=1}^{k-1} (A_t \otimes A_t) \left( \prod_{i=1}^{j-1} (B_{t-i} \otimes B_{t-i}) (A_{t-i} \otimes A_{t-i}) \right) \text{vec} \left( \left( \prod_{i=j}^{k-1} B_{t-i} A_{t-i} \right) \Lambda_{t-k} \begin{pmatrix} \lambda_{t-j}^D - \omega_D & 0 \end{pmatrix} \right). \end{aligned}$$

Since  $(B_{t-1} \otimes B_{t-1}) (A_{t-1} \otimes A_{t-1})$  and  $B_t A_t$  are i.i.d, and  $E B_t A_t = E B_t E A_t$ , we obtain

$$\begin{aligned} &E \text{vec} \left( \frac{\frac{\partial h_t^D}{\partial \sigma^{D(t-k/T)}}}{\frac{\partial h_t^N}{\partial \sigma^{D(t-k/T)}}} \right) \left( \frac{\partial}{\partial \beta_D} h_t^D \quad \frac{\partial}{\partial \beta_D} h_t^N \right) \tag{24} \\ &= \sum_{j=1}^{k-1} E (A_t \otimes A_t) E (B_{t-i} \otimes B_{t-i}) (A_{t-i} \otimes A_{t-i})^{j-1} E \text{vec} \left( \left( \prod_{i=j}^{k-1} B_{t-i} A_{t-i} \right) \Lambda_{t-k} \begin{pmatrix} \lambda_{t-j}^D - \omega_D & 0 \end{pmatrix} \right). \end{aligned}$$

By (4), we can express  $\lambda_{t-1}^D$  as a function of  $\{(m_{t-i}^D, m_{t-i+1}^N), i > 1\}$ . Note that  $B_t, A_t,$  and  $\Lambda_t$  are independent of  $\{(m_s^D, m_s^N), s \neq t\}$ . Therefore, we have

$$\begin{aligned} &E \left( \left( \prod_{i=j}^{k-1} B_{t-i} A_{t-i} \right) \Lambda_{t-k} \begin{pmatrix} \lambda_{t-j}^D - \omega_D \end{pmatrix} \right) \\ &= \gamma_D E \left( \prod_{i=j}^{k-1} B_{t-i} A_{t-i} \right) \Lambda_{t-k} \sum_{i=j+1}^k \beta_D^{i-1} (m_{t-i}^D + (m_{t-i}^D + 1) \text{sign}(e_{t-i}^D)) \\ &+ \rho_D E \left( \prod_{i=j}^{k-1} B_{t-i} A_{t-i} \right) \Lambda_{t-k} \sum_{i=j+1}^k \beta_D^{i-1} (m_{t-i+1}^N + (m_{t-i+1}^N + 1) \text{sign}(e_{t-i+1}^N)), \end{aligned}$$

with the first term

$$\begin{aligned}
& \left\| E \left( \prod_{i=j}^{k-1} B_{t-i} A_{t-i} \right) \Lambda_{t-k} \sum_{i=j+1}^k \beta_D^{i-1} (m_{t-i}^D + (m_{t-i}^D + 1) \text{sign}(e_{t-i}^D)) \right\|_{\infty} \\
& \leq \left( \sum_{i=j+1}^{k-1} \beta_D^{i-1} \right) \left\| E (B_t (m_t^D + (m_t^D + 1) \text{sign}(e_t^D)) A_t) \right\|_{\infty} \|EB_t E A_t\|_{\infty}^{k-j-1} \|E \Lambda_t\|_{\infty} \\
& + \beta_D^{k-j} \left\| E \Lambda_{t-k} (m_{t-k}^D + (m_{t-k}^D + 1) \text{sign}(e_{t-k}^D)) \right\|_{\infty} \|EB_t E A_t\|_{\infty}^{k-j} \\
& \leq \frac{\beta_D}{1 - \beta_D} \left\| E (B_t (m_t^D + (m_t^D + 1) \text{sign}(e_t^D)) A_t) \right\|_{\infty} \|E \Lambda_t\|_{\infty} \|EB_t E A_t\|_{\infty}^{k-j-1} \\
& + \beta_D^{k-j} \left\| E \Lambda_{t-k} (m_{t-k}^D + (m_{t-k}^D + 1) \text{sign}(e_{t-k}^D)) \right\|_{\infty} \|EB_t E A_t\|_{\infty}^{k-j}
\end{aligned}$$

and the second term

$$\begin{aligned}
& \left\| E \left( \prod_{i=j}^{k-1} B_{t-i} A_{t-i} \right) \Lambda_{t-k} \sum_{i=j+1}^k \beta_D^{i-1} (m_{t-i+1}^N + (m_{t-i+1}^N + 1) \text{sign}(e_{t-i+1}^N)) \right\|_{\infty} \\
& \leq \frac{\beta_D}{1 - \beta_D} \left\| E (B_t (m_t^N + (m_t^N + 1) \text{sign}(e_t^N)) A_t) \right\|_{\infty} \|E \Lambda_t\|_{\infty} \|EB_t E A_t\|_{\infty}^{k-j-1}.
\end{aligned}$$

According to the definition of  $\|\cdot\|_{\infty}$ ,

$$\left\| \text{Evec} \left( \left( \prod_{i=j}^{k-1} B_{t-i} A_{t-i} \right) \Lambda_{t-k} \begin{pmatrix} \lambda_{t-j}^D - \omega_D & 0 \end{pmatrix} \right) \right\|_{\infty} \leq \left\| E \left( \left( \prod_{i=j}^{k-1} B_{t-i} A_{t-i} \right) \Lambda_{t-k} \begin{pmatrix} \lambda_{t-j}^D - \omega_D & 0 \end{pmatrix} \right) \right\|_{\infty}$$

Therefore,

$$\left\| \text{Evec} \left( \left( \prod_{i=j}^{k-1} B_{t-i} A_{t-i} \right) \Lambda_{t-k} \begin{pmatrix} \lambda_{t-j}^D - \omega_D & 0 \end{pmatrix} \right) \right\|_{\infty} \leq c_T \|EB_t E A_t\|_{\infty}^{k-j-1} \quad (25)$$

with

$$\begin{aligned}
c_T &= \frac{\beta_D}{1 - \beta_D} |\gamma_D| \left\| E (B_t (m_t^D + (m_t^D + 1) \text{sign}(e_t^D)) A_t) \right\|_{\infty} \|E \Lambda_t\|_{\infty} \\
& + \|EB_t E A_t\|_{\infty} \left\| E \Lambda_{t-k} (m_{t-k}^D + (m_{t-k}^D + 1) \text{sign}(e_{t-k}^D)) \right\|_{\infty} \\
& + \frac{\beta_D}{1 - \beta_D} |\rho_D| \left\| E (B_t (m_t^N + (m_t^N + 1) \text{sign}(e_t^N)) A_t) \right\|_{\infty} \|E \Lambda_t\|_{\infty}.
\end{aligned}$$

Substituting (25) into (24) gives

$$\begin{aligned}
& \left\| \text{Evec} \left( \begin{pmatrix} \frac{\partial h_t^D}{\partial \sigma^{D(t-k/T)}} \\ \frac{\partial h_t^N}{\partial \sigma^{D(t-k/T)}} \end{pmatrix} \begin{pmatrix} \frac{\partial}{\partial \beta_D} h_t^D & \frac{\partial}{\partial \beta_D} h_t^N \end{pmatrix} \right) \right\|_{\infty} \\
& \leq \sum_{j=1}^{k-1} \|E (A_t \otimes A_t)\|_{\infty} \|E (B_{t-i} \otimes B_{t-i}) (A_{t-i} \otimes A_{t-i})\|_{\infty}^{j-1} c_T \|EB_t E A_t\|_{\infty}^{k-j-1} \\
& \leq c_T \|E (A_t \otimes A_t)\|_{\infty} \sum_{j=1}^{k-1} \|E (B_{t-i} \otimes B_{t-i}) (A_{t-i} \otimes A_{t-i})\|_{\infty}^{j-1} \|EB_t E A_t\|_{\infty}^{k-j-1} \\
& \leq c_T \|E (A_t \otimes A_t)\|_{\infty} \frac{\|EB_t E A_t\|_{\infty}^{k-2}}{1 - \frac{\|E(B_{t-i} \otimes B_{t-i})(A_{t-i} \otimes A_{t-i})\|_{\infty}}{\|EB_t E A_t\|_{\infty}}},
\end{aligned}$$

provided that  $\|EB_tEA_t\|_\infty < 1$  and  $\|E(B_{t-1}A_{t-1} \otimes B_{t-1}A_{t-1})\|_\infty < \|EB_tEA_t\|_\infty$ . It is then straightforward to show

$$\sum_k k \left\| \text{Evec} \left( \frac{\frac{\partial h_t^D}{\partial \sigma^D(t-k/T)}}{\frac{\partial h_t^N}{\partial \sigma^D(t-k/T)}} \right) \left( \frac{\partial}{\partial \beta_D} h_t^D \quad \frac{\partial}{\partial \beta_D} h_t^N \right) \right\|_\infty < \infty$$

and thereby

$$\sum_k k \left\| E \left( \frac{\frac{\partial h_t^D}{\partial \sigma^D(t-k/T)}}{\frac{\partial h_t^N}{\partial \sigma^D(t-k/T)}} \right) \left( \frac{\partial}{\partial \beta_D} h_t^D \quad \frac{\partial}{\partial \beta_D} h_t^N \right) \right\|_\infty < \infty.$$

■

**Lemma 4** *The score functions of  $h_t^j$  with respect to  $\beta_D, v_D$  and  $\sigma^j(t/T)$  are*

$$\begin{aligned} \begin{pmatrix} \frac{\partial}{\partial \beta_D} h_t^D \\ \frac{\partial}{\partial \beta_D} h_t^N \end{pmatrix} &= A_t \begin{pmatrix} \lambda_{t-1}^D - \omega_D \\ 0 \end{pmatrix} + A_t B_{t-1} \begin{pmatrix} \frac{\partial}{\partial \beta_D} h_{t-1}^D \\ \frac{\partial}{\partial \beta_D} h_{t-1}^N \end{pmatrix} \\ &= \sum_{j=1}^{\infty} A_t \prod_{i=1}^{j-1} B_{t-i} A_{t-i} \begin{pmatrix} \lambda_{t-j}^D - \omega_D \\ 0 \end{pmatrix}. \end{aligned} \quad (26)$$

$$\begin{aligned} \begin{pmatrix} \frac{\partial h_t^D}{\partial \sigma^D(t-k/T)} \\ \frac{\partial h_t^N}{\partial \sigma^D(t-k/T)} \end{pmatrix} &= A_t B_{t-1} \begin{pmatrix} \frac{\partial h_{t-1}^D}{\partial \sigma^D(t-k/T)} \\ \frac{\partial h_{t-1}^N}{\partial \sigma^D(t-k/T)} \end{pmatrix} \\ &= A_t \left( \prod_{i=1}^{k-1} B_{t-i} A_{t-i} \right) \Lambda_{t-k}, \quad k > 1 \\ \begin{pmatrix} \frac{\partial h_t^D}{\partial \sigma^D(t/T)} \\ \frac{\partial h_t^N}{\partial \sigma^D(t/T)} \end{pmatrix} &= \begin{pmatrix} 1 \\ 0 \end{pmatrix}; \quad \text{and} \quad \begin{pmatrix} \frac{\partial h_t^D}{\partial \sigma^D(t-1/T)} \\ \frac{\partial h_t^N}{\partial \sigma^D(t-1/T)} \end{pmatrix} = A_t \begin{pmatrix} a_{t-1}^{DD} \\ a_{t-1}^{ND} \end{pmatrix}, \end{aligned} \quad (27)$$

with  $\Lambda_t = \begin{pmatrix} a_t^{DD} \\ a_t^{ND} \end{pmatrix}$ . If the top-Lyapunov exponent of the sequence of  $A_t B_{t-1}$  is strictly negative,  $\begin{pmatrix} \frac{\partial}{\partial \beta_D} h_t^D \\ \frac{\partial}{\partial \beta_D} h_t^N \end{pmatrix}$ ,  $\begin{pmatrix} \frac{\partial h_t^D}{\partial \sigma^D(t-k/T)} \\ \frac{\partial h_t^N}{\partial \sigma^D(t-k/T)} \end{pmatrix}$  and  $\begin{pmatrix} \frac{\partial h_t^D}{\partial \beta_D} & \frac{\partial h_t^N}{\partial \beta_D} \end{pmatrix}$  are strictly stationary.

**Proof.** Since  $h_t^j = \lambda_t^j + \sigma^j(t/T)$ , we can write  $h_t^j$  in a recursive formula as

$$\begin{aligned} h_t^D &= \sigma^D(t/T) - \beta_D \sigma^D\left(\frac{t-1}{T}\right) + \omega_D(1 - \beta_D) + \beta_D h_{t-1}^D + \gamma_D m_{t-1}^D \\ &\quad + \rho_D m_t^N + \gamma_D^*(m_{t-1}^D + 1)\text{sign}(u_{t-1}^D) + \rho_D^*(m_t^N + 1)\text{sign}(u_t^N) \end{aligned} \quad (28)$$

$$\begin{aligned} h_t^N &= \sigma^N(t/T) - \beta_N \sigma^N\left(\frac{t-1}{T}\right) + \omega_N(1 - \beta_N) + \beta_N h_{t-1}^N + \gamma_N m_{t-1}^N \\ &\quad + \rho_N m_{t-1}^D + \rho_N^*(m_{t-1}^D + 1)\text{sign}(u_{t-1}^D) + \gamma_N^*(m_{t-1}^N + 1)\text{sign}(u_{t-1}^N). \end{aligned} \quad (29)$$

and  $m_t^D$  and  $m_t^N$  can be expressed as

$$\begin{aligned} m_t^D &= \frac{(1 + v_D)(u_t^D)^2 \exp(-2h_t^D)}{v_D + (u_t^D)^2 \exp(-2h_t^D)} - 1, \quad v_D > 0 \\ m_t^N &= \frac{(1 + v_N)(u_t^N)^2 \exp(-2h_t^N)}{v_N + (u_t^N)^2 \exp(-2h_t^N)} - 1, \quad v_N > 0. \end{aligned}$$

Taking the first order derivative of equation (28) and (29) with respect to  $\beta_D$  gives

$$\begin{aligned} \frac{\partial h_t^D}{\partial \beta_D} &= -\sigma^D \left( \frac{t-1}{T} \right) - \omega_D + h_{t-1}^D + \beta_D \frac{\partial}{\partial \beta_D} h_{t-1}^D + \frac{\partial}{\partial \beta_D} \gamma_D m_{t-1}^D + \frac{\partial}{\partial \beta_D} \rho_D m_t^N \\ &\quad + \frac{\partial}{\partial \beta_D} \gamma_D^* (m_{t-1}^D + 1) \text{sign}(u_{t-1}^D) + \frac{\partial}{\partial \beta_D} \rho_D^* (m_t^N + 1) \text{sign}(u_t^N) \end{aligned} \quad (30)$$

$$\begin{aligned} \frac{\partial h_t^N}{\partial \beta_D} &= \beta_N \frac{\partial}{\partial \beta_D} h_{t-1}^N + \frac{\partial}{\partial \beta_D} \gamma_N m_{t-1}^N + \frac{\partial}{\partial \beta_D} \rho_N m_{t-1}^D \\ &\quad + \frac{\partial}{\partial \beta_D} \rho_N^* (m_{t-1}^D + 1) \text{sign}(u_{t-1}^D) + \frac{\partial}{\partial \beta_D} \gamma_N^* (m_{t-1}^N + 1) \text{sign}(u_{t-1}^N) \end{aligned} \quad (31)$$

and the derivatives of  $m_{t-1}^D$  and  $m_{t-1}^N$  are

$$\begin{aligned} \frac{\partial}{\partial \beta_D} m_{t-1}^D &= \frac{\partial m_{t-1}^D}{\partial h_{t-1}^D} \frac{\partial}{\partial \beta_D} h_{t-1}^D = -2(v_D + 1) b_{t-1}^D (1 - b_{t-1}^D) \frac{\partial}{\partial \beta_D} h_{t-1}^D \\ \frac{\partial}{\partial \beta_D} m_{t-1}^N &= \frac{\partial m_{t-1}^N}{\partial h_{t-1}^N} \frac{\partial}{\partial \beta_D} h_{t-1}^N = -2(v_N + 1) b_{t-1}^N (1 - b_{t-1}^N) \frac{\partial}{\partial \beta_D} h_{t-1}^N. \end{aligned}$$

Substituting them back into (30) and (31) gives

$$\begin{aligned} \frac{\partial h_t^D}{\partial \beta_D} &= \lambda_{t-1}^D - \omega_D + (\beta_D + a_{t-1}^{DD}) \frac{\partial}{\partial \phi} h_{t-1}^D + a_t^{DN} \frac{\partial}{\partial \phi} h_t^N \\ \frac{\partial h_t^N}{\partial \beta_D} &= 0 + (\beta_N + a_{t-1}^{NN}) \frac{\partial}{\partial \phi} h_{t-1}^N + a_{t-1}^{ND} \frac{\partial}{\partial \phi} h_{t-1}^D \end{aligned}$$

with the matrix form

$$\begin{pmatrix} \frac{\partial}{\partial \beta_D} h_t^D \\ \frac{\partial}{\partial \beta_D} h_t^N \end{pmatrix} = A_t \begin{pmatrix} \lambda_{t-1}^D - \omega_D \\ 0 \end{pmatrix} + A_t B_{t-1} \begin{pmatrix} \frac{\partial}{\partial \beta_D} h_{t-1}^D \\ \frac{\partial}{\partial \beta_D} h_{t-1}^N \end{pmatrix}.$$

Note that  $A_t B_{t-1}$  and  $A_t \begin{pmatrix} \lambda_{t-1}^D - \omega_D \\ 0 \end{pmatrix}$  are strictly stationary and ergodic, by Theorem 4.27 in Douc, Moulines, and Stoffer (2014), when the top-Lyapunov exponent of the sequence of  $A_t B_{t-1}$  is strictly negative,  $\begin{pmatrix} \frac{\partial}{\partial \beta_D} h_t^D \\ \frac{\partial}{\partial \beta_D} h_t^N \end{pmatrix}$  converges and is strictly stationary.

Likewise, taking the first order derivative of  $h_t^j$  with respect to  $\sigma^D \left( \frac{t-k}{T} \right)$  yields

$$\begin{aligned} \frac{\partial h_t^D}{\partial \sigma^D((t-k)/T)} &= (\beta_D + a_{t-1}^{DD}) \frac{\partial h_{t-1}^D}{\partial \sigma^D((t-k)/T)} + a_t^{DN} \frac{\partial h_t^N}{\partial \sigma^D((t-k)/T)}, \quad k > 1 \\ \frac{\partial h_t^D}{\partial \sigma^D(t/T)} &= 1, \quad \frac{\partial h_t^D}{\partial \sigma^D((t-1)/T)} = a_{t-1}^{DD} + a_t^{DN} a_{t-1}^{ND} \end{aligned}$$

$$\begin{aligned} \frac{\partial h_t^N}{\partial \sigma^D((t-k)/T)} &= (\beta_N + a_{t-1}^{NN}) \frac{\partial h_{t-1}^N}{\partial \sigma^D((t-k)/T)} + a_{t-1}^{ND} \frac{\partial h_{t-1}^D}{\partial \sigma^D((t-k)/T)}, \quad k > 1 \\ \frac{\partial h_t^N}{\partial \sigma^D(t/T)} &= 0, \quad \frac{\partial h_t^N}{\partial \sigma^D((t-1)/T)} = a_{t-1}^{ND}, \end{aligned}$$

and (27) follows. Similarly,  $\begin{pmatrix} \frac{\partial h_t^D}{\partial \sigma^D((t-k)/T)} \\ \frac{\partial h_t^N}{\partial \sigma^D((t-k)/T)} \end{pmatrix}$  is strictly stationary across time  $t$ .

Finally, we can write

$$\begin{pmatrix} \frac{\partial h_t^D}{\partial \sigma^D((t-k)/T)} \\ \frac{\partial h_t^N}{\partial \sigma^D((t-k)/T)} \\ \frac{\partial h_t^D}{\partial \beta_D} \\ \frac{\partial h_t^N}{\partial \beta_D} \end{pmatrix} = \begin{pmatrix} A_t B_{t-1} & 0 \\ 0 & A_t B_{t-1} \end{pmatrix} \begin{pmatrix} \frac{\partial h_{t-1}^D}{\partial \sigma^D((t-k)/T)} \\ \frac{\partial h_{t-1}^N}{\partial \sigma^D((t-k)/T)} \\ \frac{\partial h_{t-1}^D}{\partial \beta_D} \\ \frac{\partial h_{t-1}^N}{\partial \beta_D} \end{pmatrix} + \begin{pmatrix} A_t \begin{pmatrix} \lambda_{t-1}^D - \omega_D \\ 0 \\ 0 \end{pmatrix} \end{pmatrix}.$$

Both  $\begin{pmatrix} \frac{\partial h_t^D}{\partial \sigma^D((t-k)/T)} \\ \frac{\partial h_t^N}{\partial \sigma^D((t-k)/T)} \\ \frac{\partial h_t^D}{\partial \beta_D} \\ \frac{\partial h_t^N}{\partial \beta_D} \end{pmatrix}$  and  $\begin{pmatrix} \frac{\partial h_t^D}{\partial \sigma^D((t-k)/T)} \\ \frac{\partial h_t^N}{\partial \sigma^D((t-k)/T)} \end{pmatrix} \begin{pmatrix} \frac{\partial h_t^D}{\partial \beta_D} & \frac{\partial h_t^N}{\partial \beta_D} \end{pmatrix}$  are strictly stationary, since the top-Lyapunov

exponent of the sequence  $\begin{pmatrix} A_t B_{t-1} & 0 \\ 0 & A_t B_{t-1} \end{pmatrix}$ , same as that of  $A_t B_{t-1}$ , is strictly negative by assumption. ■

**Lemma 5** *When Assumption A1-A4 holds, we have  $\frac{1}{T} \sum_{t=1}^T E \frac{\partial h_t^D}{\partial \theta} = 0$ .*

**Proof.** Similar to the proof of Theorem 1, we only need to show  $\sum_{t=1}^T k \left\| E \begin{pmatrix} \frac{\partial h_t^D}{\partial \sigma^D((t-k)/T)} \\ \frac{\partial h_t^N}{\partial \sigma^D((t-k)/T)} \end{pmatrix} \right\|_\infty <$

$\infty$ . Note that  $E \begin{pmatrix} \frac{\partial h_t^D}{\partial \sigma^D((t-k)/T)} \\ \frac{\partial h_t^N}{\partial \sigma^D((t-k)/T)} \end{pmatrix} = E A_t B_{t-1} A_{t-1} B_{t-2} \dots A_{t-k+2} B_{t-k+1} A_{t-k+1} \Lambda_{t-k} = A (BA)^{k-1} \Lambda$ ,

when  $k > 1$ . Obviously,  $\sum_{t=1}^T k \left\| E \begin{pmatrix} \frac{\partial h_t^D}{\partial \sigma^D((t-k)/T)} \\ \frac{\partial h_t^N}{\partial \sigma^D((t-k)/T)} \end{pmatrix} \right\|_\infty < \infty$ . ■

## 9.2 Appendix B: Derivatives in the multivariate model

We now give the first-order and second-order derivatives of the global log-likelihood function in the multivariate model, given  $\lambda_t$  and  $v$ . Without subscripts  $j$  and ignoring some unnecessary parts, the log-likelihood function is

$$l_t = \log |\Theta| - \sum_{i=1}^n \left( \frac{v_i + 1}{2} \ln \left( 1 + \frac{(\iota_i^\top \text{diag}(\exp(-\lambda_t)) \Theta u_t)^2}{v_i} \right) \right).$$

Then

$$\begin{aligned}
dl_t &= d \log |\Theta| - \sum_{i=1}^n \frac{(v_i + 1) (\iota_i^\top \text{diag}(\exp(-\lambda_t)) \Theta u_t) \exp(-\lambda_{it})}{v_i + (\iota_i^\top \text{diag}(\exp(-\lambda_t)) \Theta u_t)^2} \text{tr} u_t \iota_i^\top d\Theta \\
&= \text{tr}(\Theta^{-1} d\Theta) - \text{tr} \left( \sum_{i=1}^n \frac{(v_i + 1) \exp(-2\lambda_{it}) \iota_i^\top \Theta u_t}{v_i + \exp(-2\lambda_{it}) (\iota_i^\top \Theta u_t)^2} u_t \iota_i^\top d\Theta \right) \\
&= \text{tr} \left[ \left( \Theta^{-1} - \sum_{i=1}^n \frac{(v_i + 1) \exp(-2\lambda_{it}) \iota_i^\top \Theta u_t}{v_i + \exp(-2\lambda_{it}) (\iota_i^\top \Theta u_t)^2} u_t \iota_i^\top \right) d\Theta \right] \\
&= \left[ \text{vec} \left( \Theta^{-1} - \sum_{i=1}^n \iota_i u_t^\top \frac{(v_i + 1) \exp(-2\lambda_{it}) \iota_i^\top \Theta u_t}{v_i + \exp(-2\lambda_{it}) (\iota_i^\top \Theta u_t)^2} \right) \right]^\top d\text{vec} \Theta \\
&= \left[ \text{vec} \left( \Theta^{-1} - \sum_{i=1}^n \iota_i u_t^\top \frac{(v_i + 1) \exp(-2\lambda_{it}) \iota_i^\top \Theta u_t}{v_i + \exp(-2\lambda_{it}) (\iota_i^\top \Theta u_t)^2} \right) \right]^\top D_n d\text{vech} \Theta, \tag{32}
\end{aligned}$$

where  $D_n$  is the duplication matrix so that  $\text{vec} \Theta = D_n \text{vech} \Theta$ . Therefore, the first order derivative of the global log-likelihood function is

$$\begin{aligned}
\frac{\partial L_T(\Theta; \lambda_t, s)}{\partial \text{vech} \Theta} &= -\frac{1}{T} D_n^\top \text{vec} \sum_{i=1}^n \left( \iota_i \sum_{t=1}^T \left( K_h(s - t/T) u_t^\top \frac{(v_i + 1) \exp(-2\lambda_{it}) \iota_i^\top \Theta u_t}{v_i + \exp(-2\lambda_{it}) (\iota_i^\top \Theta u_t)^2} \right) \right) \\
&\quad + D_n^\top \text{vec}(\Theta^{-1}). \tag{33}
\end{aligned}$$

To compute the Hessian matrix, we evaluate the differential of the Jacobian matrix in (32)

$$\begin{aligned}
d\text{vec} D_n^\top \left( \Theta^{-1} - \sum_{i=1}^n \iota_i u_t^\top \frac{(v_i + 1) \exp(-2\lambda_{it}) \iota_i^\top \Theta u_t}{v_i + (\exp(-2\lambda_{it}) \iota_i^\top \Theta u_t)^2} \right) D_n \\
&= D_n^\top d\text{vec} \Theta^{-1} - D_n^\top \text{vec} \sum_{i=1}^n \left( d \frac{(v_i + 1) \exp(-2\lambda_{it}) \iota_i^\top \Theta u_t}{v_i + \exp(-2\lambda_{it}) (\iota_i^\top \Theta u_t)^2} \right) \iota_i u_t^\top \\
&= D_n^\top d\text{vec} \Theta^{-1} - D_n^\top \sum_{i=1}^n \frac{\left( v_i - \exp(-2\lambda_{it}) (\iota_i^\top \Theta u_t)^2 \right) (v_i + 1) \exp(-2\lambda_{it})}{\left( v_i + \exp(-2\lambda_{it}) (\iota_i^\top \Theta u_t)^2 \right)^2} \text{vec}(\iota_i \iota_i^\top d\Theta u_t u_t^\top) \\
&= -D_n^\top (\Theta^{-1} \otimes \Theta^{-1}) D_n d\text{vech} \Theta \\
&\quad - D_n^\top \sum_{i=1}^n \frac{\left( v_i - \exp(-2\lambda_{it}) (\iota_i^\top \Theta u_t)^2 \right) (v_i + 1) \exp(-2\lambda_{it})}{\left( v_i + \exp(-2\lambda_{it}) (\iota_i^\top \Theta u_t)^2 \right)^2} (u_t u_t^\top) \otimes (\iota_i \iota_i^\top) D_n d\text{vech} \Theta.
\end{aligned}$$

The Hessian matrix of the global log-likelihood function is thus

$$\begin{aligned}
&\frac{\partial^2 L_T(\Theta; \lambda_t, s)}{\partial \text{vech} \Theta \partial (\text{vech} \Theta)^\top} \\
&= -D_n^\top \left( \sum_{i=1}^n \left( \sum_{t=1}^T \frac{K_h(s - t/T) \left( v_i - \exp(-2\lambda_{it}) (\iota_i^\top \Theta u_t)^2 \right) (v_i + 1)}{T \left( v_i + \exp(-2\lambda_{it}) (\iota_i^\top \Theta u_t)^2 \right)^2 \exp(2\lambda_{it})} u_t u_t^\top \right) \otimes (\iota_i \iota_i^\top) \right) D_n \\
&\quad - D_n^\top (\Theta^{-1} \otimes \Theta^{-1}) D_n \tag{34}
\end{aligned}$$

■

### 9.3 Appendix C: tables and figures

Panel A: cap based deciles of NYSE/AMEX/NASDAQ stocks

decile	mean		s.e.		median		T stat.	avg. no.
	day(%)	night(%)	day(%)	night(%)	day(%)	night(%)		
1-small	0.0942	0.0606	0.0107	0.0079	0.1184	0.0642	2.5290	493.3080
2	0.0964	0.0323	0.0093	0.0060	0.1380	0.0389	5.8126	571.2961
3	0.0793	0.0308	0.0096	0.0055	0.1436	0.0371	4.3742	604.6714
4	0.0601	0.0392	0.0111	0.0061	0.1318	0.0456	1.6503	630.0765
5	0.0484	0.0414	0.0130	0.0067	0.1233	0.0546	0.4786	643.4898
6	0.0426	0.0388	0.0137	0.0070	0.1161	0.0552	0.2447	655.4365
7	0.0401	0.0376	0.0141	0.0072	0.1051	0.0492	0.1546	664.1175
8	0.0416	0.0253	0.0143	0.0073	0.1101	0.0409	1.0122	673.6501
9	0.0324	0.0324	0.0136	0.0073	0.1049	0.0487	0.0003	683.3976
10-large	0.0155	0.0270	0.0126	0.0081	0.0543	0.0441	-0.7725	699.5996

Panel B: cap based deciles of NASDAQ stocks

size	mean		s.e.		median		T stat.	avg. no.
	day(%)	night(%)	day(%)	night(%)	day(%)	night(%)		
1-small	0.1056	0.0623	0.0135	0.0104	0.1110	0.0599	2.5372	262.8418
2	0.0902	0.0497	0.0106	0.0073	0.1254	0.0542	3.1557	305.5648
3	0.1060	0.0238	0.0102	0.0065	0.1531	0.0294	6.7834	321.6926
4	0.0670	0.0461	0.0107	0.0064	0.1325	0.0548	1.6795	335.6151
5	0.0645	0.0436	0.0130	0.0070	0.1401	0.0546	1.4182	346.0700
6	0.0565	0.0552	0.0157	0.0080	0.1373	0.0670	0.0753	351.3748
7	0.0471	0.0478	0.0159	0.0081	0.1294	0.0690	-0.0388	358.4989
8	0.0382	0.0575	0.0162	0.0082	0.1069	0.0765	-1.0609	361.1587
9	0.0341	0.0439	0.0169	0.0086	0.1124	0.0569	-0.5148	368.2421
10-large	0.0028	0.0672	0.0184	0.0108	0.0686	0.0862	-3.0218	378.3676

Panel C: cap based deciles of NYSE stocks

decile	mean		s.e.		median		T stat.	avg. no.
	day(%)	night(%)	day(%)	night(%)	day(%)	night(%)		
1-small	0.0793	0.0063	0.0108	0.0056	0.1021	0.0067	6.0203	219.2011
2	0.0474	0.0014	0.0100	0.0053	0.0866	0.0044	4.0480	231.0752
3	0.0443	0.0088	0.0110	0.0057	0.0919	0.0134	2.8591	232.3123
4	0.0383	0.0145	0.0122	0.0062	0.0883	0.0136	1.7341	232.0882
5	0.0428	0.0117	0.0134	0.0068	0.0947	0.0128	2.0683	232.8432
6	0.0413	0.0134	0.0135	0.0069	0.0927	0.0152	1.8429	233.4402
7	0.0355	0.0142	0.0131	0.0068	0.0871	0.0237	1.4465	235.8511
8	0.0322	0.0190	0.0126	0.0068	0.0855	0.0325	0.9232	236.4532
9	0.0255	0.0242	0.0127	0.0073	0.0698	0.0352	0.0895	238.8781
10-large	0.0179	0.0164	0.0120	0.0079	0.0455	0.0342	0.1040	240.4777

This table gives the summary statistics for the intraday and overnight returns: mean, median, standard error of the mean, T statistics, and the average number of stocks. The T statistics are used to test the null hypothesis that the mean value of overnight returns equals the mean value of intraday returns.

Table A.1: Descriptive statistics for intraday and overnight returns



Panel A: cap based deciles of NYSE/AMEX/NASDAQ stocks							
decile	$\delta$	$\mu_D$	$\mu_N$	$\Pi_{11}$	$\Pi_{12}$	$\Pi_{21}$	$\Pi_{22}$
1-small	-0.0306 (0.0282)	0.0722 (0.0113)	0.0457 (0.0081)	0.2304 (0.0247)	0.0028 (0.0267)	0.0592 (0.0170)	0.1504 (0.0224)
2	-0.1375 (0.0391)	0.0722 (0.0097)	0.0183 (0.0063)	0.2526 (0.0239)	-0.0045 (0.0340)	0.1002 (0.0151)	0.1359 (0.0251)
3	-0.2024 (0.0514)	0.0643 (0.0101)	0.0230 (0.0060)	0.2038 (0.0247)	-0.0365 (0.0406)	0.0838 (0.0151)	0.0368 (0.0268)
4	-0.2375 (0.0495)	0.0557 (0.0117)	0.0362 (0.0065)	0.0827 (0.0260)	-0.0115 (0.0477)	0.0604 (0.0157)	-0.0171 (0.0281)
5	-0.2247 (0.0573)	0.0478 (0.0136)	0.0424 (0.0070)	0.0205 (0.0299)	-0.0070 (0.0550)	0.0411 (0.0158)	-0.0719 (0.0284)
6	-0.1841 (0.0570)	0.0428 (0.0142)	0.0403 (0.0072)	0.0079 (0.0280)	-0.0111 (0.0562)	0.0305 (0.0153)	-0.0726 (0.0290)
7	-0.1877 (0.0537)	0.0399 (0.0145)	0.0397 (0.0074)	0.0158 (0.0261)	-0.0101 (0.0524)	0.0351 (0.0143)	-0.0920 (0.0281)
8	-0.1887 (0.0573)	0.0411 (0.0147)	0.0266 (0.0074)	0.0111 (0.0274)	0.0021 (0.0551)	0.0327 (0.0148)	-0.1051 (0.0290)
9	-0.1673 (0.0547)	0.0312 (0.0140)	0.0346 (0.0074)	0.0375 (0.0257)	0.0018 (0.0520)	0.0467 (0.0143)	-0.1117 (0.0280)
10-large	-0.0482 (0.0459)	0.0164 (0.0128)	0.0289 (0.0081)	-0.0685 (0.0247)	0.0094 (0.0440)	0.0498 (0.0170)	-0.1012 (0.0286)
Panel B: cap based deciles of NYSE stocks							
decile	$\delta$	$\mu_D$	$\mu_N$	$\Pi_{11}$	$\Pi_{12}$	$\Pi_{21}$	$\Pi_{22}$
1-small	-0.3385 (0.0734)	0.0699 (0.0114)	0.0027 (0.0062)	0.1242 (0.0393)	-0.0412 (0.0804)	0.0483 (0.0225)	-0.0361 (0.0391)
2	-0.2984 (0.0895)	0.0454 (0.0105)	-0.0016 (0.0056)	0.0441 (0.0366)	-0.0351 (0.0832)	0.0644 (0.0257)	-0.0779 (0.0531)
3	-0.2602 (0.0875)	0.0434 (0.0114)	0.0069 (0.0059)	0.0253 (0.0360)	-0.0260 (0.0856)	0.0630 (0.0253)	-0.0941 (0.0526)
4	-0.2736 (0.0691)	0.0380 (0.0126)	0.0144 (0.0064)	0.0098 (0.0312)	0.0004 (0.0696)	0.0383 (0.0193)	-0.0920 (0.0399)
5	-0.2336 (0.0700)	0.0432 (0.0138)	0.0113 (0.0069)	-0.0044 (0.0330)	-0.0122 (0.0684)	0.0377 (0.0187)	-0.1049 (0.0380)
6	-0.2123 (0.0699)	0.0413 (0.0138)	0.0138 (0.0070)	-0.0033 (0.0326)	0.0157 (0.0689)	0.0282 (0.0182)	-0.1199 (0.0359)
7	-0.2305 (0.0644)	0.0347 (0.0134)	0.0147 (0.0069)	0.0225 (0.0300)	0.0063 (0.0629)	0.0335 (0.0164)	-0.1198 (0.0332)
8	-0.1973 (0.0616)	0.0315 (0.0129)	0.0200 (0.0069)	0.0291 (0.0286)	-0.0051 (0.0589)	0.0373 (0.0166)	-0.1165 (0.0318)
9	-0.1558 (0.0587)	0.0257 (0.0130)	0.0258 (0.0074)	0.0060 (0.0275)	-0.0099 (0.0553)	0.0412 (0.0171)	-0.1082 (0.0337)
10-large	-0.0505 (0.0462)	0.0193 (0.0122)	0.0171 (0.0080)	-0.0755 (0.0253)	0.0063 (0.0454)	0.0475 (0.0188)	-0.0945 (0.0300)
Panel C: cap based deciles of NASDAQ stocks							
decile	$\delta$	$\mu_D$	$\mu_N$	$\Pi_{11}$	$\Pi_{12}$	$\Pi_{21}$	$\Pi_{22}$
1-small	0.1181 (0.0240)	0.0824 (0.0134)	0.0526 (0.0106)	0.2004 (0.0194)	0.0284 (0.0264)	0.0086 (0.0155)	0.1359 (0.0190)
2	-0.0246 (0.0295)	0.0698 (0.0107)	0.0349 (0.0075)	0.2347 (0.0213)	-0.0129 (0.0267)	0.0792 (0.0142)	0.1539 (0.0207)
3	-0.0578 (0.0384)	0.0792 (0.0106)	0.0126 (0.0068)	0.2536 (0.0236)	-0.0080 (0.0330)	0.0749 (0.0143)	0.1377 (0.0253)
4	-0.1190 (0.0448)	0.0563 (0.0111)	0.0383 (0.0067)	0.1818 (0.0227)	-0.0323 (0.0345)	0.0796 (0.0139)	0.0554 (0.0231)
5	-0.1717 (0.0451)	0.0613 (0.0137)	0.0420 (0.0073)	0.0631 (0.0257)	-0.0174 (0.0433)	0.0364 (0.0136)	-0.0190 (0.0231)
6	-0.1544 (0.0496)	0.0572 (0.0164)	0.0566 (0.0083)	0.0127 (0.0278)	-0.0250 (0.0473)	0.0238 (0.0132)	-0.0492 (0.0233)
7	-0.1409 (0.0516)	0.0480 (0.0164)	0.0501 (0.0083)	-0.0018 (0.0252)	-0.0150 (0.0475)	0.0149 (0.0127)	-0.0628 (0.0238)
8	-0.1346 (0.0469)	0.0377 (0.0167)	0.0608 (0.0085)	0.0200 (0.0228)	-0.0025 (0.0436)	0.0247 (0.0117)	-0.0754 (0.0229)
9	-0.1006 (0.0486)	0.0335 (0.0173)	0.0467 (0.0087)	0.0383 (0.0225)	-0.0129 (0.0445)	0.0374 (0.0115)	-0.0923 (0.0224)
10-large	0.0152 (0.0414)	0.0009 (0.0187)	0.0737 (0.0110)	-0.0545 (0.0234)	0.0342 (0.0367)	0.0541 (0.0122)	-0.0988 (0.0223)

Estimates of mean equation parameters for cap based deciles, with standard errors in parentheses. The mean equation is specified as  $\begin{pmatrix} 1 & \delta \\ 0 & 1 \end{pmatrix} \begin{pmatrix} r_t^D \\ r_t^N \end{pmatrix} = \begin{pmatrix} \mu_D \\ \mu_N \end{pmatrix} + \begin{pmatrix} \Pi_{11} & \Pi_{12} \\ \Pi_{21} & \Pi_{22} \end{pmatrix} \begin{pmatrix} r_{t-1}^D \\ r_{t-1}^N \end{pmatrix} + \begin{pmatrix} u_t^D \\ u_t^N \end{pmatrix}$ .

Table A.2: Estimates of the mean equations

	decile1	decile2	decile3	decile4	decile5	decile6	decile7	decile8	decile9	decile10
cap nyse/amex/nasdaq	0.0230	0.0676	0.1252	0.2298	0.3747	0.6418	1.1669	2.1138	4.8682	38.9714
cap nyse	0.0993	0.2274	0.3800	0.6326	1.0605	1.7561	2.5854	4.9514	10.3084	56.4557
cap nasdaq	0.0169	0.0424	0.0786	0.1262	0.2099	0.3456	0.6023	1.0475	2.1272	22.7218
beta	1.5301	1.2385	1.0712	0.9612	0.8637	0.7639	0.6643	0.5264	0.3531	0.2501
std. dev.	0.0612	0.0391	0.0315	0.0271	0.0236	0.0212	0.0185	0.0157	0.0129	0.0091

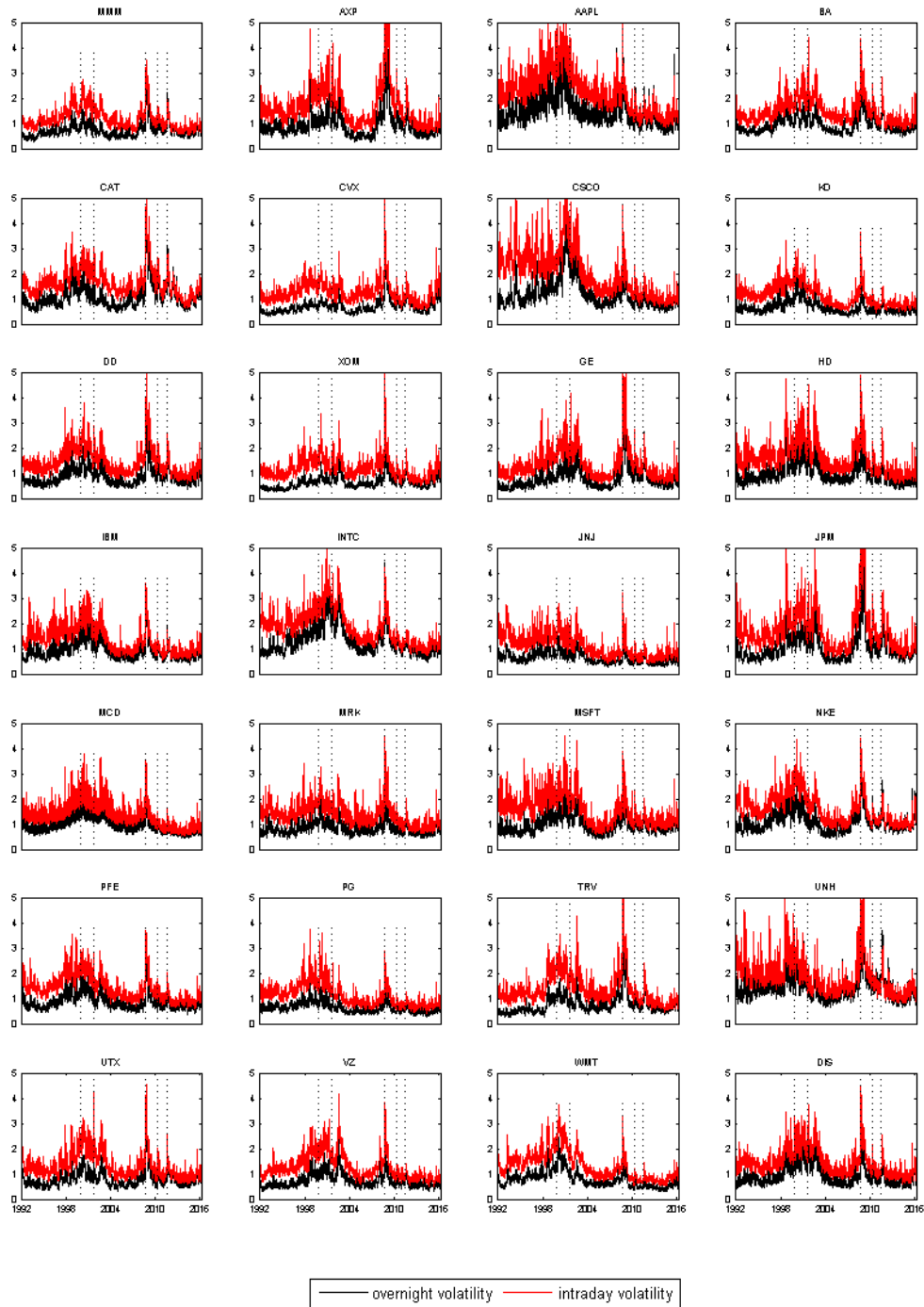
The first three rows show the average capitalization value (in million) of cap based deciles for NYSE/AMEX/NASDAQ, NYSE, and NASDAQ, respectively. Since the capitalization value varies across years, we present the average value in 2015 instead of the whole period. The fourth (last) row shows the average beta (standard deviation) value in beta (standard deviation) sorted deciles.

Table A.3: Average capitalization, beta and standard deviation values

	decile1	decile2	decile3	decile4	decile5	decile6	decile7	decile8	decile9	decile10
$\beta_D$	0.9508 (0.0077)	0.9277 (0.0106)	0.9276 (0.0101)	0.9261 (0.0100)	0.9215 (0.0103)	0.9060 (0.0117)	0.9302 (0.0087)	0.9344 (0.0077)	0.9418 (0.0068)	0.9499 (0.0056)
$\gamma_D$	0.0485 (0.0049)	0.0568 (0.0051)	0.0619 (0.0054)	0.0605 (0.0055)	0.0562 (0.0051)	0.0528 (0.0048)	0.0426 (0.0042)	0.0414 (0.0042)	0.0372 (0.0041)	0.0277 (0.0035)
$\rho_D$	0.0332 (0.0044)	0.0503 (0.0054)	0.0402 (0.0053)	0.0413 (0.0056)	0.0312 (0.0055)	0.0348 (0.0055)	0.0280 (0.0050)	0.0281 (0.0049)	0.0349 (0.0048)	0.0322 (0.0043)
$\gamma_D^*$	-0.0093 (0.0026)	-0.0097 (0.0029)	-0.0162 (0.0030)	-0.0208 (0.0032)	-0.0223 (0.0032)	-0.0268 (0.0035)	-0.0260 (0.0031)	-0.0272 (0.0030)	-0.0319 (0.0030)	-0.0363 (0.0031)
$\rho_D^*$	-0.0020 (0.0023)	-0.0102 (0.0029)	-0.0168 (0.0031)	-0.0171 (0.0031)	-0.0216 (0.0033)	-0.0219 (0.0035)	-0.0232 (0.0031)	-0.0274 (0.0032)	-0.0277 (0.0031)	-0.0282 (0.0031)
$\nu_D$	10.7398 (1.2586)	9.7630 (1.1054)	9.1173 (0.9099)	7.5708 (0.6376)	9.0529 (0.8902)	11.0662 (1.2855)	11.3517 (1.3326)	11.1961 (1.2980)	10.4456 (1.1378)	9.5211 (1.0101)
$\omega_D$	-0.4778 (0.0297)	-0.6712 (0.0273)	-0.6608 (0.0268)	-0.5677 (0.0261)	-0.4206 (0.0240)	-0.3241 (0.0216)	-0.2966 (0.0224)	-0.3039 (0.0228)	-0.3781 (0.0239)	-0.4399 (0.0232)
$\beta_N$	0.9575 (0.0060)	0.9355 (0.0083)	0.9396 (0.0073)	0.9447 (0.0069)	0.9342 (0.0080)	0.9308 (0.0083)	0.9417 (0.0074)	0.9394 (0.0075)	0.9480 (0.0065)	0.9531 (0.0058)
$\gamma_N$	0.0415 (0.0046)	0.0555 (0.0052)	0.0537 (0.0052)	0.0527 (0.0052)	0.0504 (0.0055)	0.0502 (0.0055)	0.0442 (0.0053)	0.0480 (0.0056)	0.0491 (0.0056)	0.0363 (0.0048)
$\rho_N$	0.0522 (0.0047)	0.0582 (0.0052)	0.0538 (0.0050)	0.0557 (0.0052)	0.0545 (0.0053)	0.0515 (0.0052)	0.0433 (0.0049)	0.0501 (0.0052)	0.0471 (0.0048)	0.0359 (0.0043)
$\gamma_N^*$	-0.0125 (0.0024)	-0.0195 (0.0030)	-0.0199 (0.0029)	-0.0160 (0.0027)	-0.0222 (0.0031)	-0.0236 (0.0033)	-0.0222 (0.0030)	-0.0260 (0.0034)	-0.0254 (0.0032)	-0.0330 (0.0034)
$\rho_N^*$	-0.0056 (0.0026)	-0.0106 (0.0030)	-0.0176 (0.0030)	-0.0177 (0.0029)	-0.0211 (0.0031)	-0.0227 (0.0032)	-0.0268 (0.0031)	-0.0275 (0.0033)	-0.0291 (0.0034)	-0.0311 (0.0032)
$\nu_N$	7.1157 (0.5842)	6.6378 (0.4938)	6.1400 (0.4245)	5.1110 (0.3100)	4.9166 (0.2870)	4.8815 (0.2850)	4.6815 (0.2682)	4.3985 (0.2437)	4.3945 (0.2389)	5.1849 (0.3222)
$\omega_N$	-0.9078 (0.0340)	-1.2087 (0.0293)	-1.3144 (0.0294)	-1.2991 (0.0309)	-1.2501 (0.0274)	-1.2194 (0.0263)	-1.2254 (0.0268)	-1.2657 (0.0279)	-1.3134 (0.0305)	-1.0869 (0.0272)

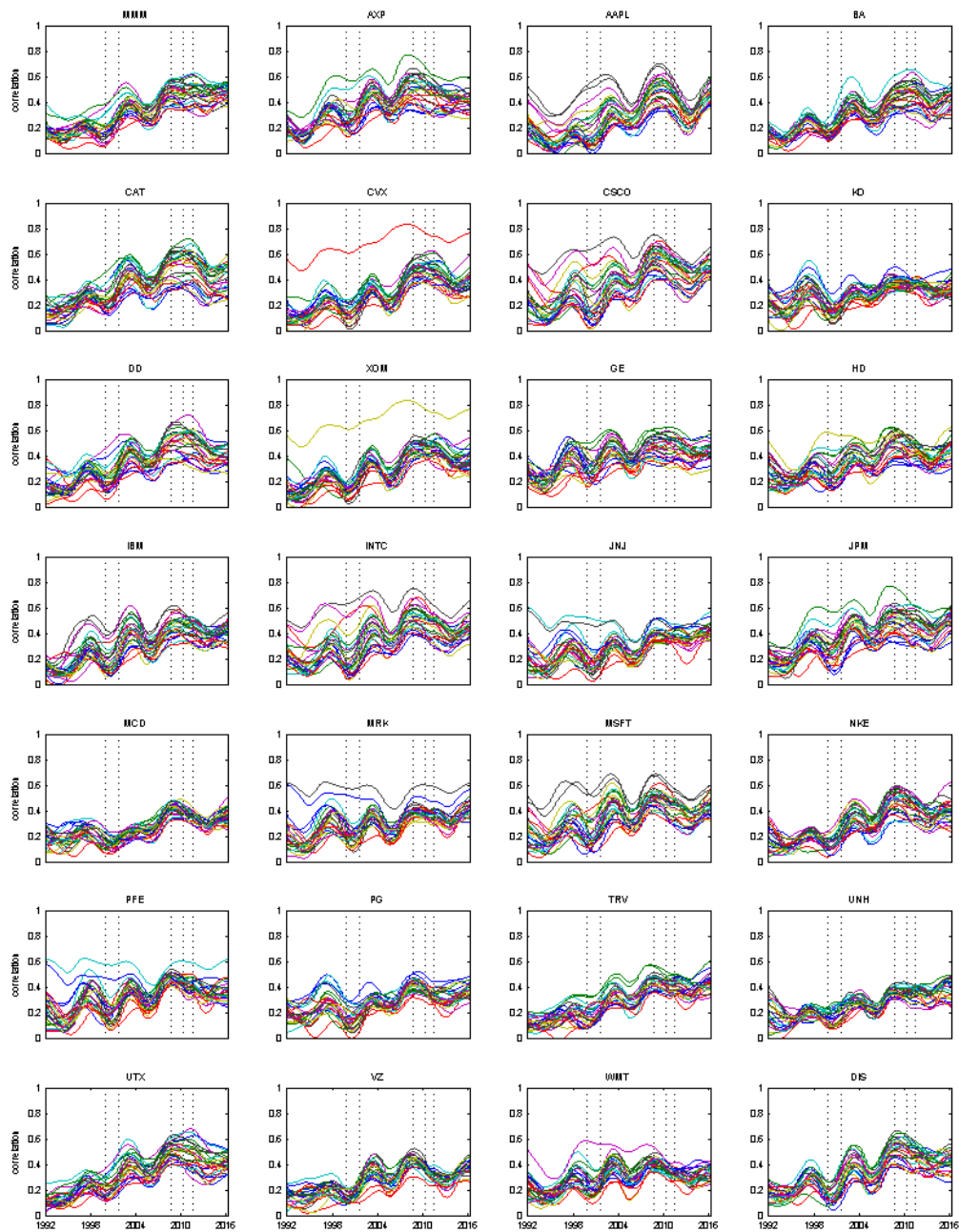
Estimates of the dynamic parameters for cap based portfolios with standard errors in parentheses.

Table A.4: Estimates of the dynamic parameters for cap based deciles: NYSE/AMEX/NASDAQ



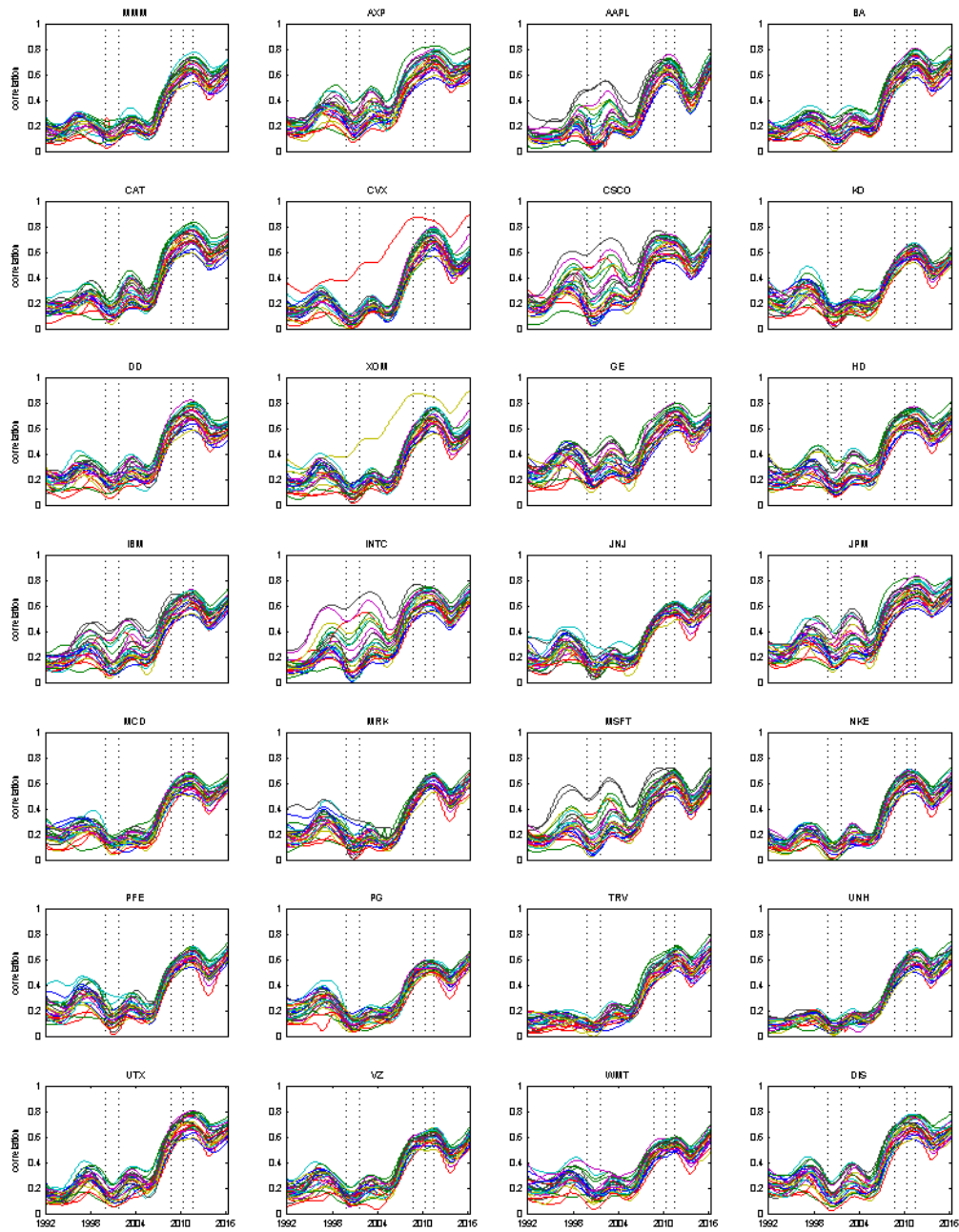
This figure shows the estimated intraday (in red) and overnight (in black) volatilities,  $\sqrt{\frac{\nu_j}{\nu_j - 2} \exp(2\lambda_t^j + 2\sigma^j(\frac{t}{T}))}$ , based on the univariate coupled component model, with one subplot for each stock. The five dashed vertical lines from left to right represent the dates: 10 March 2000 (dot-com bubble), 17 September 2011 (the September 11 attacks), 16 September 2008 (financial crisis), 6 May 2010 (flash crash) and 1 August 2011 (August 2011 stock markets fall), respectively.

Figure A.1: Intraday and overnight volatilities of Dow Jones stocks



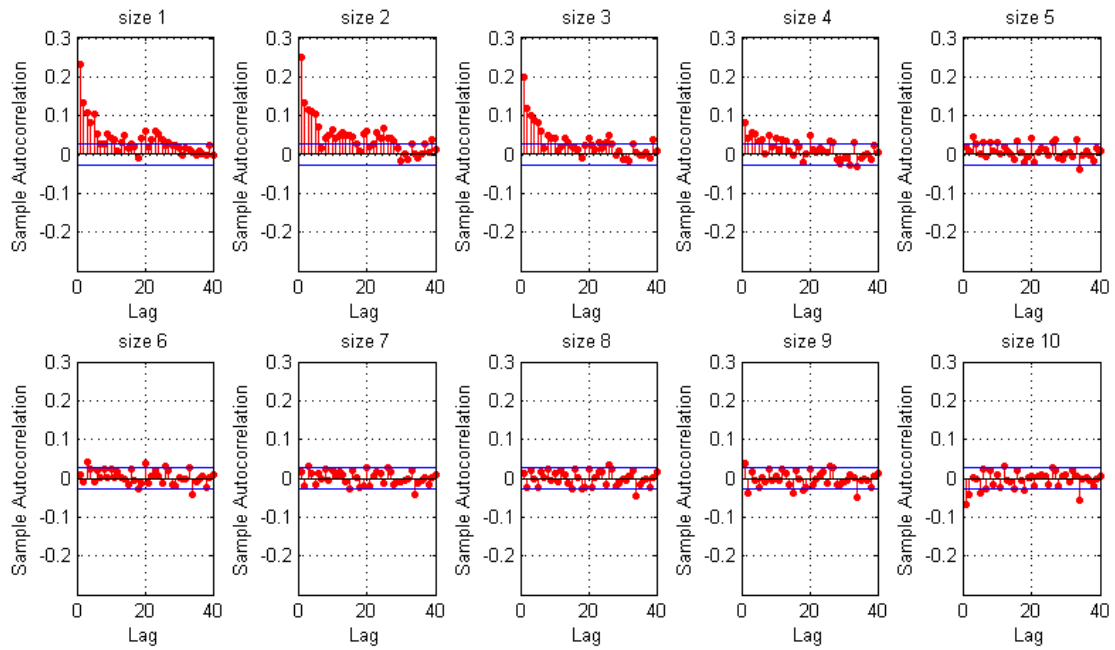
Each panel presents the long run intraday correlations between that individual stock and the remaining stocks, as implied by the multivariate coupled component model. The five dashed vertical lines from left to right represent the dates: 10 March 2000 (dot-com bubble), 17 September 2011 (the September 11 attacks), 16 September 2008 (financial crisis), 6 May 2010 (flash crash) and 1 August 2011 (August 2011 stock markets fall), respectively.

Figure A.2: Long run intraday correlations between Dow Jones stocks

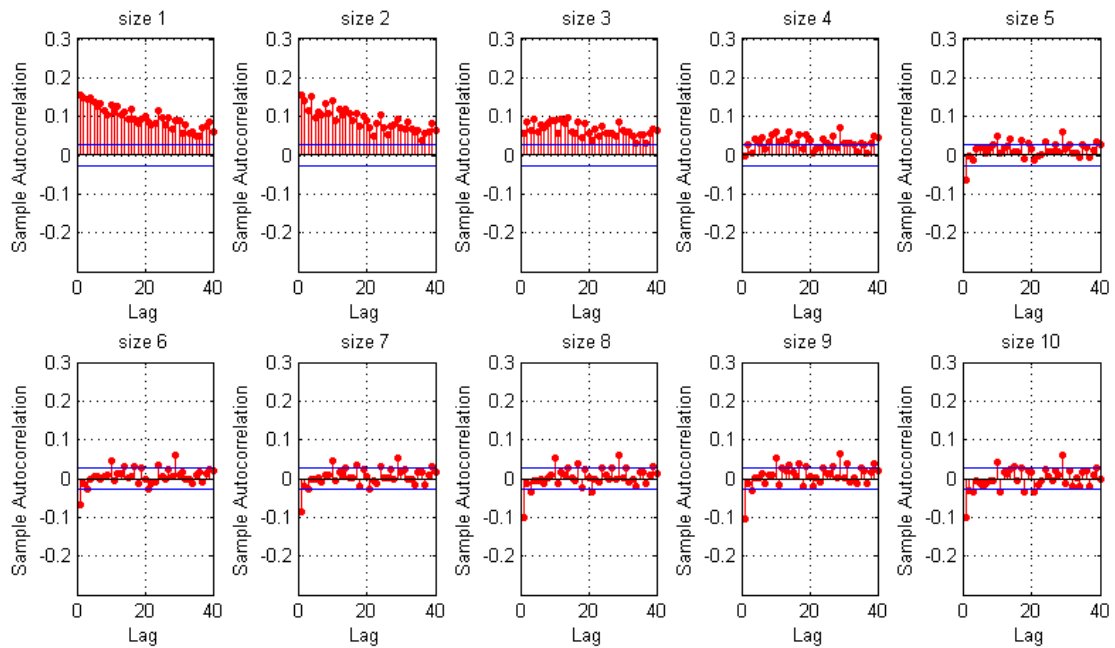


Each panel presents the long run overnight correlations between that stock and the remaining stocks, as implied by the multivariate coupled component model. The five dashed vertical lines from left to right indicate the dates: 10 March 2000 (dot-com bubble), 11 September 2001 (the September 11 attacks), 16 September 2008 (financial crisis), 6 May 2010 (flash crash) and 1 August 2011 (August 2011 stock markets fall), respectively.

Figure A.3: Long run overnight correlations between Dow Jones stocks



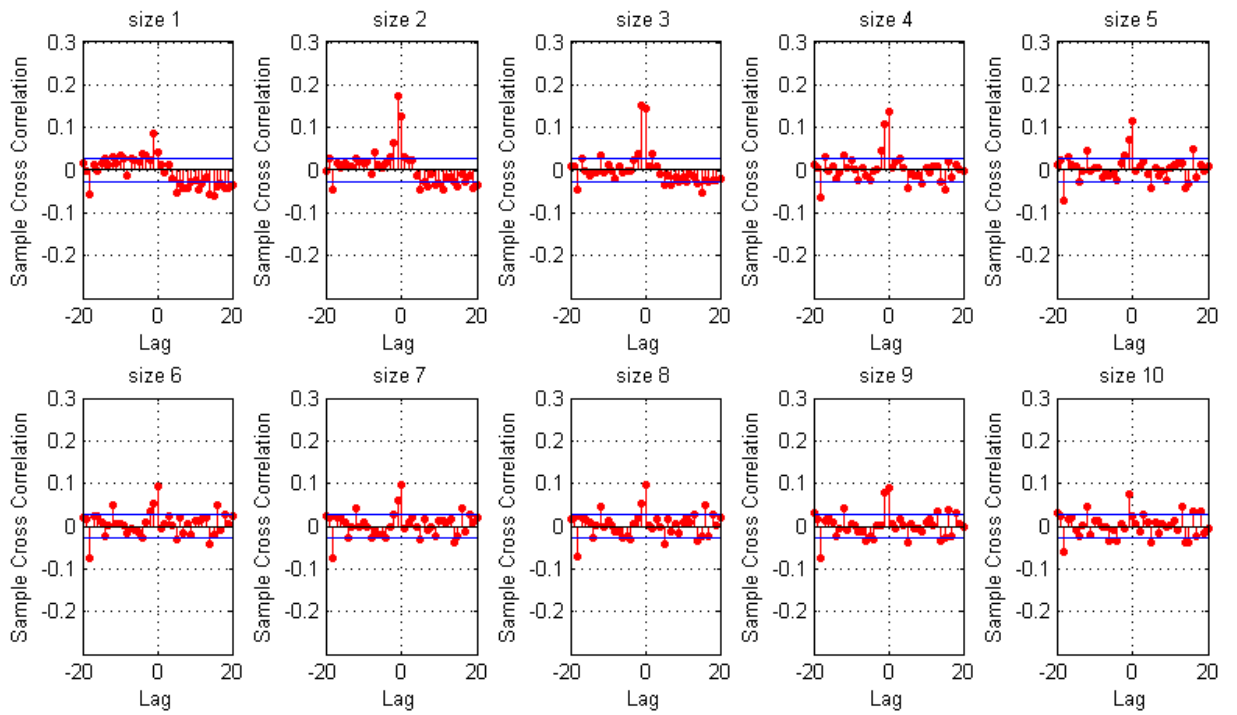
(a) intraday



(b) overnight

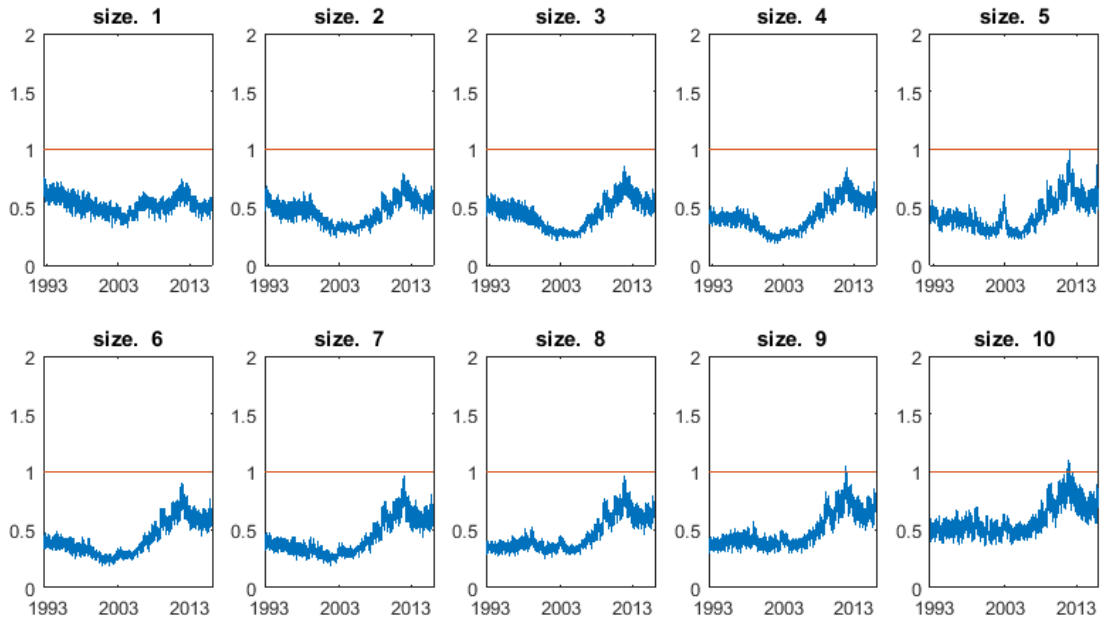
This figure plots the autocorrelations of intraday (overnight) returns for cap based portfolios on NYSE/AMEX/NASDAQ stocks in Panel A (Panel B).

Figure A.4: Autocorrelations of intraday and overnight returns

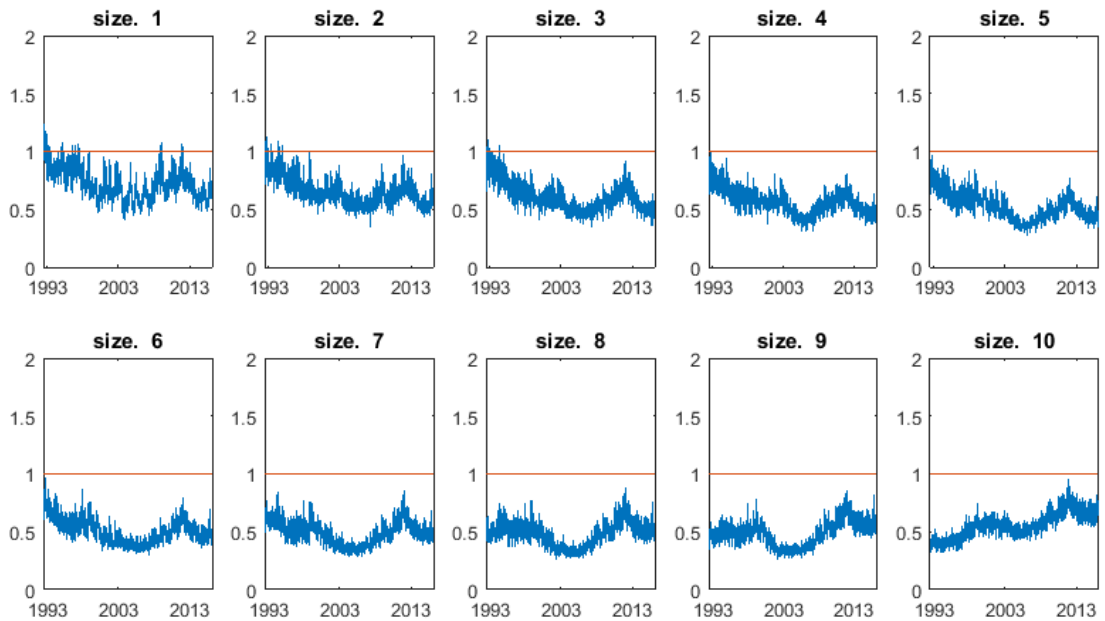


Cross correlations between overnight and intraday returns,  $r_t^N$  and  $r_{t+Lag}^D$ , for the cap based portfolios in NYSE/AMEX/NASDAQ

Figure A.5: Autocorrelation of overnight returns: NYSE/AMEX/NASDAQ



(a) NYSE

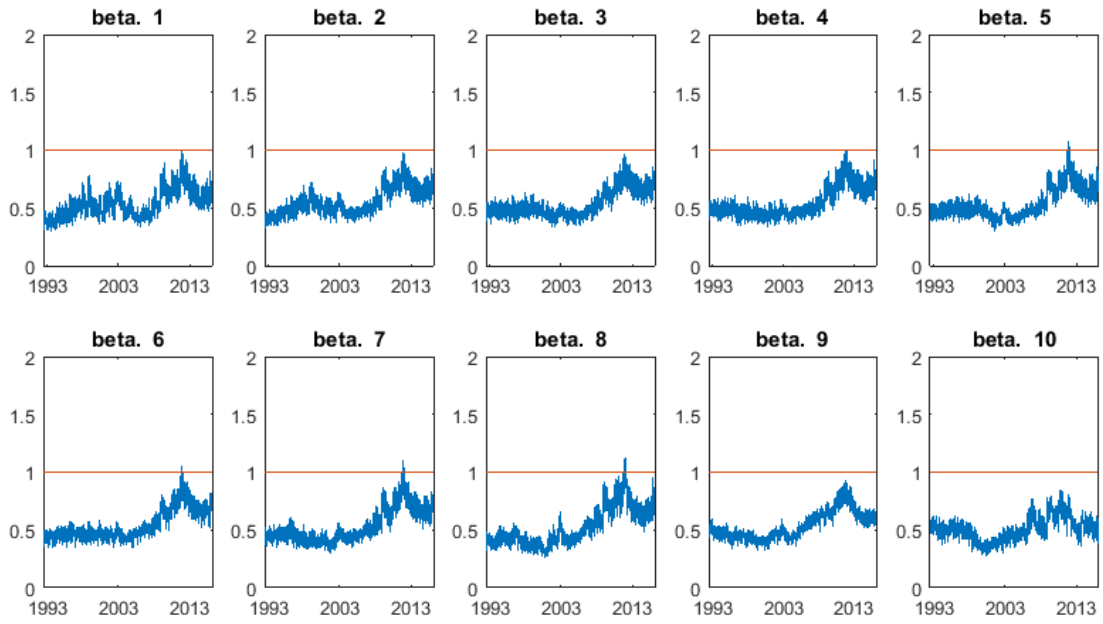


(b) NASDAQ

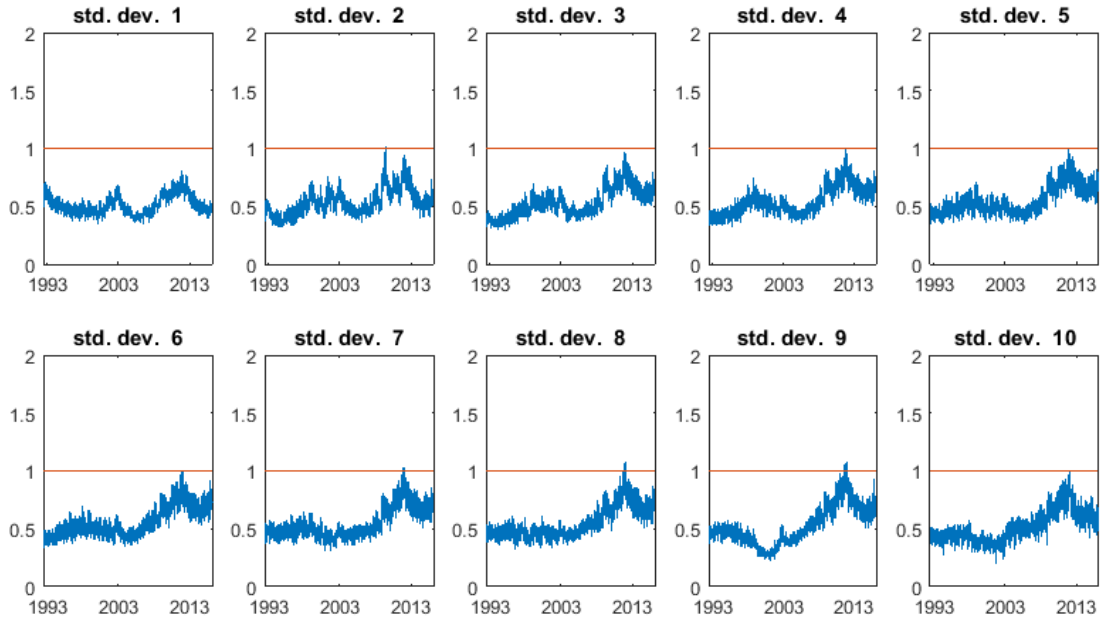
Panel A (Panel B) plots the ratio of overnight to intraday volatility for cap based portfolios for NYSE (NASDAQ) stocks: decile 1 with the smallest capitalization value and decile 10 with the largest capitalization value. Intraday and overnight volatilities are defined as  $\sqrt{\frac{\nu_j}{\nu_j - 2} \exp(2\lambda_t^j + 2\sigma^j(\frac{t}{T}))}$ , for  $j = D, N$ , respectively.

Figure A.6: Ratio of overnight to intraday volatility for cap based portfolios: NYSE and NASDAQ





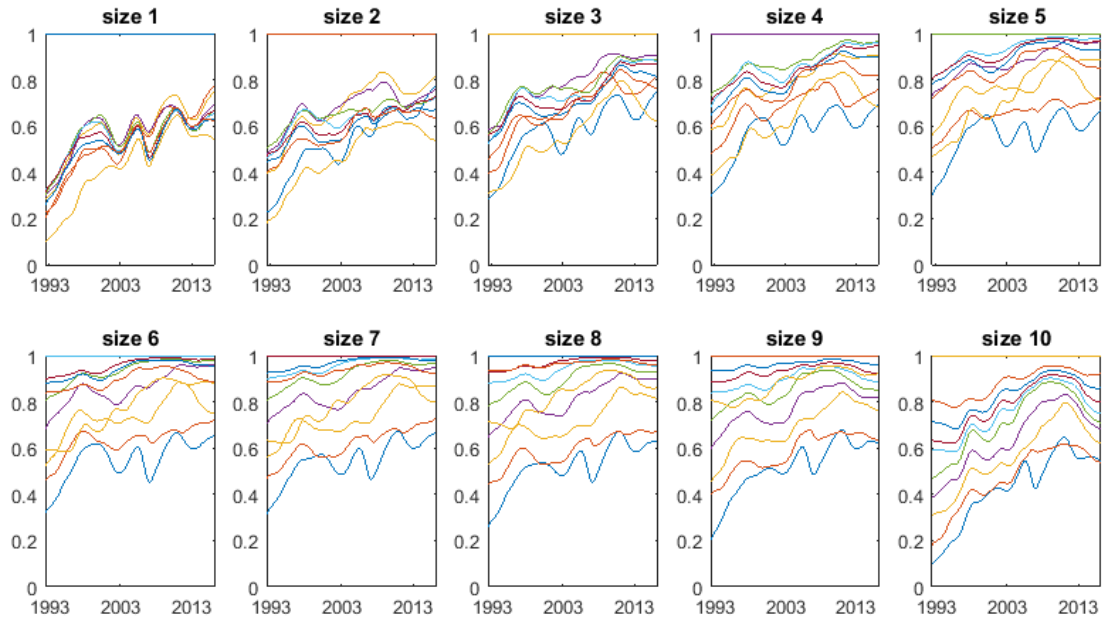
(a) beta based deciles



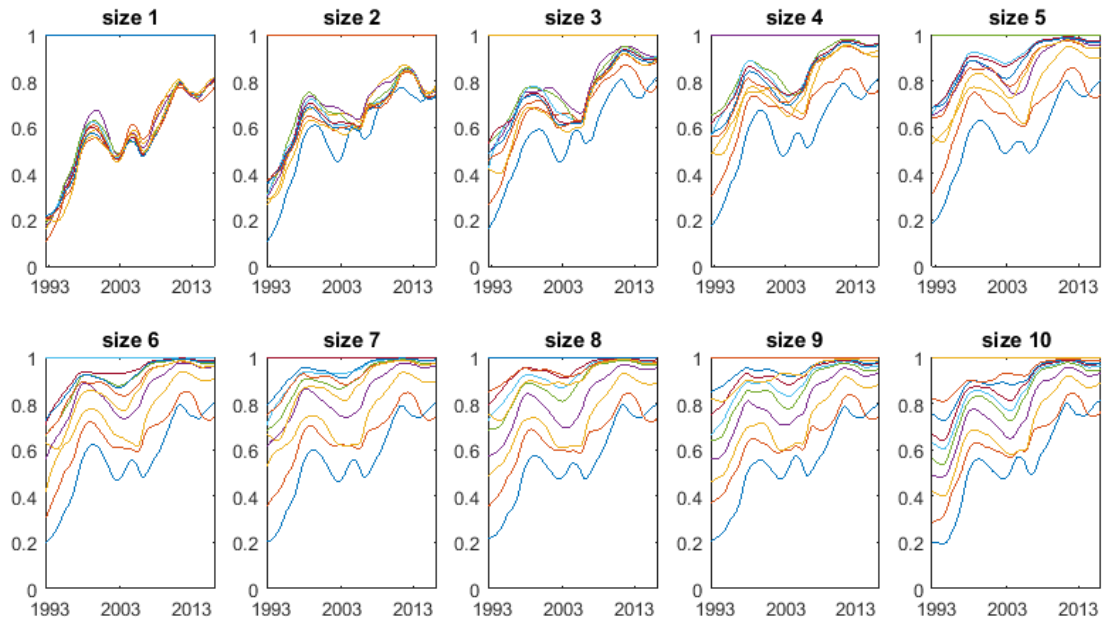
(b) standard deviation based deciles

Panel A plots the ratio of overnight to intraday volatility for beta sorted deciles. Decile 1 has the largest beta, around 1.53 on average, while decile 10 has the smallest beta, around 0.25 on average. Panel B plots the ratio for standard deviation sorted deciles. Decile 1 has the largest standard deviation, around 0.06 on average, and decile 10 has the smallest standard deviation, around 0.009 on average. Intraday and overnight volatilities are defined as  $\sqrt{\frac{\nu_j}{\nu_j-2} \exp(2\lambda_t^j + 2\sigma^j(\frac{t}{T}))}$ , for  $j = D, N$ , respectively.

Figure A.7: Ratio of overnight to intraday volatility for beta or standard deviation sorted portfolios: NYSE/AMEX/ NASDAQ



(a) intraday correlations



(b) overnight correlations

Each panel presents the long-run intraday correlations between that size decile and the remaining size deciles, as implied by the multivariate coupled component model.

Figure A.8: Long run correlations between cap based deciles

# Online Appendix to a coupled component GARCH model for intraday and overnight volatility\*

Oliver Linton<sup>†</sup>                      Jianbin Wu<sup>‡</sup>  
University of Cambridge              Xiamen University

January 17, 2017

This online appendix contains the following three items. First, we provide the first and second order derivatives of the global. Second, we provide the first and second order conditional moments of  $\lambda_t$ . Third, this document also contains several other figures and tables that are referred to in the main text.

## 1 First-order and second-order moments of $\lambda_t$

The expectation of  $\exp(2\lambda_t^D)$  given  $\mathcal{F}_{t-1}$  is

$$E [\exp(2\lambda_t^D)|\mathcal{F}_{t-1}] = \Lambda_t E [\exp(2\rho_D m_t^N + 2\rho_D^*(m_t^N + 1)\text{sign}(e_t^N))|\mathcal{F}_{t-1}],$$

We can express  $E [\exp(2\rho_D m_t^N + 2\rho_D^*(m_t^N + 1)\text{sign}(e_t^N))|\mathcal{F}_{t-1}]$  as

$$\frac{1}{2} \exp(-2\rho_D) \{ E [\exp((2\rho_D + 2\rho_D^*)(v_N + 1)b_t^N) + \exp((2\rho_D - 2\rho_D^*)(v_N + 1)b_t^N)|\mathcal{F}_{t-1}] \}.$$

Since  $b_t^N$  follows a beta  $(1/2, v_N/2)$  distribution,

$$E [\exp((2\rho_D + 2\rho_D^*)(v_N + 1)b_t^N)] = {}_1F_1(1/2, 1/2 + v_N/2, (2\rho_D + 2\rho_D^*)(v_N + 1)),$$

Hence, we have

$$E [\exp(2\lambda_t^D)|\mathcal{F}_{t-1}] = \frac{1}{2} \exp(-2\rho_D) \Lambda_t {}_1F_1(1/2, 1/2 + v_N/2, (2\rho_D + 2\rho_D^*)(v_N + 1)) \\ + \frac{1}{2} \exp(-2\rho_D) \Lambda_t {}_1F_1(1/2, 1/2 + v_N/2, (2\rho_D - 2\rho_D^*)(v_N + 1)).$$

---

\*We would like to thank Piet Sercu, Haihan Tang and Chen Wang for helpful comments.

<sup>†</sup>Faculty of Economics, Austin Robinson Building, Sidgwick Avenue, Cambridge, CB3 9DD. Email: ob120@cam.ac.uk. Thanks to the Cambridge INET for financial support.

<sup>‡</sup>School of Management, Xiamen, China. Email: jianbin.wu@xmu.edu.cn

For the unconditional second order moments, we first write the dynamic function of  $\lambda_t^j$  as

$$\begin{aligned}\lambda_t^D &= \beta_D^{t-1} \lambda_1^D + \omega_D (1 - \beta_D) \sum_{k=1}^{t-1} \beta_D^{k-1} + \gamma_D \sum_{k=1}^{t-1} \beta_D^{k-1} m_{t-k}^D + \rho_D \sum_{k=1}^{t-1} \beta_D^{k-1} m_{t-k+1}^N \\ &\quad + \gamma_D^* \sum_{k=1}^{t-1} \beta_D^{k-1} (m_{t-k}^D + 1) \text{sign}(e_{t-k}^D) + \rho_D^* \sum_{k=1}^{t-1} \beta_D^{k-1} (m_{t-k+1}^N + 1) \text{sign}(e_{t-k+1}^N) \\ \lambda_t^N &= \beta_N^{t-1} \lambda_1^N + \omega_N (1 - \beta_N) \sum_{k=1}^{t-1} \beta_N^{k-1} + \gamma_N \sum_{k=1}^{t-1} m_{t-k}^N \beta_N^{k-1} + \rho_N \sum_{k=1}^{t-1} \beta_N^{k-1} m_{t-k}^D \\ &\quad + \rho_N^* \sum_{k=1}^{t-1} \beta_N^{k-1} (m_{t-k}^D + 1) \text{sign}(e_{t-k}^D) + \gamma_N^* \sum_{k=1}^{t-1} \beta_N^{k-1} (m_{t-k}^N + 1) \text{sign}(e_{t-k}^N)\end{aligned}$$

When  $\lambda_t^j$  starts from infinite past,

$$\begin{aligned}\lambda_t^D &= \omega_D + \gamma_D \sum_{k=1}^{\infty} \beta_D^{k-1} m_{t-k}^D + \rho_D \sum_{k=1}^{\infty} \beta_D^{k-1} m_{t-k+1}^N \\ &\quad + \gamma_D^* \sum_{k=1}^{\infty} \beta_D^{k-1} (m_{t-k}^D + 1) \text{sign}(e_{t-k}^D) + \rho_D^* \sum_{k=1}^{\infty} \beta_D^{k-1} (m_{t-k+1}^N + 1) \text{sign}(e_{t-k+1}^N) \\ \lambda_t^N &= \omega_N + \gamma_N \sum_{k=1}^{\infty} m_{t-k}^N \beta_N^{k-1} + \rho_N \sum_{k=1}^{\infty} \beta_N^{k-1} m_{t-k}^D \\ &\quad + \rho_N^* \sum_{k=1}^{\infty} \beta_N^{k-1} (m_{t-k}^D + 1) \text{sign}(e_{t-k}^D) + \gamma_N^* \sum_{k=1}^{\infty} \beta_N^{k-1} (m_{t-k}^N + 1) \text{sign}(e_{t-k}^N).\end{aligned}\tag{1}$$

The unconditional second order moments  $\text{var}(u_t^D)$  and  $\text{var}(u_t^N)$  are

$$\text{var}(u_t^j) = \frac{v_j}{v_j - 2} E \exp(2\lambda_t^j) E \exp(2\sigma^j(t/T))$$

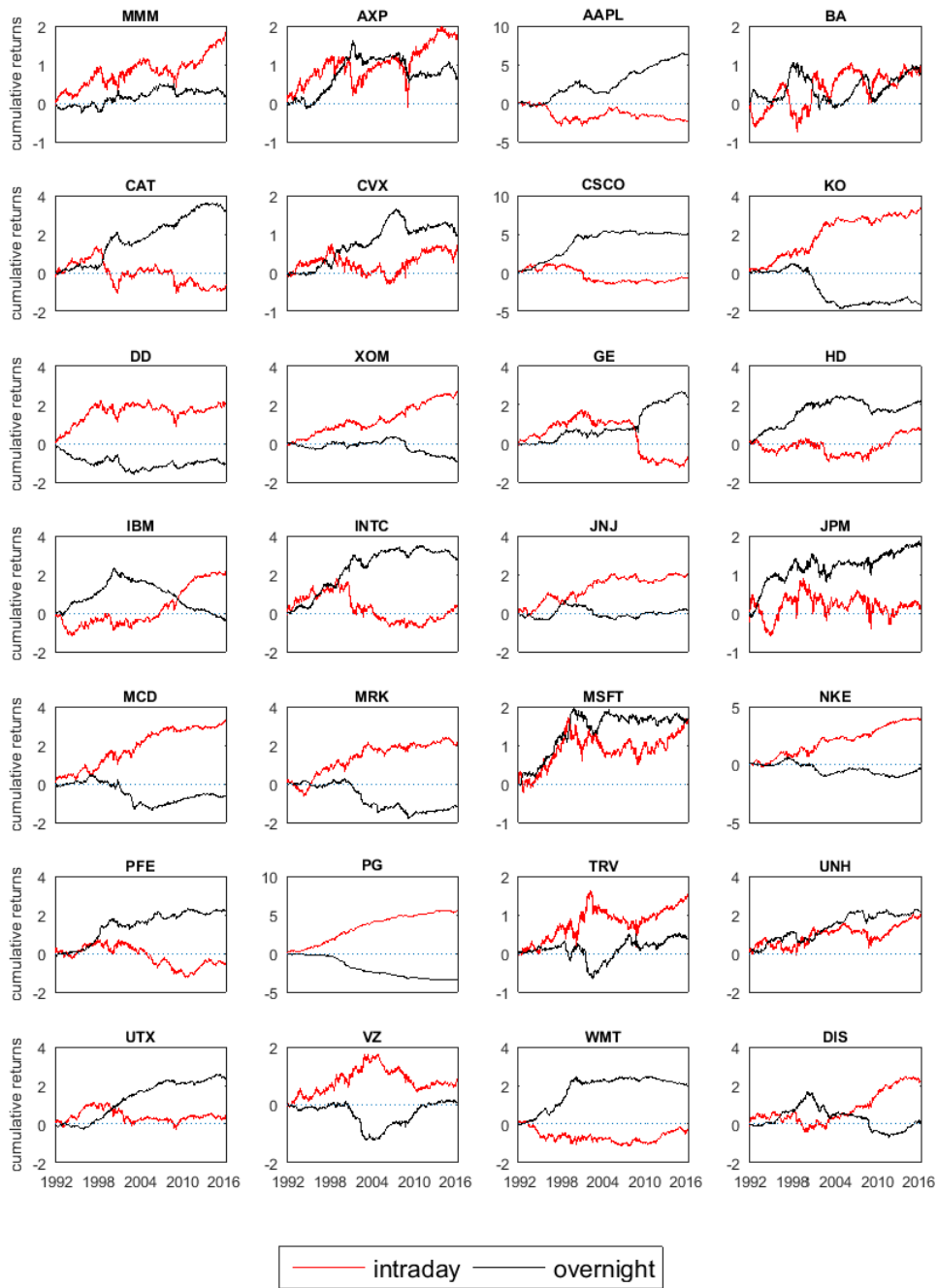
with

$$\begin{aligned}E \exp(2\lambda_t^N) &= \frac{1}{4} \exp\left(2\omega_N - \frac{2(\gamma_N + \rho_N)}{1 - \beta_N}\right) \\ &\quad \left[ \prod_{k=0}^{\infty} {}_1F_1\left(\frac{1}{2}, \frac{v^N + 1}{2}, 2(\gamma_N + \gamma_N^*)(v^N + 1)\beta_N^k\right) + \prod_{k=0}^{\infty} {}_1F_1\left(\frac{1}{2}, \frac{v^N + 1}{2}, 2(\gamma_N - \gamma_N^*)(v^N + 1)\beta_N^k\right) \right] \\ &\quad \left[ \prod_{k=0}^{\infty} {}_1F_1\left(\frac{1}{2}, \frac{v^D + 1}{2}, 2(\rho_N + \rho_N^*)(v^D + 1)\beta_N^k\right) + \prod_{k=0}^{\infty} {}_1F_1\left(\frac{1}{2}, \frac{v^D + 1}{2}, 2(\rho_N - \rho_N^*)(v^D + 1)\beta_N^k\right) \right]\end{aligned}$$

$$\begin{aligned}E \exp(2\lambda_t^D) &= \frac{1}{4} \exp\left(2\omega_D - \frac{2(\gamma_D + \rho_D)}{1 - \beta_D}\right) \\ &\quad \left[ \prod_{k=0}^{\infty} {}_1F_1\left(\frac{1}{2}, \frac{v^D + 1}{2}, 2(\gamma_D + \gamma_D^*)(v^D + 1)\beta_D^k\right) + \prod_{k=0}^{\infty} {}_1F_1\left(\frac{1}{2}, \frac{v^D + 1}{2}, 2(\gamma_D - \gamma_D^*)(v^D + 1)\beta_D^k\right) \right] \\ &\quad \left[ \prod_{k=0}^{\infty} {}_1F_1\left(\frac{1}{2}, \frac{v^N + 1}{2}, 2(\rho_D + \rho_D^*)(v^N + 1)\beta_D^k\right) + \prod_{k=0}^{\infty} {}_1F_1\left(\frac{1}{2}, \frac{v^N + 1}{2}, 2(\rho_D - \rho_D^*)(v^N + 1)\beta_D^k\right) \right].\end{aligned}$$

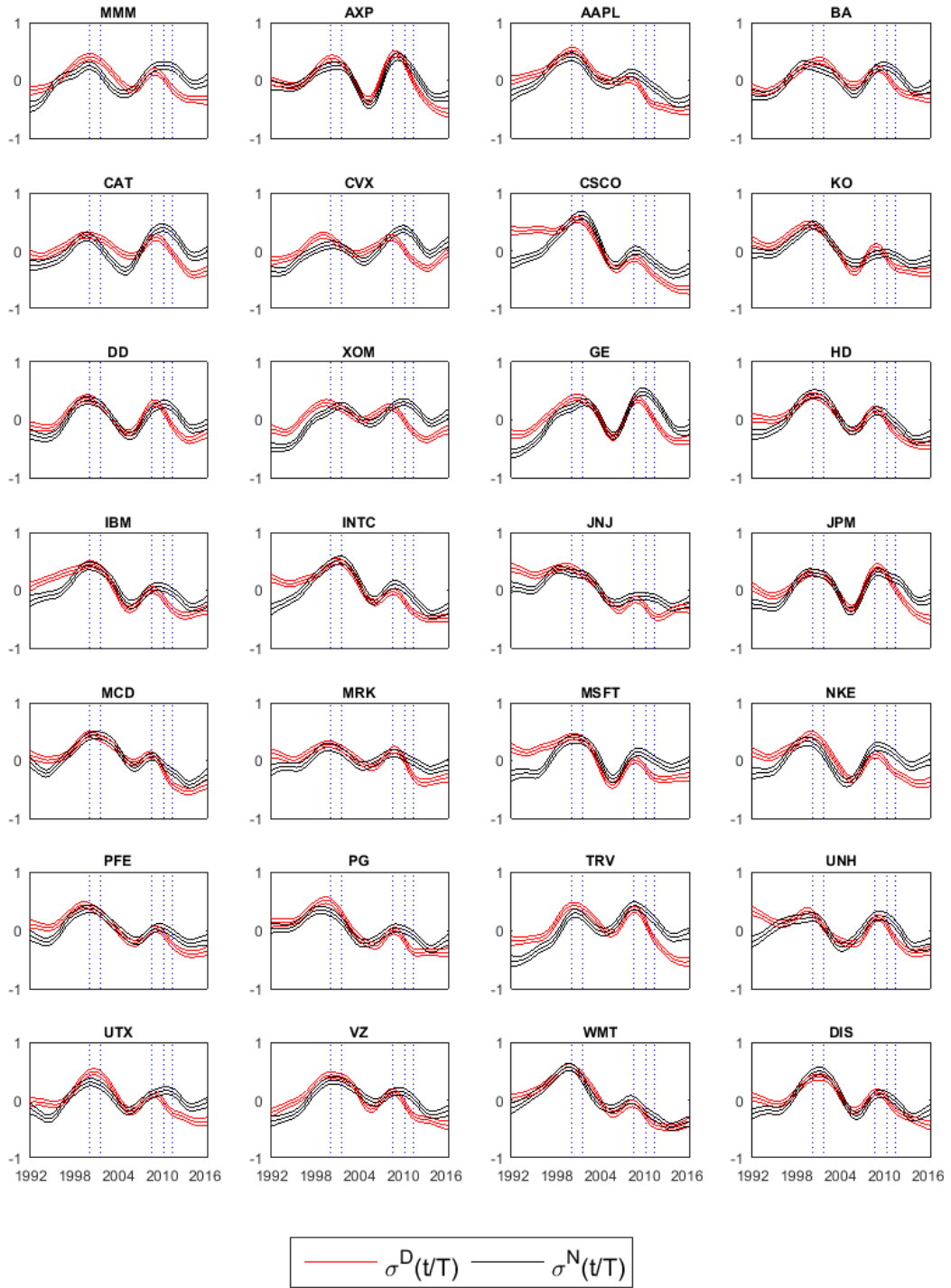
■

## 2 Figures and tables



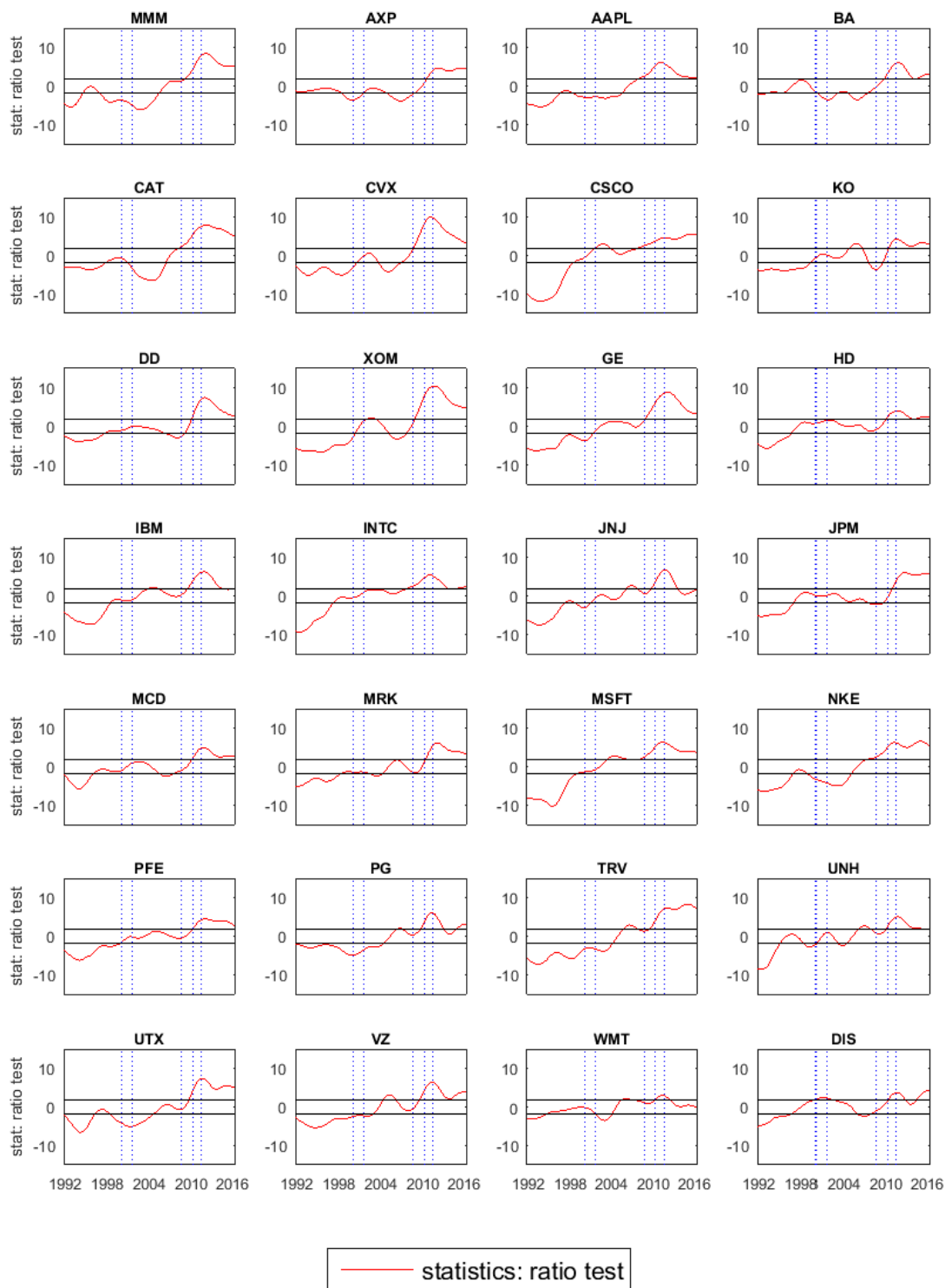
This figure shows the cumulative intraday (in red) and cumulative overnight (in black) returns with one subplot for each stock.

Figure B.1: Cumulative intraday and overnight returns



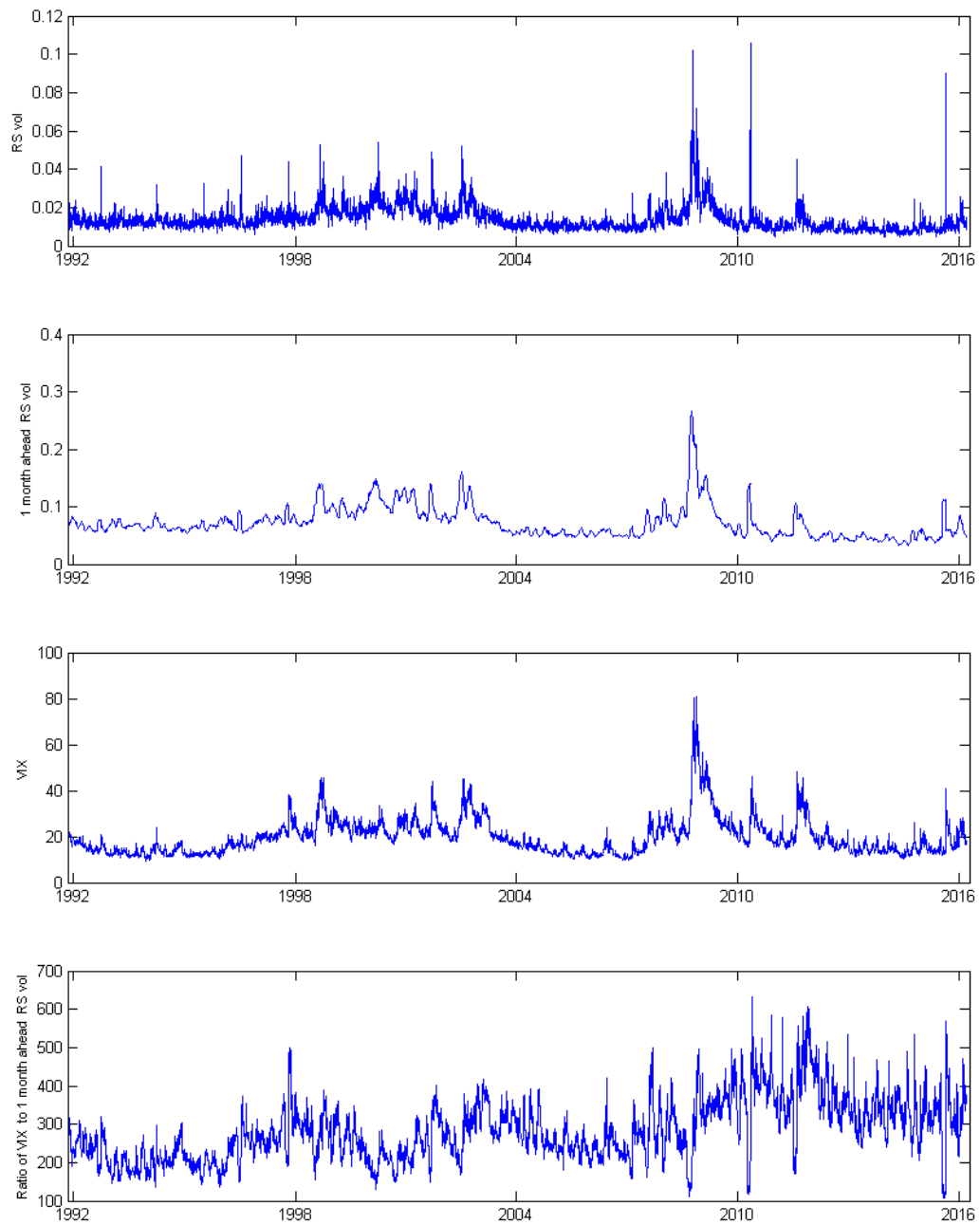
This figure shows the estimated intraday (in red) and overnight (in black) long run components,  $\sigma^D(t/T)$  and  $\sigma^N(t/T)$ , based on the univariate coupled component model, with one subplot for each stock. The five dashed vertical lines from left to right represent the dates: 10 March 2000(dot-com bubble), 17 September 2011(after the September 11 attacks), 16 September 2008(financial crisis), 6 May 2010 (flash crash) and 1 August 2011 (August 2011 stock markets fall), respectively.

Figure B.2: Long run component  $\sigma^j(\frac{t}{T})$ : univariate model



The red lines represent the statistics of the ratio tests, with the null hypothesis  $H_0 : \exp(\sigma_0^N(t/T)) = \rho \exp(\sigma_0^D(t/T))$ . The black lines indicate the 95% confidence intervals of the statistics under the null. The five dashed vertical lines from left to right represent the dates: 10 March 2000(dot-com bubble), 17 September 2001 (after the September 11 attacks), 16 September 2008(financial crisis), 6 May 2010 (flash crash) and 1 August 2011 (August 2011 stock markets fall), respectively.

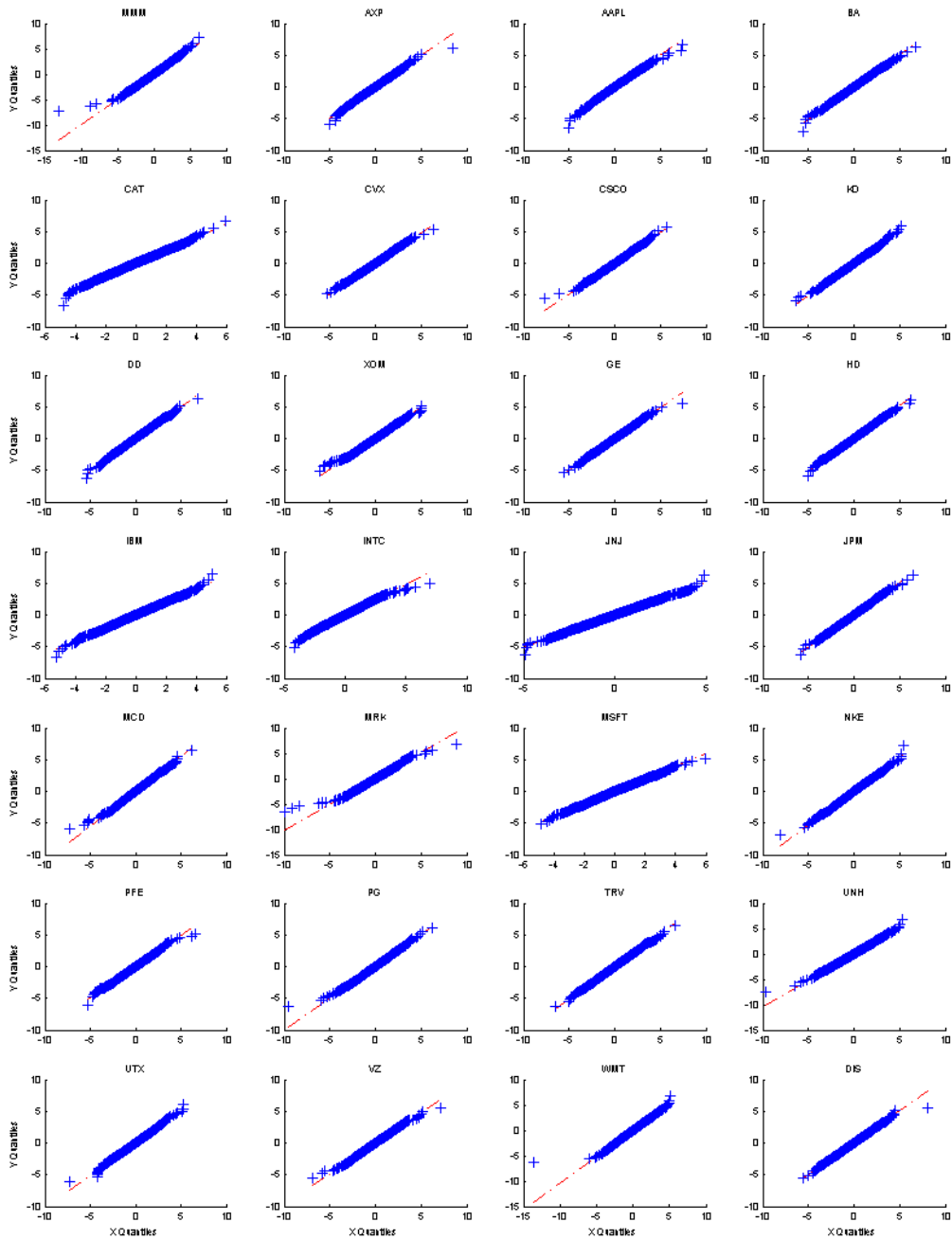
5  
Figure B.3: Statistics of ratio tests: univariate model



The figure shows the Rogers and Satchell(RS) volatility, the one-month ahead monthly RS volatility, VIX, and the ratio of VIX to the one-month ahead monthly RS volatility. The RS volatility is the average RS volatility across the 28 stocks.

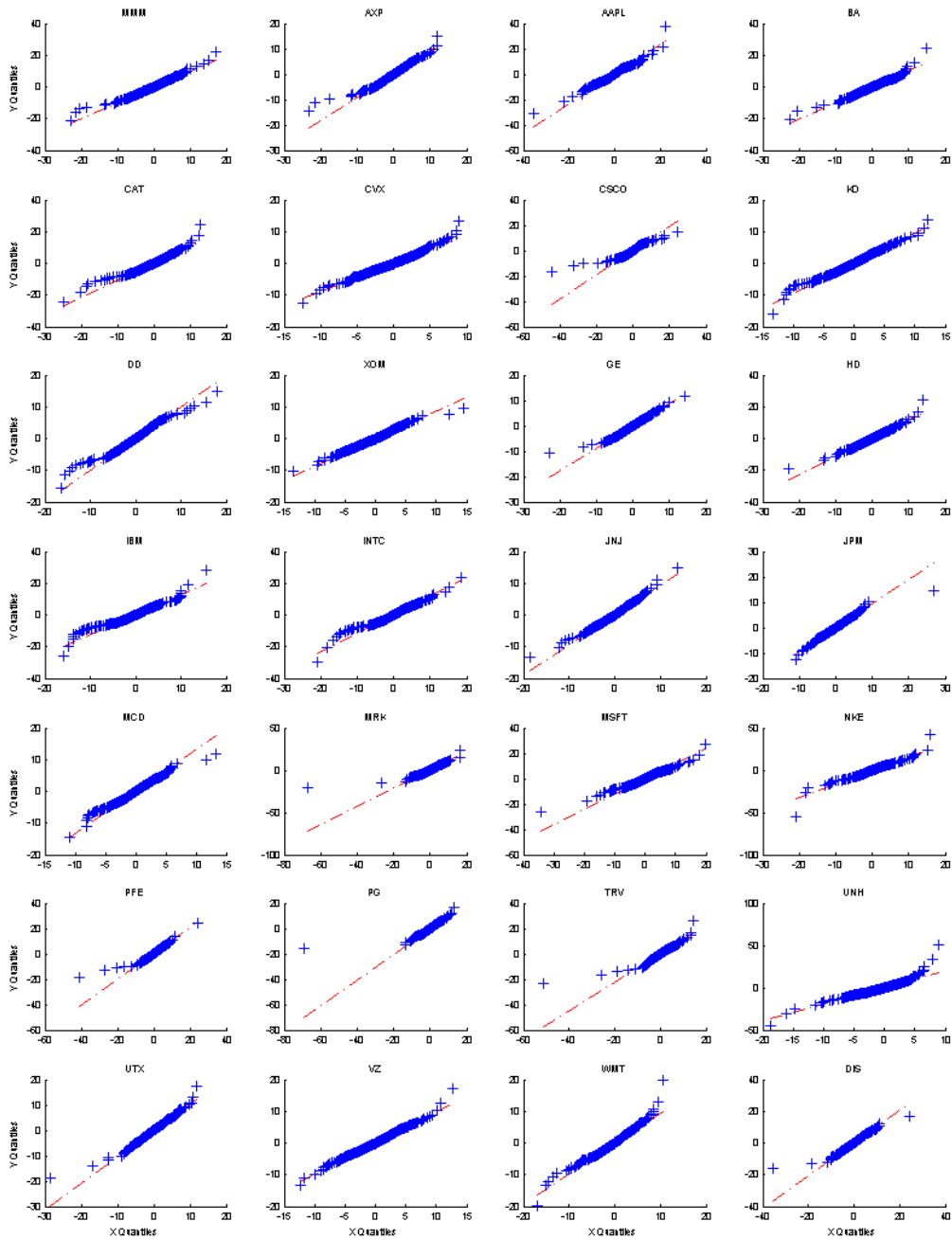
Figure B.4: RS, VIX and their ratio





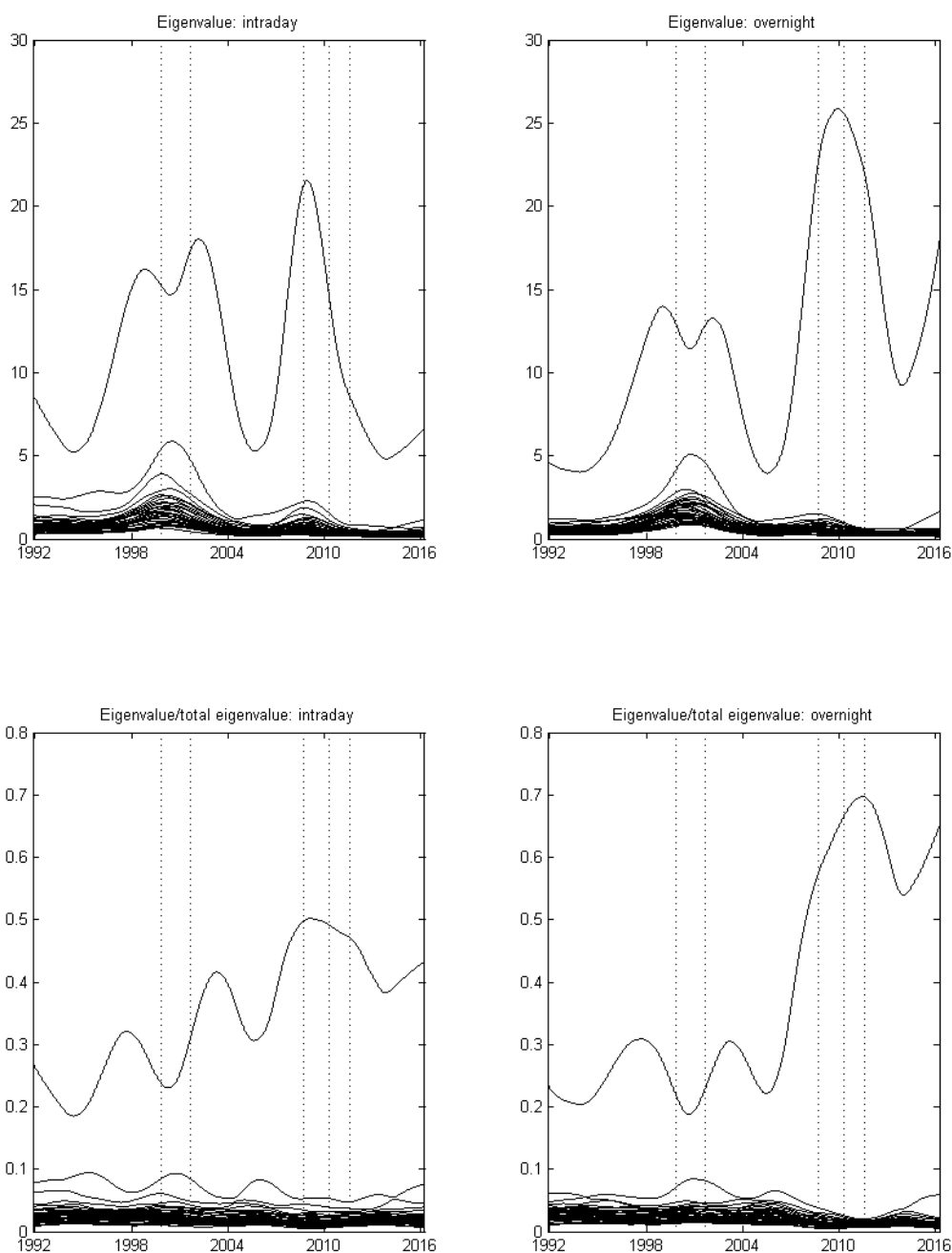
This figure displays Q-Q plots of the quantiles of the intraday innovations (X axis), versus the theoretical quantiles of the student t distribution with the  $\hat{\nu}_D$  degrees of freedom (Y axis), with one panel for each stock.

Figure B.5: QQ plot of the intraday innovations



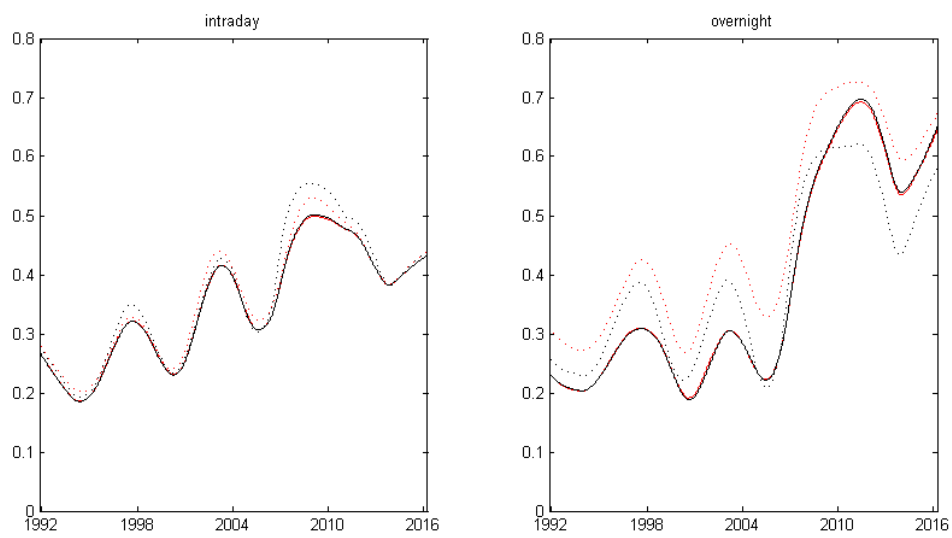
This figure displays Q-Q plots of the quantiles of the overnight innovations (X axis), versus the theoretical quantiles of the student t distribution with the  $\hat{\nu}_D$  degrees of freedom (Y axis), with one panel for each stock.

Figure B.6: QQ plot of the overnight innovations



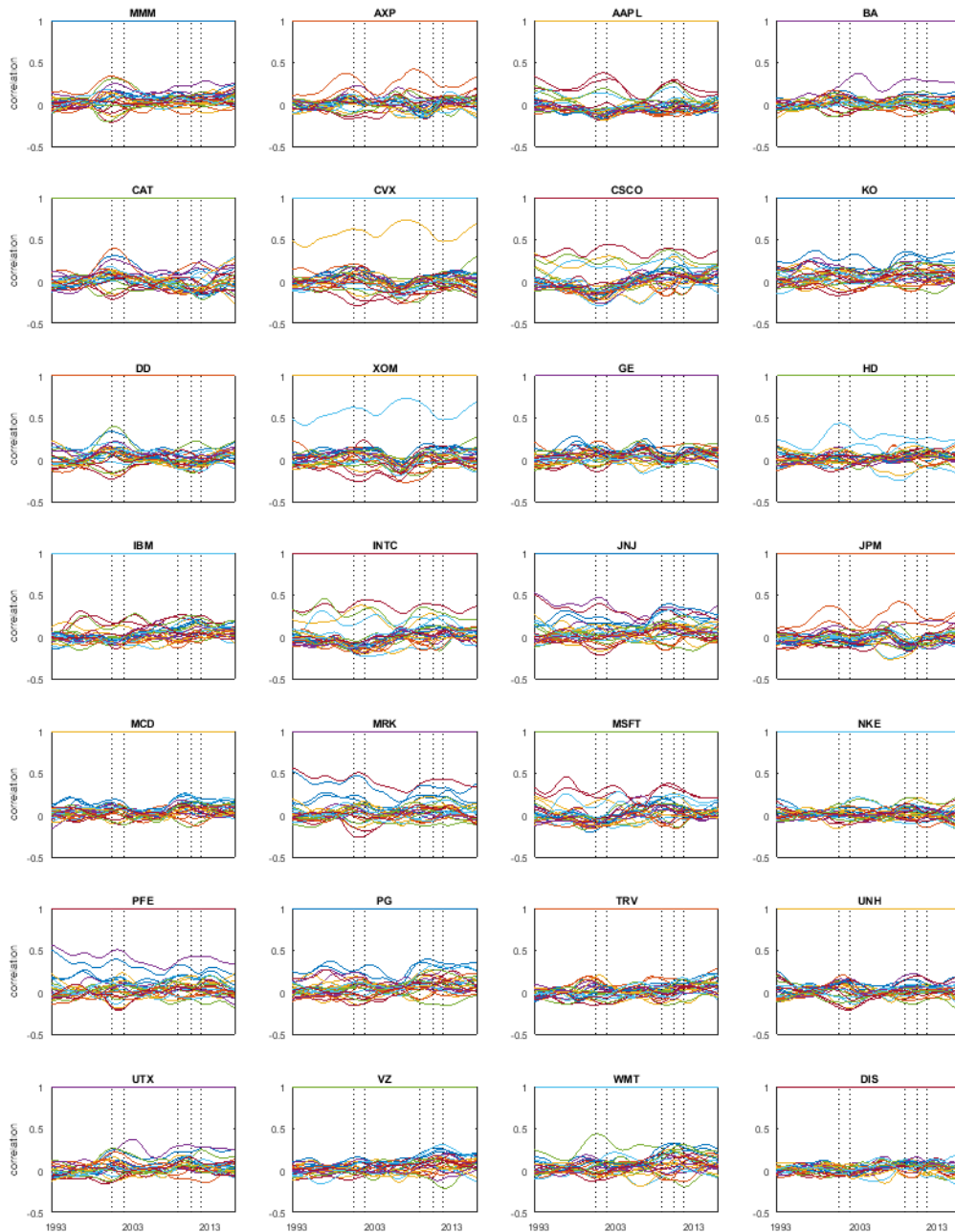
The upper panel plots the eigenvalues of the covariance matrices, and the lower panel plots the eigenvalues divided by the sum of eigenvalues. The five dashed vertical lines from left to right indicate the dates: 10 March 2000 (dot-com bubble), 17 September 2001 (after the September 11 attacks), 16 September 2008 (financial crisis), 6 May 2010 (flash crash) and 1 August 2011 (August 2011 stock markets fall), respectively.

Figure B.7: Eigenvalues of covariance matrices



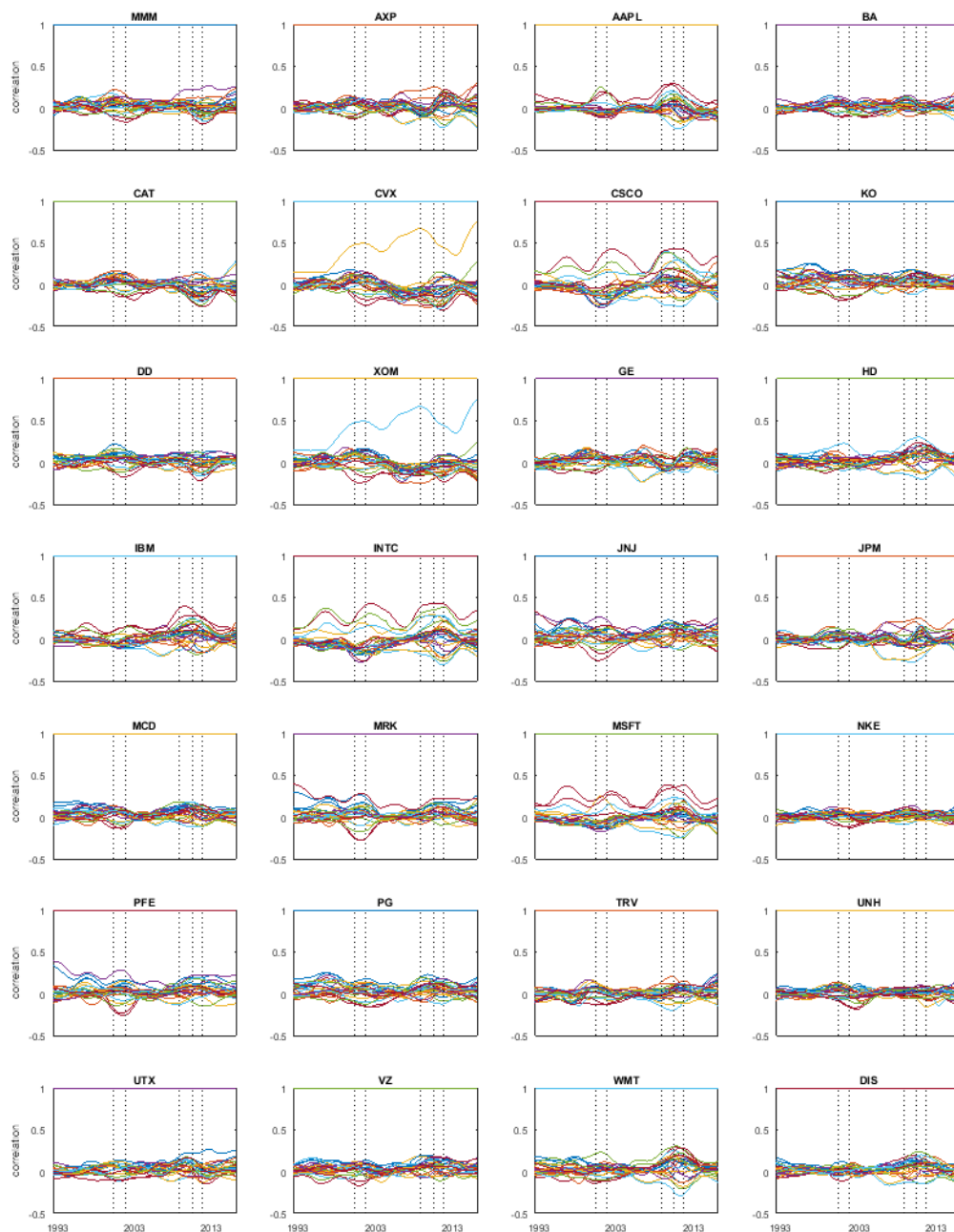
Left (right) panel plots the largest eigenvalue proportion of the estimated intraday (overnight) covariance matrix, with red (black) lines indicating the use of the non-robust (robust) correlation in the initial step. Solid (dashed) lines are further used to indicate the use of initial (updated) estimators,

Figure B.8: comparison of robust and non-robust initial correlation estimator



Each panel presents the 27 time series of long run intraday correlations between the idiosyncratic shocks of that individual stock and the remaining stocks. That is, the mean equation is specified as a CAPM model. The five dashed vertical lines from left to right indicate the dates: 10 March 2000(dot-com bubble), 17 September 2001 (after the September 11 attacks), 16 September 2008(financial crisis), 6 May 2010 (flash crash) and 1 August 2011 (August 2011 stock markets fall), respectively.

Figure B.9: Long run intraday correlations



Each panel presents the 27 time series of long run intraday correlations between the idiosyncratic shocks of that individual stock and the remaining stocks. That is, the mean equation is specified as a CAPM model. The five dashed vertical lines from left to right indicate the dates: 10 March 2000 (dot-com bubble), 17 September 2001 (after the September 11 attacks), 16 September 2008 (financial crisis), 6 May 2010 (flash crash) and 1 August 2011 (August 2011 stock markets fall), respectively.

Figure B.10: Long run overnight correlations

	intraday				overnight			
	mean	std.dev.	skew	kurt	mean	std.dev.	skew	kurt
MMM	0.0003	0.0127	0.0040	7.1842	0.0000	0.0073	-0.6030	20.3340
AXP	0.0003	0.0192	-0.0473	9.7455	0.0001	0.0109	-1.3220	30.8063
AAPL	-0.0004	0.0242	0.1903	6.3090	0.0010	0.0180	-7.2410	288.9583
BA	0.0002	0.0159	-0.0091	6.3725	0.0001	0.0103	-2.4955	59.8270
CAT	-0.0001	0.0174	0.0190	5.7938	0.0005	0.0110	-0.8610	18.7038
CVX	0.0001	0.0137	0.0810	10.6472	0.0002	0.0074	-0.9206	13.1831
CSCO	-0.0001	0.0229	0.0227	10.6339	0.0008	0.0141	-0.6753	22.9465
KO	0.0006	0.0126	0.0474	8.3962	-0.0003	0.0071	-0.3592	12.6505
DD	0.0003	0.0157	0.0273	7.1028	-0.0002	0.0091	-0.3597	16.1463
XOM	0.0004	0.0131	0.0861	10.8546	-0.0002	0.0071	-0.9341	14.7103
GE	-0.0001	0.0157	-0.0019	11.2698	0.0004	0.0101	0.1864	30.3115
HD	0.0001	0.0172	0.2999	6.9232	0.0004	0.0108	-3.0134	81.4299
IBM	0.0003	0.0150	0.0487	7.3880	-0.0001	0.0100	-0.7826	39.9142
INTC	0.0001	0.0204	0.1913	7.2270	0.0005	0.0141	-2.6159	51.1115
JNJ	0.0003	0.0120	0.0789	6.4480	0.0000	0.0071	-3.0637	79.0347
JPM	0.0000	0.0210	0.4353	14.1952	0.0003	0.0124	0.1249	19.7644
MCD	0.0005	0.0137	-0.0941	8.1253	-0.0001	0.0083	-0.4635	15.1683
MRK	0.0004	0.0149	-0.0381	7.6085	-0.0002	0.0096	-6.2306	172.5119
MSFT	0.0003	0.0171	0.1528	5.6204	0.0003	0.0109	-0.5826	32.3796
NKE	0.0006	0.0177	0.1389	9.5287	-0.0001	0.0104	-2.0513	50.5907
PFE	-0.0001	0.0152	-0.0349	5.6494	0.0004	0.0097	-2.0215	40.9346
PG	0.0009	0.0124	-0.0109	9.0587	-0.0006	0.0085	-18.5373	884.7702
TRV	0.0002	0.0163	-0.1116	16.1477	0.0001	0.0087	-1.7067	65.3085
UNH	0.0003	0.0203	-0.1451	13.8989	0.0004	0.0117	-2.9957	64.2616
UTX	0.0001	0.0145	-0.2758	9.4068	0.0004	0.0084	-1.6782	38.7102
VZ	0.0001	0.0142	0.4456	7.6871	0.0000	0.0079	-0.4672	15.4566
WMT	-0.0000	0.0147	0.1238	7.9677	0.0003	0.0084	-0.7025	16.3198
DIS	0.0004	0.0161	0.1634	7.1087	0.0000	0.0110	-1.0887	47.8462

This table gives the summary statistics for the intraday and overnight returns.

Table B.1: Summary statistics for intraday and overnight returns

	$\theta$	$\mu_D$	$\mu_N$	$\Pi_{11}$	$\Pi_{12}$	$\Pi_{21}$	$\Pi_{22}$
MMM	-0.0094 (0.0331)	0.0304 (0.0163)	0.0035 (0.0093)	-0.0201 (0.0180)	-0.0079 (0.0297)	-0.0245 (0.0108)	-0.0186 (0.0201)
AXP	-0.0482 (0.0449)	0.0302 (0.0245)	0.0112 (0.0139)	-0.0530 (0.0218)	0.0055 (0.0444)	-0.0112 (0.0141)	-0.0463 (0.0259)
AAPL	0.0473 (0.0433)	-0.0468 (0.0310)	0.1009 (0.0233)	-0.0609 (0.0172)	0.0794 (0.0262)	-0.0137 (0.0188)	0.0113 (0.0220)
BA	-0.0284 (0.0313)	0.0149 (0.0203)	0.0120 (0.0132)	-0.0048 (0.0197)	0.0162 (0.0413)	-0.0100 (0.0144)	0.0239 (0.0184)
CAT	0.0142 (0.0342)	-0.0095 (0.0223)	0.0531 (0.0140)	-0.0013 (0.0185)	-0.0159 (0.0260)	0.0155 (0.0113)	-0.0132 (0.0179)
CVX	-0.0847 (0.0435)	0.0130 (0.0176)	0.0163 (0.0095)	-0.0515 (0.0211)	-0.0449 (0.0452)	-0.0059 (0.0137)	-0.0316 (0.0226)
CSCO	0.0319 (0.0322)	-0.0120 (0.0294)	0.0832 (0.0181)	-0.0615 (0.0203)	0.0081 (0.0303)	0.0268 (0.0105)	-0.0205 (0.0181)
KO	0.0516 (0.0372)	0.0571 (0.0162)	-0.0250 (0.0091)	-0.0188 (0.0193)	0.0354 (0.0353)	-0.0134 (0.0123)	0.0537 (0.0171)
DD	0.0627 (0.0370)	0.0343 (0.0201)	-0.0174 (0.0117)	0.0025 (0.0204)	-0.0230 (0.0315)	-0.0094 (0.0114)	-0.0083 (0.0172)
XOM	-0.0482 (0.0465)	0.0475 (0.0166)	-0.0148 (0.0090)	-0.0898 (0.0220)	-0.0144 (0.0447)	-0.0287 (0.0147)	-0.0222 (0.0236)
GE	0.1066 (0.0493)	-0.0125 (0.0201)	0.0382 (0.0130)	-0.0276 (0.0283)	0.0234 (0.0429)	-0.0020 (0.0173)	0.0159 (0.0289)
HD	0.0306 (0.0414)	0.0143 (0.0220)	0.0362 (0.0139)	0.0217 (0.0191)	-0.0563 (0.0288)	0.0208 (0.0120)	-0.0054 (0.0197)
IBM	-0.0067 (0.0297)	0.0365 (0.0191)	-0.0061 (0.0127)	-0.0375 (0.0177)	0.0609 (0.0254)	0.0070 (0.0112)	-0.0477 (0.0190)
INTC	0.0335 (0.0277)	0.0034 (0.0260)	0.0475 (0.0180)	-0.0542 (0.0180)	0.0742 (0.0307)	0.0061 (0.0121)	-0.0515 (0.0192)
JNJ	0.0866 (0.0309)	0.0346 (0.0154)	0.0013 (0.0092)	-0.0327 (0.0181)	0.0016 (0.0334)	0.0254 (0.0122)	0.0271 (0.0200)
JPM	-0.0020 (0.0493)	0.0037 (0.0268)	0.0308 (0.0158)	-0.0701 (0.0288)	0.0065 (0.0462)	0.0195 (0.0161)	-0.0601 (0.0237)
MCD	0.1500 (0.0329)	0.0546 (0.0175)	-0.0089 (0.0106)	-0.0169 (0.0200)	0.0221 (0.0305)	-0.0216 (0.0112)	0.0235 (0.0177)
MRK	0.0032 (0.0292)	0.0352 (0.0190)	-0.0202 (0.0123)	-0.0084 (0.0197)	-0.0151 (0.0271)	0.0165 (0.0114)	-0.0022 (0.0187)
MSFT	-0.0200 (0.0322)	0.0268 (0.0218)	0.0277 (0.0139)	-0.0536 (0.0182)	0.0461 (0.0265)	0.0033 (0.0107)	-0.0247 (0.0153)
NKE	0.0226 (0.0339)	0.0616 (0.0227)	-0.0059 (0.0133)	0.0153 (0.0197)	-0.0228 (0.0287)	-0.0081 (0.0127)	-0.0132 (0.0160)
PFE	0.1283 (0.0285)	-0.0078 (0.0195)	0.0355 (0.0124)	0.0014 (0.0168)	-0.0094 (0.0283)	-0.0024 (0.0114)	0.0222 (0.0187)
PG	0.0929 (0.0275)	0.0986 (0.0160)	-0.0530 (0.0112)	-0.0612 (0.0216)	0.0729 (0.0289)	-0.0268 (0.0134)	-0.0029 (0.0121)
TRV	0.1594 (0.0686)	0.0264 (0.0208)	0.0070 (0.0111)	-0.0423 (0.0299)	-0.0529 (0.0460)	-0.0194 (0.0191)	-0.0312 (0.0220)
UNH	-0.0305 (0.0593)	0.0332 (0.0261)	0.0353 (0.0150)	0.0229 (0.0205)	-0.0370 (0.0400)	0.0058 (0.0145)	-0.0084 (0.0214)
UTX	-0.0565 (0.0698)	0.0096 (0.0186)	0.0395 (0.0107)	-0.0216 (0.0197)	-0.0386 (0.0323)	0.0032 (0.0105)	-0.0458 (0.0181)
VZ	0.0621 (0.0429)	0.0143 (0.0181)	0.0012 (0.0101)	-0.0405 (0.0202)	-0.0316 (0.0376)	-0.0129 (0.0119)	0.0012 (0.0188)
WMT	0.0852 (0.0347)	-0.0054 (0.0188)	0.0310 (0.0107)	-0.0436 (0.0185)	0.0315 (0.0341)	-0.0053 (0.0100)	0.0361 (0.0175)
DIS	0.0376 (0.0290)	0.0373 (0.0205)	0.0024 (0.0140)	-0.0236 (0.0197)	0.0026 (0.0369)	-0.0155 (0.0132)	-0.0019 (0.0234)
DJI	-0.0549 (0.0393)	0.0328 (0.0208)	-0.0020 (0.0128)	-0.0615 (0.0205)	0.1050 (0.0342)	0.0034 (0.0130)	-0.0282 (0.0198)
average	0.0311	0.0223	0.0165	-0.0297	0.0042	-0.0029	-0.0086
pool est.	0.0299	0.0223	0.0162	-0.0313	0.0121	-0.0011	-0.0103
pool s.e.	(0.0034)	(0.0023)	(0.0015)	(0.0018)	(0.0032)	(0.0012)	(0.0019)
num of +	18	22	20	5	15	11	9
num of -	10	6	8	23	13	17	19
num of signi +	7	6	11	0	4	2	2
num of signi -	0	0	2	12	0	2	4

This table gives the estimates of the mean equations in the univariate coupled component models, with their asymptotic standard errors in parenthesis; 'pool est.' and 'pool s.e.' represent the MLE pool estimates and their standard errors.

Table B.2: Estimates of the mean equations



	$\beta_D$	$\gamma_D$	$\rho_D$	$\gamma_D^*$	$\rho_D^*$	$\nu_D$	$\omega_D$
MMM	0.9716 (0.0055)	0.0213 (0.0036)	0.0273 (0.0042)	-0.0189 (0.0025)	-0.0107 (0.0025)	6.8817 (0.5291)	-0.0611 (0.0266)
AXP	0.9710 (0.0052)	0.0348 (0.0040)	0.0298 (0.0041)	-0.0162 (0.0025)	-0.0112 (0.0027)	9.6898 (1.0451)	0.3035 (0.0336)
AAPL	0.9177 (0.0166)	0.0394 (0.0056)	0.0381 (0.0068)	-0.0157 (0.0032)	-0.0109 (0.0035)	8.9059 (0.8917)	0.6216 (0.0213)
BA	0.9587 (0.0087)	0.0340 (0.0045)	0.0261 (0.0050)	-0.0110 (0.0026)	-0.0116 (0.0027)	8.6091 (0.8269)	0.2315 (0.0263)
CAT	0.9752 (0.0050)	0.0236 (0.0038)	0.0239 (0.0042)	-0.0157 (0.0021)	-0.0105 (0.0022)	8.1879 (0.7801)	0.3253 (0.0298)
CVX	0.9626 (0.0066)	0.0309 (0.0039)	0.0256 (0.0040)	-0.0177 (0.0025)	-0.0137 (0.0027)	14.2545 (2.1566)	0.1014 (0.0268)
CSCO	0.9527 (0.0080)	0.0305 (0.0041)	0.0314 (0.0046)	-0.0187 (0.0029)	-0.0183 (0.0028)	11.8282 (1.4338)	0.5052 (0.0239)
KO	0.9616 (0.0082)	0.0279 (0.0041)	0.0262 (0.0048)	-0.0163 (0.0027)	-0.0143 (0.0026)	8.9666 (0.9389)	-0.0507 (0.0258)
DD	0.9541 (0.0102)	0.0351 (0.0050)	0.0302 (0.0053)	-0.0130 (0.0028)	-0.0144 (0.0029)	8.8106 (0.8545)	0.1858 (0.0258)
XOM	0.9605 (0.0068)	0.0382 (0.0043)	0.0263 (0.0040)	-0.0095 (0.0026)	-0.0157 (0.0028)	12.8135 (1.6619)	0.0350 (0.0287)
GE	0.9590 (0.0065)	0.0351 (0.0041)	0.0351 (0.0045)	-0.0182 (0.0025)	-0.0152 (0.0027)	11.7415 (1.4348)	0.1273 (0.0284)
HD	0.9559 (0.0071)	0.0326 (0.0041)	0.0345 (0.0049)	-0.0245 (0.0030)	-0.0176 (0.0030)	8.7982 (0.8661)	0.2666 (0.0260)
IBM	0.9614 (0.0076)	0.0331 (0.0046)	0.0311 (0.0051)	-0.0195 (0.0028)	-0.0096 (0.0027)	8.0274 (0.7189)	0.1107 (0.0276)
INTC	0.9638 (0.0072)	0.0263 (0.0034)	0.0221 (0.0043)	-0.0116 (0.0023)	-0.0125 (0.0027)	13.8716 (1.9630)	0.4828 (0.0250)
JNJ	0.9440 (0.0084)	0.0399 (0.0045)	0.0394 (0.0051)	-0.0226 (0.0032)	-0.0131 (0.0032)	9.2874 (0.9551)	-0.1001 (0.0255)
JPM	0.9739 (0.0042)	0.0386 (0.0042)	0.0370 (0.0043)	-0.0187 (0.0025)	-0.0102 (0.0026)	8.9114 (0.8937)	0.3347 (0.0394)
MCD	0.7771 (0.1108)	0.0677 (0.0393)	0.0622 (0.0097)	0.0017 (0.0111)	0.0017 (0.0102)	9.0474 (1.0475)	0.2359 (0.0945)
MRK	0.9391 (0.0132)	0.0397 (0.0054)	0.0400 (0.0066)	-0.0153 (0.0032)	-0.0105 (0.0032)	7.6928 (0.6331)	0.1438 (0.0239)
MSFT	0.9366 (0.0108)	0.0437 (0.0047)	0.0495 (0.0063)	-0.0111 (0.0030)	-0.0073 (0.0034)	11.3473 (1.3919)	0.2991 (0.0253)
NKE	0.9670 (0.0069)	0.0315 (0.0044)	0.0290 (0.0051)	-0.0171 (0.0028)	-0.0067 (0.0026)	6.9838 (0.5738)	0.2606 (0.0292)
PFE	0.9640 (0.0071)	0.0275 (0.0038)	0.0322 (0.0046)	-0.0144 (0.0025)	-0.0077 (0.0025)	11.3019 (1.3785)	0.2051 (0.0270)
PG	0.9480 (0.0096)	0.0356 (0.0045)	0.0332 (0.0051)	-0.0163 (0.0030)	-0.0108 (0.0032)	8.7109 (0.8227)	-0.0845 (0.0246)
TRV	0.9660 (0.0067)	0.0413 (0.0050)	0.0333 (0.0050)	-0.0119 (0.0028)	-0.0101 (0.0028)	8.2381 (0.7880)	0.1086 (0.0331)
UNH	0.9470 (0.0099)	0.0405 (0.0048)	0.0344 (0.0058)	-0.0210 (0.0033)	-0.0110 (0.0033)	7.4073 (0.6330)	0.3985 (0.0254)
UTX	0.9596 (0.0075)	0.0288 (0.0044)	0.0336 (0.0048)	-0.0182 (0.0027)	-0.0163 (0.0028)	9.3467 (1.0045)	0.0982 (0.0261)
VZ	0.9676 (0.0062)	0.0278 (0.0037)	0.0279 (0.0042)	-0.0070 (0.0023)	-0.0146 (0.0026)	11.3300 (1.3386)	0.0931 (0.0280)
WMT	0.9742 (0.0062)	0.0270 (0.0037)	0.0238 (0.0042)	-0.0097 (0.0023)	-0.0085 (0.0025)	8.0639 (0.7403)	0.0663 (0.0308)
DIS	0.9516 (0.0116)	0.0344 (0.0056)	0.0329 (0.0051)	-0.0151 (0.0030)	-0.0115 (0.0031)	9.6181 (1.0518)	0.1953 (0.0298)
average	0.9515	0.0345	0.0327	-0.0151	-0.0115	9.5955	0.1943
pool est.	0.9861	0.0316	0.0314	-0.0059	-0.0022	8.0103	-0.8937
pool s.e.	(0.0004)	(0.0009)	(0.0006)	(0.0003)	(0.0003)	(0.1339)	(0.0374)

Continued on the next page.

Table B.3: Estimates of the dynamic parameters in the univariate coupled component models

	$\beta_N$	$\gamma_N$	$\rho_N$	$\gamma_N^*$	$\rho_N^*$	$\nu_N$	$\omega_N$
MMM	0.9683 (0.0063)	0.0344 (0.0054)	0.0322 (0.0049)	-0.0127 (0.0033)	-0.0235 (0.0032)	2.9893 (0.1333)	-0.9498 (0.0325)
AXP	0.9722 (0.0046)	0.0387 (0.0055)	0.0379 (0.0042)	-0.0188 (0.0032)	-0.0229 (0.0029)	3.7613 (0.1895)	-0.5535 (0.0385)
AAPL	0.9234 (0.0117)	0.0619 (0.0081)	0.0629 (0.0064)	-0.0154 (0.0045)	-0.0146 (0.0040)	2.6745 (0.0977)	-0.3351 (0.0278)
BA	0.9710 (0.0062)	0.0206 (0.0051)	0.0327 (0.0043)	-0.0120 (0.0026)	-0.0168 (0.0026)	3.0865 (0.1367)	-0.6114 (0.0298)
CAT	0.9708 (0.0057)	0.0305 (0.0058)	0.0393 (0.0049)	-0.0103 (0.0030)	-0.0197 (0.0029)	2.8998 (0.1229)	-0.5496 (0.0350)
CVX	0.9778 (0.0039)	0.0197 (0.0039)	0.0264 (0.0031)	-0.0110 (0.0023)	-0.0157 (0.0024)	4.1452 (0.2379)	-0.7624 (0.0324)
CSCO	0.9631 (0.0065)	0.0368 (0.0058)	0.0344 (0.0044)	-0.0140 (0.0029)	-0.0212 (0.0030)	3.5092 (0.1532)	-0.3252 (0.0306)
KO	0.9658 (0.0058)	0.0409 (0.0053)	0.0275 (0.0042)	-0.0189 (0.0031)	-0.0201 (0.0029)	3.7388 (0.1821)	-0.8462 (0.0319)
DD	0.9566 (0.0084)	0.0337 (0.0060)	0.0425 (0.0050)	-0.0175 (0.0035)	-0.0159 (0.0030)	3.5630 (0.1734)	-0.6296 (0.0290)
XOM	0.9729 (0.0052)	0.0258 (0.0043)	0.0310 (0.0037)	-0.0122 (0.0026)	-0.0140 (0.0025)	5.0318 (0.3115)	-0.7701 (0.0322)
GE	0.9614 (0.0062)	0.0401 (0.0056)	0.0463 (0.0046)	-0.0204 (0.0031)	-0.0221 (0.0030)	4.7818 (0.2773)	-0.6118 (0.0340)
HD	0.9537 (0.0076)	0.0452 (0.0062)	0.0373 (0.0048)	-0.0220 (0.0039)	-0.0259 (0.0036)	3.1685 (0.1418)	-0.6014 (0.0299)
IBM	0.9632 (0.0064)	0.0414 (0.0062)	0.0389 (0.0048)	-0.0121 (0.0033)	-0.0218 (0.0030)	2.7722 (0.1088)	-0.7656 (0.0330)
INTC	0.9662 (0.0083)	0.0300 (0.0064)	0.0305 (0.0047)	-0.0131 (0.0033)	-0.0155 (0.0027)	2.8768 (0.1116)	-0.4046 (0.0295)
JNJ	0.9596 (0.0063)	0.0323 (0.0050)	0.0348 (0.0043)	-0.0166 (0.0030)	-0.0262 (0.0030)	4.0828 (0.2189)	-0.8547 (0.0281)
JPM	0.9754 (0.0038)	0.0350 (0.0046)	0.0366 (0.0040)	-0.0198 (0.0027)	-0.0226 (0.0026)	4.0152 (0.2098)	-0.4103 (0.0397)
MCD	0.8012 (0.0159)	0.0488 (0.0477)	0.0800 (0.0787)	-0.0018 (0.0082)	-0.0000 (0.0069)	4.0211 (0.1751)	-0.2824 (0.0458)
MRK	0.9458 (0.0111)	0.0398 (0.0064)	0.0435 (0.0062)	-0.0135 (0.0036)	-0.0209 (0.0035)	3.2409 (0.1456)	-0.6822 (0.0271)
MSFT	0.9433 (0.0102)	0.0543 (0.0076)	0.0452 (0.0053)	-0.0098 (0.0038)	-0.0115 (0.0035)	2.8706 (0.1101)	-0.6569 (0.0293)
NKE	0.9543 (0.0095)	0.0396 (0.0068)	0.0456 (0.0061)	-0.0147 (0.0037)	-0.0177 (0.0038)	2.3998 (0.0876)	-0.8391 (0.0301)
PFE	0.9619 (0.0074)	0.0424 (0.0058)	0.0364 (0.0045)	-0.0112 (0.0032)	-0.0118 (0.0031)	3.4040 (0.1577)	-0.6243 (0.0324)
PG	0.9445 (0.0097)	0.0292 (0.0058)	0.0370 (0.0050)	-0.0206 (0.0035)	-0.0235 (0.0033)	3.6016 (0.1717)	-0.9050 (0.0240)
TRV	0.9740 (0.0049)	0.0398 (0.0060)	0.0347 (0.0044)	-0.0125 (0.0031)	-0.0170 (0.0029)	2.9686 (0.1268)	-0.9225 (0.0393)
UNH	0.9354 (0.0109)	0.0521 (0.0077)	0.0547 (0.0066)	-0.0076 (0.0045)	-0.0202 (0.0042)	2.2533 (0.0836)	-0.7491 (0.0293)
UTX	0.9708 (0.0048)	0.0303 (0.0048)	0.0324 (0.0041)	-0.0202 (0.0030)	-0.0195 (0.0027)	3.3906 (0.1623)	-0.7534 (0.0332)
VZ	0.9661 (0.0057)	0.0302 (0.0052)	0.0325 (0.0040)	-0.0224 (0.0031)	-0.0138 (0.0028)	3.7265 (0.1886)	-0.7555 (0.0300)
WMT	0.9756 (0.0052)	0.0240 (0.0047)	0.0302 (0.0038)	-0.0111 (0.0026)	-0.0126 (0.0026)	3.4965 (0.1641)	-0.7485 (0.0328)
DIS	0.9552 (0.0074)	0.0369 (0.0073)	0.0396 (0.0074)	-0.0147 (0.0034)	-0.0183 (0.0032)	3.4211 (0.1618)	-0.6600 (0.0320)
Average	0.9553	0.0369	0.0394	-0.0145	-0.0180	3.4247	-0.6629
pool est.	0.9823	0.0426	0.0307	-0.0086	-0.0130	3.2019	-1.5104
pool s.e.	(0.0006)	(0.0010)	(0.0009)	(0.0005)	(0.0005)	(0.0265)	(0.0322)

This table presents the estimates of the dynamic parameters in the univariate coupled component models, and their asymptotic standard errors in parenthesis; 'pool est.' and 'pool s.e.' represent the MLE pool estimates and their standard errors.

Table B.3: Estimates of the dynamic parameters in the univariate coupled component models (cont.)

	$\beta_D = \beta_N$	$\gamma_D = \gamma_N$	$\rho_D = \rho_N$	$\gamma_D^* = \gamma_N^*$	$\rho_D^* = \rho_N^*$	$\nu_D = \nu_N$	$\omega_D = \omega_N$	$\gamma_N = \rho_D$	$(\beta_D, \gamma_D, \rho_D, \gamma_D^*, \rho_D^*)$ $= (\beta_N, \gamma_N, \rho_N, \gamma_N^*, \rho_N^*)$
MMM	0.4463	0.0404	0.4074	0.1300	0.0015	0.0000	0.0000	0.1158	0.0015
AXP	0.7387	0.5529	0.1337	0.5090	0.0031	0.0000	0.0000	0.0587	0.0004
AAPL	0.6655	0.0175	0.0047	0.9604	0.5031	0.0000	0.0000	0.0016	0.0000
BA	0.0412	0.0357	0.2624	0.7881	0.1553	0.0000	0.0000	0.2269	0.0222
CAT	0.2142	0.2870	0.0058	0.1250	0.0090	0.0000	0.0000	0.1444	0.0015
CVX	0.0010	0.0332	0.8557	0.0381	0.5759	0.0000	0.0000	0.1356	0.0106
CSCO	0.0811	0.3699	0.6042	0.2516	0.4850	0.0000	0.0000	0.3166	0.0169
KO	0.5108	0.0408	0.8287	0.5255	0.1401	0.0000	0.0000	0.0035	0.0122
DD	0.7178	0.8493	0.0533	0.2979	0.7134	0.0000	0.0000	0.5036	0.0953
XOM	0.0113	0.0358	0.3672	0.4597	0.6693	0.0000	0.0000	0.9082	0.0377
GE	0.5704	0.4586	0.0643	0.5741	0.0904	0.0000	0.0000	0.2692	0.0004
HD	0.7339	0.0834	0.6725	0.6071	0.0790	0.0000	0.0000	0.0616	0.1236
IBM	0.7507	0.2660	0.2244	0.0799	0.0027	0.0000	0.0000	0.0597	0.0032
INTC	0.7053	0.6005	0.1628	0.7053	0.4233	0.0000	0.0000	0.1713	0.1426
JNJ	0.0149	0.2568	0.4710	0.1707	0.0027	0.0000	0.0000	0.1627	0.0049
JPM	0.5514	0.5603	0.9484	0.7509	0.0008	0.0000	0.0000	0.6026	0.0012
MCD	0.8264	0.8265	0.8190	0.8200	0.8627	0.0000	0.0001	0.7875	0.9999
MRK	0.4594	0.9906	0.6508	0.7012	0.0283	0.0000	0.0000	0.9729	0.1458
MSFT	0.4468	0.2405	0.5895	0.7901	0.3990	0.0000	0.0000	0.5058	0.3634
NKE	0.0625	0.2967	0.0206	0.5988	0.0159	0.0000	0.0000	0.0646	0.0362
PFE	0.7098	0.0303	0.4915	0.4023	0.2893	0.0000	0.0000	0.0508	0.0377
PG	0.6715	0.3739	0.5645	0.3481	0.0069	0.0000	0.0000	0.4775	0.0481
TRV	0.0957	0.8364	0.8171	0.8814	0.0976	0.0000	0.0000	0.2369	0.0499
UNH	0.2059	0.1949	0.0139	0.0167	0.0901	0.0000	0.0000	0.0113	0.0028
UTX	0.0310	0.8085	0.8380	0.6094	0.4181	0.0000	0.0000	0.4670	0.0098
VZ	0.7429	0.6957	0.3921	0.0001	0.8273	0.0000	0.0000	0.6222	0.0015
WMT	0.7214	0.5910	0.2347	0.6712	0.2528	0.0000	0.0000	0.9611	0.4234
DIS	0.5415	0.7408	0.2892	0.9213	0.1324	0.0000	0.0000	0.4689	0.0731

This table presents the  $p$ -values of the Wald tests for several sets of null hypothesis:  $H_0 : \beta_D = \beta_N$ ,  $H_0 : \gamma_D = \gamma_N$ ,  $H_0 : \rho_D = \rho_N$ ,  $H_0 : \gamma_D^* = \gamma_N^*$ ,  $H_0 : \rho_D^* = \rho_N^*$ ,  $H_0 : \nu_D = \nu_N$ ,  $H_0 : \omega_D = \omega_N$ ,  $H_0 : \gamma_N = \rho_D$ , and  $H_0 : (\beta_D, \gamma_D, \rho_D, \gamma_D^*, \rho_D^*) = (\beta_N, \gamma_N, \rho_N, \gamma_N^*, \rho_N^*)$ .

Table B.4: Wald tests

	student t log-likelihood				quasi Gaussian log-likelihood			
	$l_{cogarch}$	$l_{garch}$	GW stat.	p-val.	$l_{cogarch}$	$l_{garch}$	GW stat.	p-val.
MMM	1.1832	1.1963	6.3242	0.0119	1.1901	1.2092	6.2041	0.0127
AXP	1.3335	1.3473	2.7307	0.0984	1.3727	1.3974	2.2438	0.1342
AAPL	1.6569	1.6701	2.5099	0.1131	1.6642	1.6854	2.0921	0.1481
BA	1.4584	1.4715	4.7922	0.0286	1.4830	1.5048	5.5787	0.0182
CAT	1.5693	1.5761	1.9846	0.1589	1.5834	1.5915	1.4751	0.2245
CVX	1.6026	1.6058	0.2129	0.6445	1.6135	1.6178	0.2728	0.6015
CSCO	1.3807	1.3936	3.5761	0.0586	1.3832	1.4027	3.4340	0.0639
KO	1.1211	1.1347	2.3200	0.1277	1.1281	1.1483	2.6316	0.1048
DD	1.4821	1.4956	2.8619	0.0907	1.4996	1.5218	3.2895	0.0697
XOM	1.4198	1.4284	1.9184	0.1660	1.4304	1.4448	3.1887	0.0742
GE	1.3125	1.3328	1.8666	0.1719	1.3371	1.3638	0.7425	0.3889
HD	1.4018	1.4148	3.1614	0.0754	1.4179	1.4408	2.4230	0.1196
IBM	1.3442	1.3538	3.0191	0.0823	1.3586	1.3730	2.1378	0.1437
INTC	1.5674	1.5736	0.6431	0.4226	1.5913	1.6025	1.4440	0.2295
JNJ	1.1759	1.1807	0.2140	0.6436	1.1863	1.2141	1.0331	0.3094
JPM	1.3844	1.3902	0.4479	0.5033	1.3933	1.4047	0.5767	0.4476
MCD	1.1675	1.1772	0.6391	0.4240	1.2151	1.2332	0.6079	0.4356
MRK	1.4255	1.4298	0.4247	0.5146	1.4483	1.4694	1.0146	0.3138
MSFT	1.5373	1.5511	3.8529	0.0497	1.5612	1.5889	4.4249	0.0354
NKE	1.4760	1.4811	0.6902	0.4061	1.4872	1.5010	1.2014	0.2730
PFE	1.3581	1.3701	1.4091	0.2352	1.3698	1.3924	1.0637	0.3024
PG	1.0967	1.0992	0.1259	0.7227	1.1153	1.1345	1.0687	0.3012
TRV	1.1117	1.1185	0.5408	0.4621	1.1186	1.1280	0.8314	0.3619
UNH	1.6005	1.6018	0.1291	0.7193	1.5949	1.5961	0.0506	0.8219
UTX	1.3216	1.3336	2.1103	0.1463	1.3437	1.3566	0.7855	0.3755
VZ	1.1679	1.1791	3.5395	0.0599	1.1797	1.2149	1.9419	0.1635
WMT	1.2735	1.2720	0.0452	0.8316	1.4252	1.4429	1.3135	0.2518
DIS	1.3163	1.3222	0.4560	0.4995	1.3300	1.3439	0.9672	0.3254

The table presents the GW test of the null that the one-component and the coupled component model have equal expected loss, with minus the out-of-sample t log-likelihood or quasi Gaussian log-likelihood as the loss function.  $l_{cogarch}$  represents the average loss value of the coupled component model, and  $l_{garch}$  represents the average loss value of the one component BETA-T-EGARCH model with open-close returns.

Table B.5: GW tests: univariate model

	$ \epsilon_d $	$ \epsilon_n $	$ r_d $	$ r_n $	$\epsilon_d^2$	$\epsilon_n^2$	$r_d^2$	$r_n^2$
MMM	0.7102	0.2692	0.0000	0.0000	0.9611	0.9923	0.0000	0.0000
AXP	0.3953	0.1358	0.0000	0.0000	0.1828	0.9900	0.0000	0.0000
AAPL	0.7447	0.4793	0.0000	0.0000	0.0757	0.9997	0.0000	0.9558
BA	0.1846	0.2596	0.0000	0.0000	0.2914	0.9962	0.0000	0.0000
CAT	0.9292	0.2899	0.0000	0.0000	0.7909	0.9988	0.0000	0.0000
CVX	0.3064	0.5760	0.0000	0.0000	0.0637	0.5412	0.0000	0.0000
CSCO	0.0739	0.7701	0.0000	0.0000	0.0170	1.0000	0.0000	0.0000
KO	0.5040	0.7539	0.0000	0.0000	0.5222	0.9752	0.0000	0.0000
DD	0.6311	0.7901	0.0000	0.0000	0.0710	0.2432	0.0000	0.0000
XOM	0.4986	0.1337	0.0000	0.0000	0.3109	0.7145	0.0000	0.0000
GE	0.1884	0.8045	0.0000	0.0000	0.0138	0.9978	0.0000	0.0000
HD	0.3390	0.4095	0.0000	0.0000	0.1141	0.9977	0.0000	0.0120
IBM	0.4555	0.2208	0.0000	0.0000	0.7846	0.9603	0.0000	0.0000
INTC	0.3869	0.0606	0.0000	0.0000	0.8838	0.9853	0.0000	0.0003
JNJ	0.2579	0.4742	0.0000	0.0000	0.5205	0.9366	0.0000	0.0286
JPM	0.2962	0.4567	0.0000	0.0000	0.3807	1.0000	0.0000	0.0000
MCD	0.1996	0.3503	0.0000	0.0000	0.3556	0.9685	0.0000	0.0000
MRK	0.2003	0.7233	0.0000	0.0000	0.0000	1.0000	0.0000	1.0000
MSFT	0.5201	0.8494	0.0000	0.0000	0.7620	1.0000	0.0000	0.0000
NKE	0.0407	0.8972	0.0000	0.0000	0.0924	0.9980	0.0000	0.9857
PFE	0.1066	0.6689	0.0000	0.0000	0.0957	1.0000	0.0000	0.0025
PG	0.8185	0.8830	0.0000	0.0000	0.9378	1.0000	0.0000	1.0000
TRV	0.4188	0.3676	0.0000	0.0000	0.1089	0.9992	0.0000	0.0000
UNH	0.0045	0.4844	0.0000	0.0000	0.2356	0.9829	0.0000	0.0000
UTX	0.0096	0.1683	0.0000	0.0000	0.0018	0.9999	0.0000	0.0017
VZ	0.1302	0.2894	0.0000	0.0000	0.5510	0.0343	0.0000	0.0000
WMT	0.1704	0.5944	0.0000	0.0000	0.9867	0.9023	0.0000	0.0000
DIS	0.9257	0.1840	0.0000	0.0000	0.7475	1.0000	0.0000	0.0000

This table gives the  $p$ -values of the Ljung-Box Q-tests for absolute(squared) residuals and returns.

Table B.6: Diagnostic checking for GARCH effects

	$\beta_D$	$\gamma_D$	$\rho_D$	$\gamma_D^*$	$\rho_D^*$	$\nu_D$	$\omega_D$
MMM	0.8504 (0.0811)	0.0350 (0.0097)	0.0788 (0.0226)	-0.0094 (0.0053)	0.0001 (0.0047)	5.1024 (0.3138)	-0.1047 (0.0196)
AXP	0.9332 (0.0132)	0.0442 (0.0054)	0.0466 (0.0066)	-0.0138 (0.0033)	-0.0082 (0.0035)	8.5370 (0.8093)	-0.0540 (0.0247)
AAPL	0.8056 (0.0419)	0.0587 (0.0080)	0.0646 (0.0100)	-0.0169 (0.0047)	0.0026 (0.0049)	7.4693 (-0.6579)	-0.0421 (0.0190)
BA	0.7165 (0.0519)	0.0636 (0.0079)	0.0721 (0.0098)	0.0000 (0.0050)	0.0089 (0.0059)	7.8943 (0.7117)	-0.0268 (0.0176)
CAT	0.9447 (0.0158)	0.0271 (0.0047)	0.0311 (0.0072)	-0.0098 (0.0026)	-0.0004 (0.0028)	7.3387 (0.6330)	-0.0276 (0.0221)
CVX	0.9475 (0.0139)	0.0331 (0.0050)	0.0285 (0.0056)	-0.0116 (0.0029)	-0.0038 (0.0030)	9.7347 (1.1058)	-0.0069 (0.0238)
CSCO	0.9282 (0.0154)	0.0412 (0.0057)	0.0412 (0.0067)	-0.0152 (0.0035)	-0.0134 (0.0031)	8.3211 (0.7676)	-0.0515 (0.0229)
KO	0.8383 (0.0471)	0.0477 (0.0078)	0.0567 (0.0101)	-0.0139 (0.0042)	0.0001 (0.0049)	8.9520 (0.9210)	-0.0161 (0.0189)
DD	0.7722 (0.0409)	0.0523 (0.0072)	0.0792 (0.0093)	-0.0018 (0.0049)	-0.0009 (0.0050)	7.0406 (0.5741)	-0.0625 (0.0180)
XOM	0.9316 (0.0188)	0.0417 (0.0063)	0.0334 (0.0065)	0.0029 (0.0032)	-0.0031 (0.0033)	11.2320 (1.3386)	0.0081 (0.0229)
GE	0.9905 (0.0015)	0.0307 (0.0029)	0.0366 (0.0048)	-0.0093 (0.0023)	-0.0065 (0.0021)	7.4505 (1.0314)	-0.1456 (0.0300)
HD	0.8657 (0.0430)	0.0573 (0.0098)	0.0591 (0.0114)	-0.0155 (0.0042)	-0.0081 (0.0044)	7.8864 (0.7215)	-0.0342 (0.0208)
IBM	0.9459 (0.0279)	0.0324 (0.0046)	0.0186 (0.0049)	-0.0097 (0.0021)	-0.0066 (0.0023)	6.3196 (0.4762)	-0.0476 (0.0903)
INTC	0.9108 (0.0264)	0.0322 (0.0059)	0.0294 (0.0077)	-0.0062 (0.0032)	-0.0046 (0.0033)	8.7912 (0.8483)	-0.0289 (0.0192)
JNJ	0.7695 (0.0555)	0.0648 (0.0087)	0.0760 (0.0109)	-0.0137 (0.0051)	0.0043 (0.0063)	7.3108 (0.6096)	-0.0319 (0.0185)
JPM	0.9661 (0.0065)	0.0407 (0.0047)	0.0367 (0.0051)	-0.0108 (0.0027)	-0.0026 (0.0027)	7.1034 (0.5958)	-0.0644 (0.0333)
MCD	0.7385 (0.0757)	0.0545 (0.0089)	0.0691 (0.0121)	-0.0059 (0.0054)	0.0033 (0.0057)	7.1915 (0.5940)	-0.0341 (0.0174)
MRK	0.7964 (0.0443)	0.0649 (0.0082)	0.0799 (0.0110)	-0.0090 (0.0051)	-0.0066 (0.0052)	6.8163 (0.5228)	-0.0495 (0.0190)
MSFT	0.8637 (0.0247)	0.0554 (0.0063)	0.0675 (0.0085)	0.0003 (0.0040)	0.0042 (0.0044)	8.8889 (0.8994)	-0.0320 (0.0205)
NKE	0.9706 (0.0069)	0.0200 (0.0023)	0.0187 (0.0037)	-0.0062 (0.0021)	0.0005 (0.0016)	5.8409 (-0.3850)	-0.0863 (0.0303)
PFE	0.9422 (0.0147)	0.0316 (0.0049)	0.0375 (0.0064)	-0.0049 (0.0030)	0.0014 (0.0032)	8.5675 (0.8417)	-0.0273 (0.0230)
PG	0.7537 (0.0910)	0.0369 (0.0037)	0.0639 (0.0080)	-0.0130 (0.0026)	-0.0092 (0.0025)	10.1869 (1.4107)	0.0162 (0.0305)
TRV	0.9248 (0.0154)	0.0517 (0.0060)	0.0502 (0.0075)	-0.0078 (0.0035)	-0.0002 (0.0035)	7.3641 (0.6169)	-0.0564 (0.0248)
UNH	0.9465 (0.0098)	0.0178 (0.0071)	-0.0073 (0.0091)	-0.0275 (0.0032)	-0.0209 (0.0036)	13.3228 (3.6346)	0.2249 (0.0761)
UTX	0.8583 (0.0331)	0.0511 (0.0070)	0.0591 (0.0092)	-0.0072 (0.0041)	-0.0071 (0.0042)	8.4000 (0.8074)	-0.0176 (0.0201)
VZ	0.9098 (0.0222)	0.0350 (0.0059)	0.0528 (0.0077)	0.0000 (0.0034)	-0.0085 (0.0035)	8.9866 (0.8905)	-0.0281 (0.0206)
WMT	0.9397 (0.0222)	0.0355 (0.0063)	0.0291 (0.0081)	-0.0031 (0.0031)	-0.0034 (0.0032)	7.1862 (0.5837)	-0.0342 (0.0227)
DIS	0.8600 (0.0350)	0.0279 (0.0050)	0.0593 (0.0087)	-0.0066 (0.0040)	-0.0017 (0.0039)	7.2250 (0.5754)	-0.0372 (0.0175)
Average	0.8793	0.0423	0.0489	-0.0088	-0.0032	8.0879	-0.0321

Continued on the next page.

Table B.7: Estimates of the dynamic parameters in the multivariate coupled component model

	$\beta_N$	$\gamma_N$	$\rho_N$	$\gamma_N^*$	$\rho_N^*$	$\nu_N$	$\omega_N$
MMM	0.8804 (0.0339)	0.0483 (0.0076)	0.0383 (0.0073)	0.0039 (0.0046)	-0.0076 (0.0050)	2.9933 (0.1300)	-1.0124 (0.0228)
AXP	0.9295 (0.0138)	0.0595 (0.0081)	0.0444 (0.0060)	-0.0066 (0.0042)	-0.0102 (0.0039)	3.2091 (0.1363)	-0.9629 (0.0271)
AAPL	0.8619 (0.0196)	0.0800 (0.0098)	0.0798 (0.0081)	-0.0005 (0.0055)	-0.0141 (0.0051)	2.3334 (0.0781)	-1.2202 (0.0241)
BA	0.7390 (0.0478)	0.0558 (0.0111)	0.0706 (0.0095)	-0.0001 (0.0064)	-0.0039 (0.0063)	2.5584 (0.0950)	-1.0268 (0.0194)
CAT	0.9330 (0.0157)	0.0449 (0.0084)	0.0496 (0.0071)	0.0055 (0.0041)	-0.0104 (0.0039)	2.4952 (0.0918)	-1.0838 (0.0267)
CVX	0.9692 (0.0080)	0.0139 (0.0043)	0.0232 (0.0038)	-0.0016 (0.0024)	-0.0069 (0.0024)	3.4551 (0.1676)	-0.8353 (0.0244)
CSCO	0.9394 (0.0137)	0.0547 (0.0086)	0.0444 (0.0062)	0.0003 (0.0037)	-0.0138 (0.0039)	2.7603 (0.1023)	-1.1515 (0.0283)
KO	0.8793 (0.0330)	0.0422 (0.0077)	0.0404 (0.0079)	-0.0074 (0.0045)	-0.0141 (0.0047)	3.1641 (0.1354)	-0.9414 (0.0205)
DD	0.8112 (0.0406)	0.0585 (0.0098)	0.0546 (0.0083)	-0.0072 (0.0055)	0.0021 (0.0055)	3.0657 (0.1278)	-0.9734 (0.0199)
XOM	0.9375 (0.0158)	0.0329 (0.0065)	0.0330 (0.0051)	-0.0023 (0.0034)	0.0007 (0.0034)	4.0204 (0.2057)	-0.8168 (0.0228)
GE	0.9930 (0.0009)	0.0345 (0.0046)	0.0393 (0.0032)	-0.0055 (0.0023)	-0.0079 (0.0022)	3.4604 (0.1365)	-1.0347 (0.0408)
HD	0.9001 (0.0231)	0.0420 (0.0080)	0.0540 (0.0080)	-0.0070 (0.0044)	-0.0183 (0.0045)	2.7342 (0.1052)	-1.0060 (0.0225)
IBM	0.8994 (0.0642)	0.0474 (0.0089)	0.0490 (0.0067)	-0.0028 (0.0037)	-0.0150 (0.0038)	2.3921 (0.0844)	-1.1149 (0.0833)
INTC	0.8185 (0.0341)	0.0799 (0.0112)	0.0611 (0.0089)	0.0005 (0.0061)	-0.0028 (0.0055)	2.2863 (0.0772)	-1.1842 (0.0219)
JNJ	0.9383 (0.0158)	0.0284 (0.0072)	0.0334 (0.0066)	-0.0031 (0.0034)	-0.0172 (0.0035)	3.3619 (0.1521)	-0.8759 (0.0226)
JPM	0.9683 (0.0063)	0.0387 (0.0059)	0.0391 (0.0048)	-0.0103 (0.0029)	-0.0093 (0.0028)	3.3407 (0.1506)	-0.9096 (0.0350)
MCD	0.8857 (0.0349)	0.0353 (0.0093)	0.0441 (0.0088)	-0.0046 (0.0043)	-0.0117 (0.0043)	2.9313 (0.1162)	-0.9419 (0.0201)
MRK	0.9148 (0.0205)	0.0484 (0.0094)	0.0430 (0.0081)	-0.0056 (0.0042)	-0.0100 (0.0042)	2.7916 (0.1113)	-1.0097 (0.0240)
MSFT	0.8783 (0.0251)	0.0725 (0.0100)	0.0494 (0.0075)	0.0040 (0.0049)	-0.0022 (0.0047)	2.4788 (0.0850)	-1.1938 (0.0233)
NKE	0.8054 (0.0842)	0.0584 (0.0122)	0.0628 (0.0128)	-0.0084 (0.0046)	-0.0159 (0.0062)	2.2388 (0.0766)	-1.1941 (0.0240)
PFE	0.9505 (0.0113)	0.0434 (0.0068)	0.0375 (0.0053)	-0.0001 (0.0036)	0.0008 (0.0034)	2.9088 (0.1175)	-0.9905 (0.0285)
PG	0.7464 (0.0823)	0.0492 (0.0066)	0.0486 (0.0060)	-0.0188 (0.0037)	-0.0070 (0.0032)	3.1622 (0.1351)	-0.9233 (0.0259)
TRV	0.9478 (0.0105)	0.0548 (0.0072)	0.0408 (0.0060)	-0.0060 (0.0036)	-0.0065 (0.0037)	2.7246 (0.1042)	-0.9799 (0.0300)
UNH	0.8028 (0.0158)	0.0429 (0.0480)	0.0800 (0.0489)	0.0013 (0.0079)	-0.0132 (0.0067)	3.4955 (0.1653)	-0.5698 (0.0722)
UTX	0.9419 (0.0131)	0.0323 (0.0058)	0.0361 (0.0058)	-0.0080 (0.0033)	-0.0104 (0.0035)	2.9737 (0.1238)	-0.9300 (0.0246)
VZ	0.9333 (0.0133)	0.0429 (0.0071)	0.0364 (0.0055)	-0.0104 (0.0035)	-0.0027 (0.0035)	3.1833 (0.1345)	-0.8965 (0.0244)
WMT	0.9604 (0.0127)	0.0249 (0.0054)	0.0294 (0.0055)	-0.0005 (0.0028)	-0.0061 (0.0029)	2.9159 (0.1159)	-0.9766 (0.0254)
DIS	0.8282 (0.0322)	0.0800 (0.0108)	0.0708 (0.0094)	0.0010 (0.0056)	0.0010 (0.0056)	2.8703 (0.1147)	-1.0500 (0.0223)
Average	0.8926	0.0481	0.0476	-0.0036	-0.0083	2.9395	-0.9931

This table gives the estimates of the dynamic parameters in the multivariate coupled component model, and their asymptotic standard errors in parenthesis. The last row shows the average estimated values.

Table B.7: Estimates of the dynamic parameters in the multivariate coupled component model(cont.)

	$\alpha_D$	$\beta^{DD}$	$\beta^{DN}$	$\alpha_N$	$\beta^{NN}$	$B\beta^{DN}$
MMM	0.0078 (0.0137)	0.7605 (0.0195)	0.0902 (0.0339)	-0.0140 (0.0078)	0.7149 (0.0215)	-0.0294 (0.0115)
AXP	-0.0036 (0.0183)	1.3586 (0.0307)	0.1044 (0.0451)	-0.0227 (0.0101)	1.3036 (0.0388)	-0.0380 (0.0145)
AAPL	-0.0495 (0.0275)	1.2499 (0.0367)	-0.4008 (0.0519)	0.0692 (0.0214)	1.2795 (0.0410)	-0.0129 (0.0345)
BA	0.0032 (0.0175)	0.8752 (0.0259)	0.0260 (0.0395)	-0.0173 (0.0112)	0.9944 (0.0437)	-0.0018 (0.0204)
CAT	-0.0381 (0.0180)	1.1038 (0.0251)	-0.0173 (0.0446)	0.0225 (0.0111)	1.1490 (0.0260)	0.0200 (0.0144)
CVX	-0.0084 (0.0146)	0.7938 (0.0279)	0.1060 (0.0411)	-0.0040 (0.0075)	0.7782 (0.0254)	-0.0308 (0.0106)
CSCO	-0.0362 (0.0239)	1.4340 (0.0364)	-0.2393 (0.0518)	0.0353 (0.0143)	1.5125 (0.0398)	0.0271 (0.0186)
KO	0.0439 (0.0144)	0.6008 (0.0246)	-0.1229 (0.0363)	-0.0450 (0.0080)	0.6220 (0.0199)	-0.0273 (0.0116)
DD	0.0087 (0.0164)	0.9774 (0.0255)	0.0814 (0.0410)	-0.0401 (0.0094)	0.9410 (0.0236)	0.0016 (0.0138)
XOM	0.0259 (0.0141)	0.7638 (0.0278)	0.0563 (0.0383)	-0.0360 (0.0070)	0.7708 (0.0237)	-0.0412 (0.0102)
GE	-0.0359 (0.0146)	1.1506 (0.0272)	-0.1242 (0.0568)	0.0069 (0.0086)	1.2827 (0.0397)	0.0132 (0.0192)
HD	-0.0042 (0.0175)	1.1193 (0.0273)	-0.1750 (0.0421)	0.0046 (0.0114)	1.0824 (0.0320)	-0.0066 (0.0156)
IBM	0.0199 (0.0160)	0.9031 (0.0221)	-0.0778 (0.0320)	-0.0340 (0.0105)	1.0056 (0.0325)	0.0031 (0.0150)
INTC	-0.0166 (0.0206)	1.3354 (0.0324)	-0.1999 (0.0436)	0.0093 (0.0151)	1.4196 (0.0435)	-0.0262 (0.0180)
JNJ	0.0232 (0.0137)	0.5839 (0.0208)	-0.1028 (0.0289)	-0.0119 (0.0081)	0.6256 (0.0240)	-0.0006 (0.0121)
JPM	-0.0285 (0.0196)	1.5187 (0.0431)	-0.1691 (0.0719)	-0.0121 (0.0105)	1.5754 (0.0423)	-0.0152 (0.0193)
MCD	0.0401 (0.0159)	0.6222 (0.0230)	-0.1375 (0.0354)	-0.0288 (0.0094)	0.6937 (0.0205)	0.0166 (0.0113)
MRK	0.0188 (0.0169)	0.7569 (0.0255)	-0.0463 (0.0360)	-0.0392 (0.0113)	0.7590 (0.0270)	-0.0313 (0.0130)
MSFT	0.0081 (0.0171)	1.1223 (0.0242)	-0.0564 (0.0376)	-0.0053 (0.0112)	1.1081 (0.0287)	-0.0329 (0.0131)
NKE	0.0502 (0.0202)	0.8567 (0.0280)	-0.0060 (0.0476)	-0.0301 (0.0120)	0.8211 (0.0273)	-0.0162 (0.0138)
PFE	-0.0216 (0.0170)	0.7967 (0.0239)	-0.1187 (0.0356)	0.0153 (0.0111)	0.8099 (0.0307)	0.0023 (0.0131)
PG	0.0773 (0.0145)	0.5619 (0.0244)	-0.0952 (0.0335)	-0.0706 (0.0103)	0.5988 (0.0187)	-0.0227 (0.0133)
TRV	0.0044 (0.0183)	0.9263 (0.0382)	0.0345 (0.0655)	-0.0163 (0.0096)	0.8511 (0.0454)	-0.0340 (0.0167)
UNH	0.0131 (0.0240)	0.8234 (0.0448)	0.0093 (0.0769)	0.0126 (0.0142)	0.7748 (0.0378)	0.0031 (0.0229)
UTX	-0.0194 (0.0154)	0.8836 (0.0217)	0.1891 (0.0485)	0.0175 (0.0085)	0.9107 (0.0344)	-0.0117 (0.0125)
VZ	0.0001 (0.0163)	0.7322 (0.0239)	-0.1011 (0.0375)	-0.0185 (0.0086)	0.7536 (0.0227)	0.0019 (0.0129)
WMT	-0.0202 (0.0164)	0.7811 (0.0240)	-0.1636 (0.0339)	0.0144 (0.0094)	0.7311 (0.0238)	-0.0169 (0.0116)
DIS	0.0103 (0.0167)	1.0073 (0.0241)	0.0580 (0.0395)	-0.0250 (0.0120)	1.0557 (0.0464)	0.0070 (0.0190)

Estimates of the CAPM structure in the mean equations.  $r_{it}^D = a_i^D + \beta_i^{DD} r_{mt}^D + \beta_i^{DN} r_{mt}^N + u_{it}^D$  and  $r_{it}^N = a_i^N + \beta_i^{NN} r_{mt}^N + \beta_i^{ND} r_{mt-1}^D + u_{it}^N$ .

Table B.8: Estimates of the mean equations